UNIVERSITY OF CALIFORNIA
RIVERSIDE

A Study on High-Throughput Technologies for the Identification of Citrus Pathogens and the Characterization of Host Responses to Infections

A Dissertation submitted in partial satisfaction
of the requirements for the degree of

Doctor in Philosophy

in

Microbiology

by

Tyler Dang

September 2021

Dissertation Committee:
Dr. Georgios Vidalakis, Chairperson
Dr. James Borneman
Dr. Norman Ellstrand

The Dissertation of Tyler Dang is approved:

_____

_____

_____

Committee Chairperson

University of California, Riverside

ACKNOWLEDGMENTS

This dissertation would not have been completed without the help and support from so many people, both present and past. First and foremost, I would like to acknowledge and thank my advisor, Dr. Georgios Vidalakis, for his constant support and encouragement through the graduate school journey. Under his mentorship, I have developed significantly at the professional and personal level from my initial start as undergraduate laboratory assistant, to graduate student, and finally as an independent scientist. The lesions I have learned under his tutelage will have lasting effects as I continue to develop my professional career.

I would also like to extend my gratitude to my dissertation committee members, Dr. James Borneman and Dr. Norman Ellstrand, for their guidance and support in completion of my dissertation. I would also thank the professors serving on my qualifying exam committee: Dr. James Borneman, Dr. Sharon Walker, Dr. Caroline Roper, Dr. Emma Aronson, and Dr. Timothy Paine.

In addition, I would like to acknowledge the personnel from Vidalakis lab that had provided enormous help to make my research possible and contributed to my development: Dr. Sohrab Bodaghi and Greg Greer, Dr. Fatima Osman, Dr. Irene Lavagi-Craddock, Dr. Rock Christiano, Dr. Deborah Pagliaccia, Carolyn Anderson, Alexandra Syed, Bailey Van Zanten, Iman Mimou, and Gerardo Uribe.

I would like to show my appreciation to the past members of the Vidalakis lab for their support: Dr. Jinbo Wang, Dr. Shih-hua Tan, Dr. Sophia Kamenidou, Amy Huang, Brandon Ramirez, Tavia Rucker, Sarah Hammado, Shurooq Abu-Hajar, Ning Chen,

Xingyu Chen, Adilene Gomez, Ramon Serna, Brittany Nguyen, Noora Siddiqui, Emily Dang, German Torres-Contreras, Isaac Menchaca, Silvia Abdulnour, Alice Hsieh, Jocelyn Sun, Michael Voeltz, Roya Campos, and Harry Bae.

I would also like to extend my acknowledgements to the collaborators Dr. Robert Krueger and Dr. MaryLou Polek from USDA ARS National Clonal Germplasm Repository for Citrus and Dates and Dr. Kitty Cardwell and Dr. Andres Camacho Espindola from Institute of Biosecurity and Microbial Forensics at Oklahoma State University, Stillwater for their support.

Last, but not least, my journey in graduate school would not be completed without the unconditional support from my family and close friends.

The work in this dissertation could not be done without the financial support from Citrus Research Board projects “Next generation sequencing as a CCPP routine diagnostic tool for citrus variety introduction” and “Phase II of high-throughput sequencing as a CCPP routine diagnostic tool for variety introduction” (5300-179 and 5300-205), California Department of Food and Agriculture, and United States Department of Agriculture (USDA) National Institute of Food and Agriculture (NIFA), Hatch (project 233744) and the National Clean Plant Network (NCPN) which operates under the auspices of USDA Animal and Plant Health Inspection Service (APHIS) (12-8100-1544-CA; 14-, 15-, 16- 8130-0419-CA; AP17PPQS&T00C118; AP18PPQS&T00C107).

I acknowledge the Cahuilla people as the Traditional Custodians of the Land on which the experimental work was completed.

Note: The contents of this thesis are adapted from: 1) Dang, T. et al. 2021. High-throughput RNA extraction from citrus tissues for the detection of viroids. In: Rao, A., Lavagi-Craddock, I., Vidalakis, G., (Eds), Methods Molecular Biology, Viroids. Vol. 2316 Springer *In press*. 2) Dang et. al. (2018). First report of Citrus viroid V naturally infecting grapefruit and calamondin trees in California. Plant Dis. 102:2055 3) Dang et al. (2020). First report of Citrus leaf blotch virus infecting bears lime tree in California. Plant Dis. 104:3088. 4) Dang, T. et al. 2021. An *In-silico* Detection of a Citrus Viroid from Raw High Throughput Sequencing Data. In: Rao, A., Lavagi-Craddock, I., Vidalakis, G., (Eds), Methods Molecular Biology, Viroids. Vol. 2316 Springer *In press*. 5) Dang et. al. (2021) Front Microbio. 12. 980.

DEDICATION

This dissertation is dedicated to my parents, Phat Dang and Tina Dang, and my sister Emily Dang for their sacrifices and unconditional support through my journey towards my PhD. I also want to express appreciation for my dog, Neil. for accompanying me while I wrote this thesis.

ABSTRACT OF THE DISSERTATION

A Study on High-Throughput Technologies for the Identification of Citrus Pathogens and the Characterization of Host Responses to Infections

by

Tyler Dang

Doctor of Philosophy, Graduate Program in Microbiology
University of California, Riverside, September 2021
Dr. Georgios Vidalakis, Chairperson

High-throughput technologies for citrus diagnostic and characterization of host response in response to infection were evaluated. The high-throughput extraction using the MagMax 96 (Thermo Fisher Scientific, Waltham, MA) was found to be comparable to other existing RNA extractions methods for viroid and viruses testing. The method was adopted by the Citrus Clonal Protection Program and immediately utilized for nursery stock testing and field surveys. This resulted in significantly lowering the virus and viroid infections in the CA nursery stock program and the led to the discovery of citrus viroid V (CVd V) and citrus leaf blotch virus (CLBV), two exotic pathogens of California (CA). I was able to confirm the presence of CVd V by fulfilling Koch's postulate through biological indexing and sanger sequencing. Alternatively, CLBV was confirmed by high-throughput sequencing (HTS). I expanded the HTS for the detection of citrus pathogens and utilized the e-probe diagnostic nucleic acid analysis (EDNA) online platform to simplify the data analysis. As proof-of-concept e-probes were developed for citrus

tristeza virus (CTV), citrus exocortis viroid (CEVd), and *Candidatus* Liberibacter asiaticus (CLas). The e-probes worked as well as the currently approved diagnostic tools such as polymerase chain reaction (PCR). HTS was also applied for the characterization of citrus response in response to citrus dwarfing viroid (CDVd) infection. I discovered 4 conserved (3 from and 1 roots) and 3 novel miRNAs (stem only). The miRNA target host functions are associated with plant development and cellular growth that is consistent with the observed dwarfing phenotype in sweet orange trees on trifoliate rootstocks. In summary, the present dissertation provides in-depth application of high throughput methods for citrus diagnostics and characterization of host response to infection. These studies lead to the application of important high-throughput tools which have been utilized by the CCPP and provide insights into viroid-host interaction for future research.

TABLE OF CONTENTS

LIST OF FIGURES

CHAPTER 1

LIST OF TABLES

GENERAL INTRODUCTION

The California citrus industry is valued at $7.12 billion and is under constant threat from endemic and exotic pathogens (Babcock 2018). Over the years, the citrus industry has been protected by the advances in technology which have allowed for the removal and exclusion of citrus pathogens by the Citrus Clonal Protection Program (CCPP). In the 1930's citrus diagnosis was limited to visual identification of symptoms observed by Dr. H.S. Fawcett. This method provided some level of pathogen exclusion, however not all pathogens will show symptoms, thus potentially allowing infected plants to still be used as prerogative material. By the 1950's a breakthrough occurred with the development of citrus biological indexing for the detection of graft-transmissible diseases by Drs. J.W. Wallace and E.C. Calavan. Indicator plants inoculated with infected trees will express the exact same symptoms for a specific disease under greenhouse conditions. In the 1970's diagnostics transitioned from the greenhouse to the laboratory with the development of enzyme-linked immunosorbent assay (ELISA) by Drs. D. Gumpf and J.S. Semancik. The highly controlled laboratory setting allowed for testing to be performed year-round and results to be obtained faster. By the 2000's citrus diagnostic tests had largely become molecular with polymerase chain reaction (PCR) and quantitative PCR by Dr. G. Vidalakis.

As a Ph.D. student in microbiology under the tutelage of Dr. Vidalakis, the current director of the CCPP. This research is focused on continuing developing and improving technology for citrus diagnostics. Throughout this dissertation, high-throughput extraction and sequencing technologies were utilized for identification of

citrus pathogens and the characterization of citrus host response in response to pathogen infections.

Chapter I

A comparative study of RNA extraction protocols optimized for citrus tissues and application for high throughput detection and identification of citrus pathogens

Note: This has been adapted from: Dang, T. et al. (2021). High-throughput RNA extraction from citrus tissues for the detection of viroids. In: Rao, A., Lavagi-Craddock, I., Vidalakis, G., (Eds), Methods Molecular Biology, Viroids. Vol. 2316 Springer *In press*.

ABSTRACT

High quality RNA (i.e. purity, concentration, & integrity) is required for reliable detection of citrus pathogens using polymerase chain reaction (PCR) based methods. Citrus tissues are known to have high levels of polyphenols and polysaccharides that can affect RNA quality and inhibit RT-qPCR. We compared three RNA isolation methods: TRIzol™, a phenol-chloroform based method; Qiagen Plant RNeasy Mini Kit, a silica column-based method; and MagMAX-96 Viral RNA Isolation Kit (MME-96), a magnetic-bead based high-throughput method, by processing citrus tissues infected with different citrus pathogens (viruses and viroids) and healthy controls. We assessed the RNA purity and concentration with spectrophotometry and RNA integrity with RT-qPCR targeting the citrus gene NADH dehydrogenase subunit 5 (Nad5). All methods produced RNA with acceptable purity and integrity for use in PCR based applications. TRIzol™ yielded the highest concentrations (473.59 ± 132.44 ng/uL, median= 466.16, n= 43),

purity (260/280: 1.97 ± 0.09, median= 1.95) and good integrity (Nad5 Cq: 18.18 ± 1.46, median= 17.80), however it required serial dilutions to remove RT-qPCR inhibitors and effectively detect the targeted citrus pathogens. Qiagen produced the second highest concentrations (147.34 ± 72.52 ng/uL, median= 142, n= 43), purity (260/280: 2.20 ± 0.08, median= 2.21) and similar integrity to TRIzol™ (Nad5 Cq: 18.97 ± 1.69, median= 18.83). MM-96 extraction provided quality RNA, with uniform concentrations (57.75 ± 15.93 ng/uL, median= 54.4, n= 43), purity (260/280: 2.30 ± 0.12, median= 2.30) and consistent integrity (Nad5 Cq: 21.30 ± 0.89, median= 21.12). PCRs for the detection of citrus viruses and viroids were performed to verify the RNA extraction quality. The respective pathogens were detected regardless of extraction method. Ultimately, MME-96 was implemented by the Citrus Clonal Protection Program (CCPP) because it enables thousands of samples to be rapidly tested for citrus pathogens in a relatively small amount of time. As a result, infection rates have gone down significantly since the implementation of high throughput MM-96 extraction and RT-qPCR. This workflow and technology can be integrated to regulatory state and federal clean stock germplasm programs ensuring the availability of pathogen tested citrus propagative materials.

INTRODUCTION

Diagnostic tools for the detection of citrus viruses and viroids have been evolving as new technologies become available. Biological indexing (Roistacher, 1991; Garnsey et al., 2005), enzyme-linked immunosorbent assay (ELISA) (Bar-Joseph et al., 1979), imprint hybridization (de Noronha Fonseca et al., 1996; Palacio-Bielsa et al., 1999), sequential polyacrylamide gel electrophoresis (Rivera-Bustamante et al., 1986), and

direct blot immunoassay based detection (Garnsey et al., 1993), have been developed for the detection of citrus viruses and viroids. In more recent years, nucleic acid-based molecular detection methods such as reverse transcription polymerase chain reaction (RT-PCR) and RT-quantitative PCR (qPCR) have become the standard methods for the detection of citrus viruses and viroids. RT-PCR and RT-qPCR high-throughput capabilities and the availability of nucleic acid extraction protocols allowing for high sensitivity, specificity, and reliability of the molecular testing made them the system of choice for the detection of various citrus viruses and viroids from plant purified RNA (Bertolini et al., 2008; Rizza et al., 2009; Ruiz-Ruiz et al., 2009; Loconsole et al., 2010; Yokomi et al., 2010; Papayiannis, 2014; Osman et al., 2015, 2017). The application and adoption of RT-PCR and RT-qPCR assays in diagnostics has played an important role in disease management programs monitoring the sanitary status of germplasm and propagative materials, nursery stock and certification, and commercial plantings of citrus and other agriculturally significant crops (Bostock et al. 2014; Gergerich et al. 2015; Osman et al. 2015; Fuchs et al. 2021).

The quality of RNA is one of the most critical components for successful citrus pathogen detection using RT-qPCR (Glasel, 1995; Manchester, 1996). RNA quality is determined by purity, concentration and integrity. Reliable RNA extraction methods remove PCR inhibitors such as polyphenols and polysaccharides, which are found in various woody and perennial plants including citrus (Newbury and Possingham 1977; Porebski et al. 1997; Gasic et al. 2004; Gambino et al. 2008). Phenolic compounds can bind nucleic acids (Salzman et al., 1999) while polysaccharides can co-precipitate with

RNA, thus hindering absorbance readings from spectrophotometers and can inhibit enzymatic reactions (Wilkins and Smart, 1996). This results in the inhibition of polymerase activity during PCR amplification and compromises the accuracy of pathogen detection. Various techniques have been used to overcome these RNA extraction and purification limitations from woody plant tissues, including the addition of chemicals or detergents such as polyvinylpyrrolidone (PVP), 2-mercaptoethanol, and sodium dodecyl sulphate (SDS) or the serial dilutions of the sample prior of the PCR reaction set up (Sipahioglu et al., 2006; Schrader et al., 2012).

Different RNA extraction methods from citrus tissue have been successful for downstream detection of viruses and viroids with RT-qPCR. Traditional low throughput phenol-chloroform based methods with Cetrimonium bromide (CTAB) or TRIzol™ (Thermo Fisher Scientific, Waltham, MA) and silica column-based kits such as the Plant RNeasy Mini Kit (Qiagen, Valencia, CA) or Spectrum Plant RNA (Sigma-Aldrich, St. Louis, MO) have been effectively utilized on citrus tissues (Li et al. 2008; Saponari et al. 2008; Damaj et al. 2009; Wang et al. 2013). Semi-automated high-throughput total RNA isolation systems such as the MagMAX™ Express-96 (Thermo Fisher Scientific), BioSprint 96 (Qiagen), and QIAxtractor® (Qiagen), have the capability of purifying RNA up to 96 samples at once. These high-throughput methods have been utilized for various plants such as ornamentals, weed plants, and grapevines. Direct comparisons between semi-automated systems and silica column-based extraction methods for PCR diagnostics have been previously reported for grapevine and lily but not for citrus (Osman et al., 2012; Sun et al., 2014).

The assessment of quality RNA is typically described by the concentration, purity and integrity (Manchester 1996; Teare et al. 1997; Imbeaud et al. 2005; Becker et al. 2010). UV measurements for concentration is important, if concentrations are too low, not enough pathogen representation of pathogen or if concentration too high, could inhibit the reaction; these can lead to false negative results. This can be achieved because RNA absorbs max at 260nm (Manchester 1996). For a given RNA extract, the ratio of 260nm and 280nm can provide insight into the purity of the sample beacuase proteins measure strongest at 280nm (Teare et al. 1997). Ratios above 1.8 would indicate a pure sample where lower values indicate contaminants such as protein (Teare et al. 1997; Imbeaud et al. 2005). Integrity commonly measured by the 2100 bioanalyzer algorithm that calculates RNA integrity number (RIN), the method is reliable but can become expensive if you need to check many samples. Alternative way to check integrity is by testing for housekeeping genes and their expression levels via RT-qPCR (Imbeaud et al. 2005).

In this study, we compared three different RNA extractions methods for citrus tissues: MagMAX-96 Viral RNA Isolation Kit (MM-96), Qiagen Plant RNeasy Mini Kit, and TRIzol™ reagent to determine which method can extract quality RNA that be reliably used for downstream RT-PCR and RT-qPCR based detection of citrus viruses and viroids. In addition, we present data from the implementation of the selected RNA extraction and purification method (MM-96) used to process over 15,000 citrus samples for regulatory testing from budwood tree sources, orchards, and nurseries in California.

MATERIALS AND METHODS

Plant material and sample collection for RNA extraction comparison and pathogen testing

Healthy (n= 10) and infected (n= 33) (virus and viroid) citrus plant materials for RNA extraction comparisons were maintained *in planta* under screenhouse or greenhouse conditions at the Citrus Clonal Protection Program (CCPP) Lindcove Foundation Facility at the UC-ANR Lindcove Research and Extension Center (LREC) and the Rubidoux Quarantine Facility at the University of California, Riverside, respectively. Citrus pathogens targeted in this study included citrus tristeza virus (CTV), citrus psorosis virus (CPsV), citrus leaf blotch virus (CLBV), citrus tatter leaf virus (CTLV), citrus vein enation virus (CVEV), citrus bent leaf viroid (CBLVd), citrus dwarfing viroid (CDVd), citrus viroid-V (CVd-V), CVd-VI, citrus exocortis viroid (CEVd), hop stunt viroid (HSVd), and citrus bark cracking viroid (CBCVd) (**Table 1.1**). Stem samples (i.e., shoots with removed leaves and thorns) were collected from the last mature vegetative flush (approximately 12 to 18 months old) and around the tree canopy to account for any unequal distribution of the viruses or viroids in the plant. Between sampling of each tree, the pruners were sanitized with 10% household bleach solution (0.5% sodium hypochlorite) and dried with a paper towel to avoid cross contaminations. Stem samples were packaged into a resealable bag, placed on an ice chest, transported to the CCPP, and immediately stored in 4°C until further processing within 10-14 days from collection.

Citrus samples for regulatory pathogen testing were collected by the California Department of Agriculture (CDFA) from propagative sources of various nurseries

throughout California. Stem samples were collected around the entire canopy of the tree as described above and shipped overnight in an ice chest to the CCPP. The stem samples were immediately stored in 4°C until further processing within 10-14 days from collection.

Sample handling and preparation

For all stem samples, the phloem rich bark tissue was peeled using a disposable single edge razor blade. The peeled bark tissue was finely chopped into small pieces (4 to 5 mm) on small disposable chipboards, and 250 mg of small bark tissue pieces were placed into a 2 mL safe-lock tube (Eppendorf, Hamburg, Germany). Between each sample, the chipboards were disposed and the bench working area was sanitized with 10% household bleach followed by application of 70% ethanol to remove any residual sodium hypochlorite. Three tubes for each sample were prepared, one for each of the different RNA extraction methods tested, and one tube was prepared for samples used for regulatory pathogen testing.

All sample tubes were barcoded, kept in ice during processing, sanitized externally by dipping in a series of 10% household bleach and water baths and placed in a -80°C freezer for at least two hours prior to lyophilization for 24 to 26 hours in a FreeZone® Triad™ 74000 freeze-dryer (Labconco®, Kansas City, MO). After lyophilization, a single sterile 4-mm stainless steel grinding ball was added into each sample tube and stored at -80°C until tissue pulverization and RNA extraction.

Tissue pulverization and RNA extraction

Sample tubes were placed into stainless steel Cryo-Blocks (SPEX SamplePrep, Metuchen, NJ) and chilled with liquid nitrogen using the Cryo-Station (SPEX SamplePrep) for 20 minutes. The samples were ground into fine powder using a Geno/Grinder® 2010 (SPEX SamplePrep) at 1680 rpm for 20 seconds, twice.

The pulverized and homogenized citrus tissue samples were treated with three different extraction methods: MagMAX™ Viral RNA Isolation protocol, TRIzol™ according to the manufacturer's recommended protocol, and Qiagen RNeasy Plant Mini Kit. Reagents were scaled proportionally to the increased volume of starting citrus tissues in agreement with the manufacturer's protocols for the three RNA extraction methods.

Extraction #1, with modified MagMax™ 96 Viral RNA Isolation Kit (MM-96)

The MagMAX™ Express-96 Deep Well Magnetic Particle Processor (Thermo Fisher Scientific, Waltham, MA) instrument utilizing the MagMAX™ 96 Viral RNA Isolation Kit (MM-96 kit) was used to purify RNA. The standard kit procedures were adjusted and optimized for the extraction of total RNA from citrus tissues. Upon tissue pulverization, 750 µl of 4 M guanidine lysis buffer (4 M guanidine thiocyanate, 0.2 M sodium acetate pH 5.0, 2 mM EDTA, 2.5% (w/v) PVP-40 at pH 5.0) were added to each sample. Samples were homogenized using the Geno/Grinder® 2010 at 1680 rpm for 20 seconds, twice. The crude homogenized extracts were incubated at 4°C for 15 min and centrifuged at 4°C for 45 min at 17,200 x g. RNA was isolated using the default MagMAX™ protocol recommended by the manufacturer "AM1836_DW_50_V2". Two mL deep well plates were used for the MagMAX™ Express-96 and were prepared as

follows; lysate plate (position 1) which consisted of 139 µl of Lysis/Binding Solution Concentrate (premixed with 40 mL of isopropanol), 22 µl of Bead Mix (10 µl of RNA Binding Beads, 10 µl of Lysis/Binding Enhancer and 2 µl of Carrier RNA), 139 µl of isopropanol, and 150 µl of the processed supernatant; first set of wash plates that consisted of 500 µl of MagMAX™ Wash Solution 1 (position 2-3); a second set of wash plates that consisted of 500 µl of MagMAX™ Wash Solution 2 (positions 4–5); the elution plate (position 6) contained of 100 µl of elution buffer; and the tip comb plate loaded with the MagMAX™ Express-96 Deep Well Tip Comb (position 7). At the end of the MagMAX run, the elution plate was placed on a magnetic rack for 5 mins to collect any residual beads. The obtained purified RNA was transferred to individual 1.5 µl microcentrifuge tubes and stored in the -80°C freezer.

Extraction #2, with TRIzol™ reagent

The pulverized tissue was treated with TRIzol™ using the manufacturer's recommended protocol adjusted and optimized for citrus tissues. The protocol was as follows; 2.5 mL of TRIzol™ reagent was added to each sample. Samples were homogenized with a vortex for 20 seconds, centrifuged at 4°C for 5 minutes at 12,000 x g and the supernatant was then transferred to a new 5 mL Eppendorf tube. Five hundred µL (500 µL) of chloroform were added and the samples were incubated at room temperature for 3 minutes. Samples were centrifuged for 15 minutes at 12,000 x g at 4°C. The aqueous phase was transferred to a new 1.5 mL microcentrifuge tube and 1.25 mL of isopropanol were added to each sample. Samples were then incubated at room temperature for 10 minutes and subsequently centrifuged at 4°C for 10 minutes at 12,000

x g. The supernatant was discarded, and 2.5 mL of 75% ethanol were added. The samples were vortexed briefly and centrifuged at 4°C for 5 minutes at 7,500 x g. Ethanol was discarded and the pellet was left to air dry for 30 minutes to 1 hour. The RNA pellet was resuspended in 100 µL of UltraPure™ DNase/RNase-free distilled water (Thermo Fisher Scientific, Waltham, MA) and stored at -80°C.

Extraction #3, with Qiagen RNeasy® Plant Mini Kit (Qiagen)

The pulverized tissue was treated with the Qiagen RNeasy® Plant Mini Kit following the manufacturer's protocol adjusted and optimized for citrus tissues. The protocol was as follows, 1125 µL of RLT buffer and 11.25 µL of β-mercaptoethanol were added to each sample and subsequently vortexed. The lysate was transferred to a QIAshredder spin column and centrifuged at room temperature for 2 minutes at 17,200 x g. The flow-through was transferred to a clean 2.0 mL collection tube and 562.5 µL of 200 proof ethanol were added and mixed by pipetting. Six hundred fifty µL of the sample were transferred to the RNeasy Mini spin column and centrifuged for 15 seconds at 8,000 x g; this step was repeated until the remaining sample was used up. The RNeasy spin column was washed with 700 µL RW1 Buffer and centrifuged for 15 seconds at 8,000 x g at room temperature. A second wash with 500 µL of RPE was added to the column and centrifuged for 15 seconds 8,000 x g, twice. The column was centrifuged for 1 minute at 12,000 x g at room temperature to remove the excess wash buffer. The column was transferred to a clean 1.5 mL standard microcentrifuge tube and 100 µL of UltraPure™ DNase/RNase-free distilled water were added to each sample and incubated at room

temperature for 2 minutes. The samples were centrifuged for 1 minute at 8,000 x g at room temperature and the eluted RNA was stored at -80°C.

RNA quality assessment and PCR citrus pathogen testing

For all RNA samples, the concentration and purity (ratio of A_{260} and A_{280}) of RNA was assessed using the Infinite M1000 Pro plate reader (Tecan, Männedorf, Switzerland). The integrity of RNA was assessed by performing RT-qPCR targeting the citrus gene NAD dehydrogenase (nad5) (**Table 1.1**). For the RNA extraction method comparisons, RT-PCR and RT-qPCR were performed for the detection of five citrus viruses (CTV, CPsV, CLBV, CVEV, and CTLV) and seven citrus viroids as previously described (**Table 1.1**). For the regulatory testing, multiplex RT-qPCR (Taqman®) was performed for the detection of three citrus viruses (CTV, CPsV and CLBV) (Osman et al. 2015) and universal RT-qPCR (SYBR™ Green) was performed for the detection of seven citrus viroids as previously described (**Table 1.1**).

All RT-PCRs detection was performed with the ProFlex PCR System (Thermo Fisher Scientific, Waltham, MA). PCR products were analyzed using electrophoresis on a 1.5% TAE agarose gel; stained with ethidium bromide and visualized with the ChemiDoc™ Imaging System (Bio-Rad, Hercules, CA). Multiplex RT-qPCRs were carried out using the QuantStudio 12K Flex System (Thermo Fisher Scientific, Waltham, MA) and universal RT-qPCRs using the CFX96 Touch Real-Time PCR Detection System (Bio-Rad, Hercules, CA). All reactions were repeated at least twice for each sample. All reactions were performed with the appropriate positive, negative, and non-template controls.

Regulatory testing of California citrus nursery samples

All samples for regulatory testing were processed and extracted with the MagMAX™ 96 protocol as described above. Multiplex Taqman® RT-qPCR was performed for the detection of CTV, CPsV and CLBV and SYBR™ Green RT-qPCR for the universal detection of citrus viroids as previously described (**Table 1.1**) and approved by the CDFA according to the "QC 1388, Permit for PCR Protocol for Virus Testing in Citrus Nursery Stock Pest Cleanliness Program" and "QC 1354, Permit For PCR Protocol For Viroid Testing In Citrus Nursery Stock Pest Cleanliness Program".

Software and analysis

RT-qPCR data were collected and analyzed with the QuantStudio Flex software version 1.3 and Bio-Rad CFX Manager version 3.1. Statistics using Dunn's test of multiple comparisons (Dunn's test, $p < 0.05$) and figures were generated using Prism version 9.1.1.

RESULTS

Assessment of RNA quality, concentration, purity, and integrity, extracted from citrus tissues using three different methods

The concentration and purity of RNA obtained from the different extraction methods tested were assessed to determine the suitability of each of the methods for downstream RT-PCR and RT-qPCR use. MM-96 yielded the most uniform concentration of RNA among the samples with a mean concentration of 57.74 ± 15.93 ng/µL (median = 54.4) (n= 43) (**Figure 1.1**) and absorbance $A_{260/280}$ with a mean of 2.30 ± 0.12 (median = 2.30) and a range of 2.05 to 2.55 (**Figure 1.2**). Qiagen and TRIzol™ extracted RNA

yielded a mean concentration of 147.83 ± 72.69 ng/µL (median = 142), $A_{260/280}$ mean 2.20 ± 0.08 (median = 2.21) and a range of 2.01 to 2.36 and 473.59 ± 132.44 ng/µL (median = 466.16), absorbance $A_{260/280}$ mean 1.97 ± 0.09 (median = 1.95) and range of 1.71 to 2.17, respectively (**Figures 1.1 & 1.2**). The RNA concentrations obtained from Qiagen and TRIzol™ were higher and more variable as reflected by the significant differences between the mean and median values compared to the MM-96. All three extraction methods showed statistical significant differences ($p < 0.05$) in concentration and $A_{260/280}$ (**Figures 1.1 & 1.2**). The mean and median values for the $A_{260/280}$ ratios for all extraction methods were similar indicating less variability within the extraction methods.

To determine the integrity of extracted RNA, RT-qPCR was performed on the citrus housekeeping gene NADH dehydrogenase subunit 5 (nad5). The Cq values from MM-96-extracted RNA were the highest and most consistent (mean = 21.30 ± 0.89; median = 21.12) compared to the Qiagen (mean = 18.97 ± 1.69; median = 18.39) and TRIzol™ (mean = 18.18 ± 1.46; median = 17.80) extracted RNA (**Figure 1.3**). The nad5 Cq values showed significant differences between MM-96 vs TRIzol™ and MM-96 vs Qiagen extraction methods ($p < 0.05$), however there was no significant difference between TRIzol™ vs Qiagen ($p > 0.05$). The mean and median nad5 values for all extraction methods were close together indicating minimal variability in the Cq values.

RT-PCR and RT-qPCR citrus pathogen detection results for different RNA extraction methods

RT-PCRs and RT-qPCRs were performed for the detection of citrus viruses and viroids on RNA obtained from the three different extraction methods. All targeted citrus

pathogens were detected in singleplex, multiplex and universal PCR reactions regardless of the RNA extraction method used. However, the TRIzol™ extracted RNA was highly concentrated inhibiting the PCR reactions and required a serial dilution between 1:10 or 1:100 to detect the targeted citrus pathogen (**Tables 1.2A-G**).

Citrus pathogens were identified in mixed infections in 14 samples and the obtained results were consistent among all three extraction methods compared in this study (**Tables 1.2A-G**). Samples that tested positive for citrus viroids with SYBR™ Green RT-qPCR were further analyzed with RT-PCR to identify the specific viroid species. RNA extracts of all three compared methods provided accurate detection of individual citrus viroid RNA species. Citrus dwarfing viroid was detected in most of the samples (5/16), followed by hop stunt viroid (4/16) and citrus bent leaf viroid (3/16). Citrus exocortis viroid, citrus viroid I-LSS, citrus bent leaf viroid, and citrus viroid V were detected in one of the tested samples (**Tables 1.2D & 1.2E**).

Healthy control samples from different citrus varieties were tested in the study. No pathogens were detected in any of the control samples for the different extraction methods (**Table 1.3**).

Evaluation of semiautomated high throughput MM-96 extraction on California citrus nursery and orchard samples

Based on the comparison of the three RNA extraction methods all methods were suitable for citrus tissues, however, MM-96 was the most suitable protocol for large scale RNA extraction because of the uniformity and consistency based on the concentrations, purity, and integrity. In addition, the high throughput and automated capabilities of the

MM-96 RNA extraction made it ideal for the rapid testing of over 15,000 citrus samples from budwood sources, orchards, and nurseries in California.

The extracted RNA concentration of 6,461 samples ranged from 8.16 to 256.96 ng/µl with a mean of 67.97 ± 33.13 ng/µL (**Figure 1.4**). In addition, the majority of the samples (84.2%) had concentrations ≥100 ng/µl. The purity of the extracted RNA was high with the majority of the $A_{260/280}$ ratios ranging from 1.8 to 2.5 (**Figure 1.5**), which was close to the desirable 2.0 indicating low protein contaminants (Manchester, 1996). The mean 260/280 ratio was 2.22 ± 0.28 (n= 6,461) (**Figure 1.5**). A subset (n= 255) of RNA extracts were analyzed for RNA integrity by RT-qPCR targeting the nad5 citrus gene. The mean Cq value from the RT-qPCRs was 19.39 ± 1.54, n= 255 with minimum and maximum values of 15.4 and 25.43, respectively (**Figure 1.6**).

RT-qPCR results of high throughput California citrus nursery stock virus and viroid testing program

From 2004-05 to 2009-10 viroid testing was limited to greenhouse biological indexing experiments that averaged 455 samples per year. Because of the low diagnostic throughput, infection rates hovered at an average of 5.67% (**Figure 1.7**). The implementation of the high-throughput MM-96 RNA extraction method and RT-qPCR testing for citrus viruses and viroids, allowed for a high number of samples to be tested per year. For citrus viroid testing, the MM-96 was used for an average of 1,665 samples per year from 2010-11 to 2019-20 (**Figure 1.7**). The initial year of the high throughput testing saw the highest rate of infection at 7.81%. The infection progressively decreased from year to year and by 2013-14, the infection dropped to 2.22% (**Figure 1.7**). From

2014-15 to 2019-20 the viroid infection rate dropped and remained below 1% (**Figure 1.7**).

From 2004-05 to 2011-12, the primary detection methods for virus detection were enzyme-linked immunosorbent assay (ELISA) for CTV and biological indexing using Dweet tangor (*Citrus reticulata* Blanco) for CPsV. With the ELISA method, it was able to process an average of 3,491 and biological indexing 640 samples per year. Through the 2004-05 to 2011-12 testing period, citrus virus infection rates maintained below 0.5% **(Figure 1.8)**. In 2011-12, only biological indexing testing data was for CPsV and no testing data was found for CTV ELISA. In addition, no virus testing was performed in 2012-13 **(Figure 1.8)**. Molecular testing for citrus viruses was implemented in 2014-15 along with the high throughput MM-96 RNA extraction. The RT-qPCR allowed for the simultaneous detection of 3 citrus viruses in one reaction (CTV, CPsV, and CLBV). Since the implementation of the method, an average of 2,111 samples were tested per year. The initial virus infection was 0.05% and then spiked to 1% in 2015-16. From 2017-19 to 2019-20 the infection dipped and remained below 0.5%. **(Figure 1.8).**

DISCUSSION

The California citrus industry has tripled in size in the last 20 years and is valued at $3.4 billion dollars with an estimated economic impact of $7.1 billion (Babcock 2018). With the spread of deadly Huanglongbing and other diverse citrus pathogens that can devastate the citrus industry, it is imperative to have reliable citrus diagnostic tools for the maintenance of pathogen free citrus propagative materials (Gottwald 2010; da Graça et al. 2016). The application and adoption of PCR based assays in diagnostics has played

an critical role in disease management programs monitoring the sanitary status of germplasm and propagative materials, nursery stock and certification, and commercial plantings of citrus and other agriculturally significant crops (Bostock et al. 2014; Gergerich et al. 2015; Osman et al. 2015; Fuchs et al. 2021).

To obtain reliable diagnostic results, high quality input RNA for PCR based testing is required (Imbeaud et al. 2005). There are many commercially developed RNA extraction kits in the market, however RNA extraction from woody plant tissues is not necessarily a "one size fits all" and requires optimization and testing to ensure the method works properly. In many cases, PCR based diagnostic protocols are primarily focused on primer and probe designs, conditions of reaction (Bustin et al. 2009), but the importance of the quality of nucleic acids can be overlooked. The common computer science colloquially: "garbage in, garbage out" indicates that "the quality of the input determines the output" (Kilkenny and Robinson 2018). This concept can also be applied to describe PCR based methods in which the PCR results are only as good as the quality of the RNA obtained from the extraction. The quality of extracted RNA is well defined and is based on the concentration, purity, and integrity. Poor or unoptimized nucleic acid extractions can yield low quality RNA or leave behind inhibitors such as polysaccharides and proteins which can compromise the detection and quantification of PCR amplified products (Newbury and Possingham 1977; Porebski et al. 1997; Gasic et al. 2004; Imbeaud et al. 2005; Gambino et al. 2008).

Comparisons of different RNA extraction methods for citrus tissues had been previously reported for various applications (Changjie et al. 2004; Damaj et al. 2009),

however the results need to be validated to ensure the methods are compatible with stem tissues. In this study, three different RNA extraction methods (magnetic beads, silica column-based kits, and traditional phenol chloroform RNA extraction) were evaluated to determine which method can be used on phloem rich citrus stems tissues and reliably produce high quality RNA for downstream PCR based detection of citrus viruses and viroids. The quality of RNA extracts are typically evaluated by measuring concentration, purity, and integrity. Our analysis determined that all three extraction methods were capable of extracting quality RNA from citrus stem tissues for downstream PCR applications (**Figures 1.1 to 1.3**) and regardless of the extraction method, the citrus pathogens were detected by PCR from infected control samples (**Tables 1.2A to G)**.

In conjunction with our analysis, we evaluated the potential for automation and high throughput capacity of the different RNA extraction methods. Our experience with the different methods we found that TRIzol™ had restricted throughput capacity because of the limited number (12-20) of samples that can be reliably handled in one sitting. Qiagen has the potential to scale from the individual columns to the 96 well plate format to allow for high throughput extractions, however we found difficulties adjusting the extraction volumes when using more than 100mg of citrus tissues. MM-96 extraction was the preferred RNA extraction protocol because of the consistent results and versatile high throughput capabilities. The implementation of MM-96 for the CA nursery stock citrus virus and viroid testing program allowed the CCPP to process and test an average over 1500 samples per year for citrus viruses and viroids. The sustained high throughput

testing has caused citrus virus and viroid infection rates to decline and have been constantly hovering below 1% (**Figures 1.7 & 1.8**).

Our results indicated that all three methods produce a quality RNA from citrus tissues that can be successfully utilized for downstream applications such as RT-PCR and RT-qPCR for the detection and identification of a large range of citrus virus and viroids. Qiagen and TRIzol™ are capable of handling citrus tissues, MM-96 uniquely stands out because of its high-throughput extraction capabilities without jeopardizing the quality of the RNA for citrus nursery testing. Our current MM-96 protocol has been streamlined that laboratory technicians and undergraduate laboratory assistance are able to perform large scale RNA extractions without the need of high-level scientists, hence significantly reducing labor cost. In addition, the MM-96 technology can be further incorporated with semi or fully automated pipette machines and automated qPCR plate feeders (12K) that can further speed up time to obtain results and reduce potential human errors. In addition, previously studies have demonstrated that the MM-96 based extraction for DNA on citrus tissues types (stems, leaves, and roots) have been suitable for HTS based microbiome studies (Ginnan et al. 2018; Ginnan et al. 2020; Pagliaccia et al. 2020), further supporting the MM-96 platform's versatility. Ultimately, the nucleic acid extraction method of choice will depend on many factors such as the total number of extractions, available resources and infrastructure for equipment, and time.

Pathogen	Reference	Table in this paper	# of samples
RT-qPCR Taqman®			
Citrus tristeza virus (CTV)	Osman et al. 2015	Table 2a	7
Citrus psorosis virus (CPsV)	Osman et al. 2015	Table 2b	3
Citrus leaf blotch virus (CLBV)	Osman et al. 2015	Table 2c	3
Citrus bent leaf viroid (CBLVd)	Osman et al 2017	Table 2e	1
Hop stunt viroid (HSVd)	Osman et al 2017	Table 2e	5
Citrus exocortis viroid (CEVd)	Osman et al 2017	Table 2e	1
RT-qPCR SYBR® Green			
Citrus bent leaf viroid, Citrus dwarfing viroid, Citrus viroid V, CVd VI, CVd VII	Vidalakis and Wang 2013	Table 2d	9
Citrus exocortis viroid, Hop stunt viroid, Citrus bark cracking viroid	Vidalakis and Wang 2013	Table 2e	7
Internal control NADH dehydrogenase (nad5)	Saponari et al. 2008		
RT-PCR			
Citrus vein enation virus (CVEV)	Vives et al. 2013	Table 2f	9
Citrus tatter leaf virus (CTLV)	Roy et al. 2005	Table 2g	5
Citrus leaf bent viroid (CLBVd)	Wang et al. 2013	Table 2d	4
Citrus dwarfing viroid (CDVd)	Wang et al. 2013	Table 2d	4
Citrus viroid V (CVd-V)	Wang et al. 2013	Table 2d	2
Citrus viroid VI (CVd-VI)	Wang et al. 2013	Table 2d	

Table 1.1 List of PCR primers used for the detection of citrus pathogens and characterization of specific citrus viroids used in this study

Table 1.2A Cq values for *Citrus tristeza virus* (CTV) with MagMAX-96, Qiagen, and TRIzol® extractions.

Tree ID	Experiment Number	MagMAX-96	TRIzol®*	Qiagen	Infection	
					Single (S) or Mix (M)	Other pathogens
SY558	2987-56	24.50 ± 1.97	22.58 ± 0.14	24.30 ± 2.34	S	
SY568	2247-15	22.79 ± 4.90	24.10 ± 0.36	25.50 ± 4.50	S	
T517	3347-57	27.87 ± 4.40	33.46 ± 0.66	30.87 ± 5.64	S	
T525	3347-63	27.00 ± 6.51	31.25 ± 1.19	29.43 ± 5.88	S	
TL113	3291-10	27.59 ± 0.25	23.21 ± 0.8	28.53 ± 0.9	M	Apsca, CTLV
TL114	3291-11	25.38 ± 3.92	29.39 ± 0.5	24.15 ± 0.23	M	Apsca,HSVd, CTLV

* The TRIzol® extracted RNA was diluted to 1:10 or 1:100 for the reported Cq values.

Table 1.2B Cq values for *Citrus psorosis virus* (CPsV) with MagMAX-96, Qiagen, and TRIzol® extractions.

					Infection	
Tree ID	**Experiment Number**	**MagMAX-96**	**TRIzol®***	**Qiagen**	**Single (S) or Mix (M)**	**Other pathogens**
LB250		26.46 ± 2.26	26.88 ± 3.12	25.80 ± 1.9	S	
P215	3347-14	29.11 ± 2.51	25.11 ± 3.84	30.31 ± 1.08	M	CDVd
P250	3347-15	30.51 ± 5.24	32.55 ± 4.88	30.65 ± 2.80	S	

* The TRIzol® extracted RNA was diluted to 1:10 or 1:100 for the reported Cq values.

Table 1.2C Cq values for *Citrus leaf blotch virus* (CLBV) with MagMAX-96, Qiagen, and TRIzol® extractions.

					Infection	
Tree ID	**Experiment Number**	**MagMAX-96**	**TRIzol®***	**Qiagen**	**Single (S) or Mix (M)**	**Other pathogens**
DMV930	2351-1	21.91 ± 1.59	22.43 ± 4.86	20.95 ± 1.50	M	CDVd, HSVd
DMV931	2352-2	35.77 ± 0.69	29.72 ± 0.46	31.61 ± 0.62	S	
K-1	3069-2	24.88 ± 3.13	25.09 ± 0.36	22.49 ± 2.62	S	

* The TRIzol® extracted RNA was diluted to 1:10 or 1:100 for the reported Cq values.

Table 1.2D Cq values for samples Apsca viroids with MagMAX-96, Qiagen, and TRIzol® extractions.

					Infection		
Tree ID	**Experiment Number**	**MagMAX-96**	**Qiagen**	**TRIzol®***	**Viroid**	**Single (S) or Mix (M)**	**Other pathogens**
2765-2	2765-2	27.93 ± 2.19	26.02 ± 1.68	26.36 ± 2.45	CBLVd	S	
2765-12	2765-12	27.28 ± 0.4	26.56 ± 2.10	28.02 ± 1.70	CDVd	S	
3198-5	3198-5	31.22 ± 0.8	31.67 ± 1.10	32.26 ± 2.30	CVd V	M	
DMV930 CVd	2356-1	29.47 ± 0.15	25.59 ± 1.45	28.75 ± 1.52	CDVd CVd	M	CLBV, HSVd
ILSS	3237-3	29.45 ± 0.47	31.00 ± 0.12	28.74 ± 0.09	ILSS	S	
2765-11	2765-11	31.28 ± 0.81	30.79 ± 0.99	32.26 ± 2.3	CDVd	S	
IV402	2923-10	25.59 ± 1.35	25.67 ± 1.40	25.59 ± 1.35	CDVd	S	
P215	3347-14	28.50 ± 0.31	33.55 ± 0.43	33.51 ± 0.95	CDVd	M	CPsV
TL113	3291-10	26.36 ± 0.6	26.37 ± 0.6	25.12± 0.92	CBLVd	M	CTV, CTLV
TL114	3291-11	30.01 ± 1.13	27.02 ± 1.47	25.75 ± 2.98	CBLVd	M	CTV, CTLV, HSVd

* The TRIzol® extracted RNA was diluted to 1:10 or 1:100 for the reported Cq values.

Table 1.2E Cq values for Nonapsca viroids with MagMAX-96, Qiagen, and TRIzol® extractions.

					Infection		
Tree ID	**Experiment Number**	**MagMAX-96**	**Qiagen**	**TRIzol®***	**Viroid**	**Single (S) or Mix (M)**	**Other pathogens**
2765-1	2765-1	30.26 ± 0.95	26.64 ± 2.18	27.89 ± 0.69	CEVd	S	
2765-6	2765-6	27.5 ± 0.51	24.36 ± 0.82	24.21 ± 0.51	HSVd	S	
3200-1	3200-1	27.04 ± 1.81	24.42 ± 2.45	26.22 ± 0.89	CVd IV	S	
DMV930	2351-1	23.36 ± 0.15	21.13 ± 0.29	21.62 ± 1.02	HSVd	M	CLBV, Apsca
TL114	3291-11	22.61 ± 0.79	20.39 ± 0.68	22.08 ± 1.45	HSVd	M	CTV, Apsca, CTLV
VE701	2923-1	22.9 ± 1.19	21.09 ± 0.69	20.82 ± 0.29	HSVd	M	CVEV

* The TRIzol® extracted RNA was diluted to 1:10 or 1:100 for the reported Cq values.

Table 1.2F Results for *Citrus vein enation virus* (CVEV) with MagMAX-96, Qiagen, and TRIzol® extractions.

					Infection	
Tree ID	**Experiment Number**	**MagMAX-96**	**Qiagen**	**TRIzol®***	**Single (S) or Mix (M)**	**Other pathogens**
VE701	2923-1	(+)	(+)	(+)	M	HSVd
VE702	2923-2	(+)	(+)	(+)	S	
VE703	2923-3	(+)	(+)	(+)	S	
VE704	2923-4	(+)	(+)	(+)	S	
VE705	2923-5	(+)	(+)	(+)	S	
VE706	2833-1	(+)	(+)	(+)	S	
VE708	3273-13	(+)	(+)	(+)	S	
VE709	3354-5	(+)	(+)	(+)	S	
VE823	2923-6	(+)	(+)	(+)	S	

Table 1.2G Results for *Citrus tatter leaf virus* (CTLV) with MagMAX-96, Qiagen, and TRIzol® extractions.

					Infection	
Tree ID	**Experiment Number**	**MagMAX-96**	**Qiagen**	**TRIzol®**	**Single (S) or Mix (M)**	**Other pathogens**
TL100	1713-1	(+)	(+)	(+)	S	
TL101	3347-76	(+)	(+)	(+)	S	
TL110	3288-4	(+)	(+)	(+)	S	
TL113	3291-10	(+)	(+)	(+)	M	CTV, Apsca
TL114	3291-11	(+)	(+)	(+)	M	CTV, Apsca, HSVd

Table 1.2A to 1.2G- Comparison of RT-qPCR and RT-PCR results (Cq values and standard deviation) between the different extraction methods: MagMax-96, TRIzol™, and Qiagen. Known viral and viroid infected trees maintained under greenhouse conditions were used for the comparaison (n=32 for each RNA isolation method combination).

Variety		CTV	CPsV	CLBV	Apsca	NonApsca	CVEV	CTLV	NAD5
Persian Lime	*Citrus. latifolia* Tan.	(-)	(-)	(-)	(-)	(-)	(-)	(-)	(+)
Chandler Pummelo	*C.grandis* (L.) Osb.	(-)	(-)	(-)	(-)	(-)	(-)	(-)	(+)
Eureka Lemon	*C. limon* (L.) Burn.f.	(-)	(-)	(-)	(-)	(-)	(-)	(-)	(+)
Page Mandarin	*C. reticulata* Blanco	(-)	(-)	(-)	(-)	(-)	(-)	(-)	(+)
Cara Cara Navel	*C. sinesis* (L.) Osbeck	(-)	(-)	(-)	(-)	(-)	(-)	(-)	(+)
Campbell Nuclear Valencia	*C. sinesis* (L.) Osbeck	(-)	(-)	(-)	(-)	(-)	(-)	(-)	(+)
Nagami Kumquat	*Fortunella margarita* (Lour.) Swing.	(-)	(-)	(-)	(-)	(-)	(-)	(-)	(+)
Red Blush Grapefruit	*C. paradisi* Macf.	(-)	(-)	(-)	(-)	(-)	(-)	(-)	(+)
Carrizo Citrange	*C. trifoliata x C. sinensis*	(-)	(-)	(-)	(-)	(-)	(-)	(-)	(+)
Rich 16-6 Trifolate	*C. trifoliata* (L.) Raf.	(-)	(-)	(-)	(-)	(-)	(-)	(-)	(+)

Table 1.3 Healthy control samples from different citrus varieties used in this study. No pathogens were detected, while nad5 was present in all healthy control samples between the different extraction methods (MagMax-96, TRIzol™, and Qiagen) (n=10).

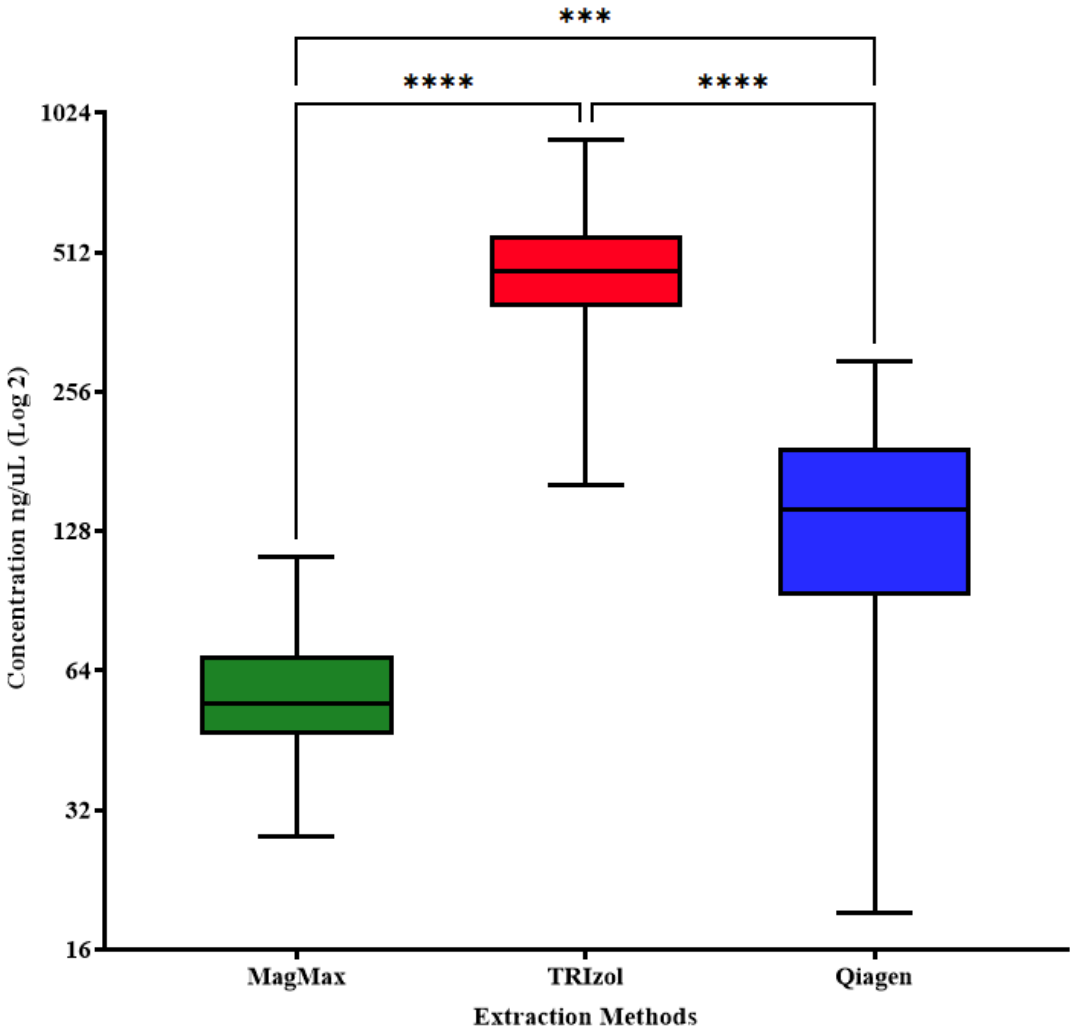

Figure 1.1- Comparison of concentrations (ng/uL) between the different RNA extractions methods: MagMax, TRIzol™, and Qiagen (n=43). Error bars represent the minimum and maximum values. Asterisks (*) indicate statistically significant differences based on Dunn's test of multiple comparisons ($p < 0.05$). Data has been transformed to Log 2.

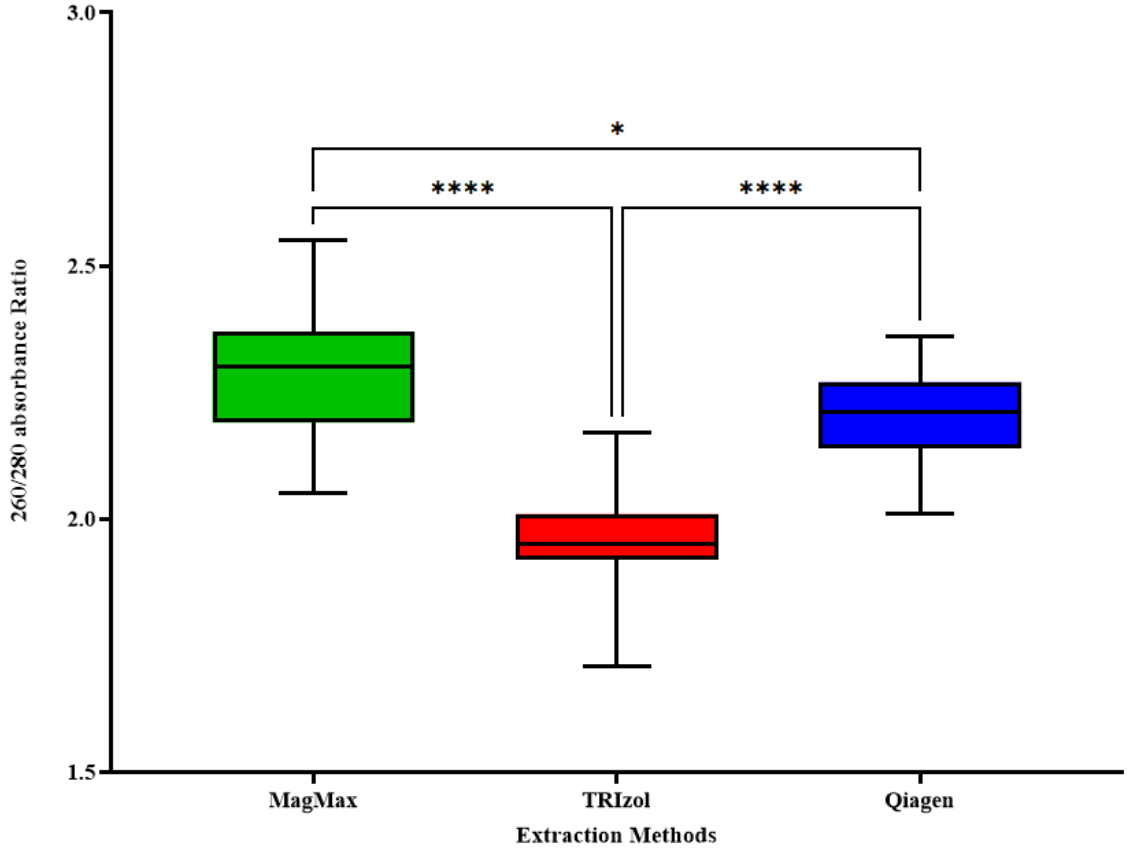

Figure 1.2 Comparison of A260/280 ratios among the different RNA extractions methods: MagMax-96, TRIzol™, and Qiagen (n=43). Error bars represent the minimum and maximum values. Asterisks (*) indicate statistically significant differences based on Dunn's test of multiple comparisons ($p < 0.05$).

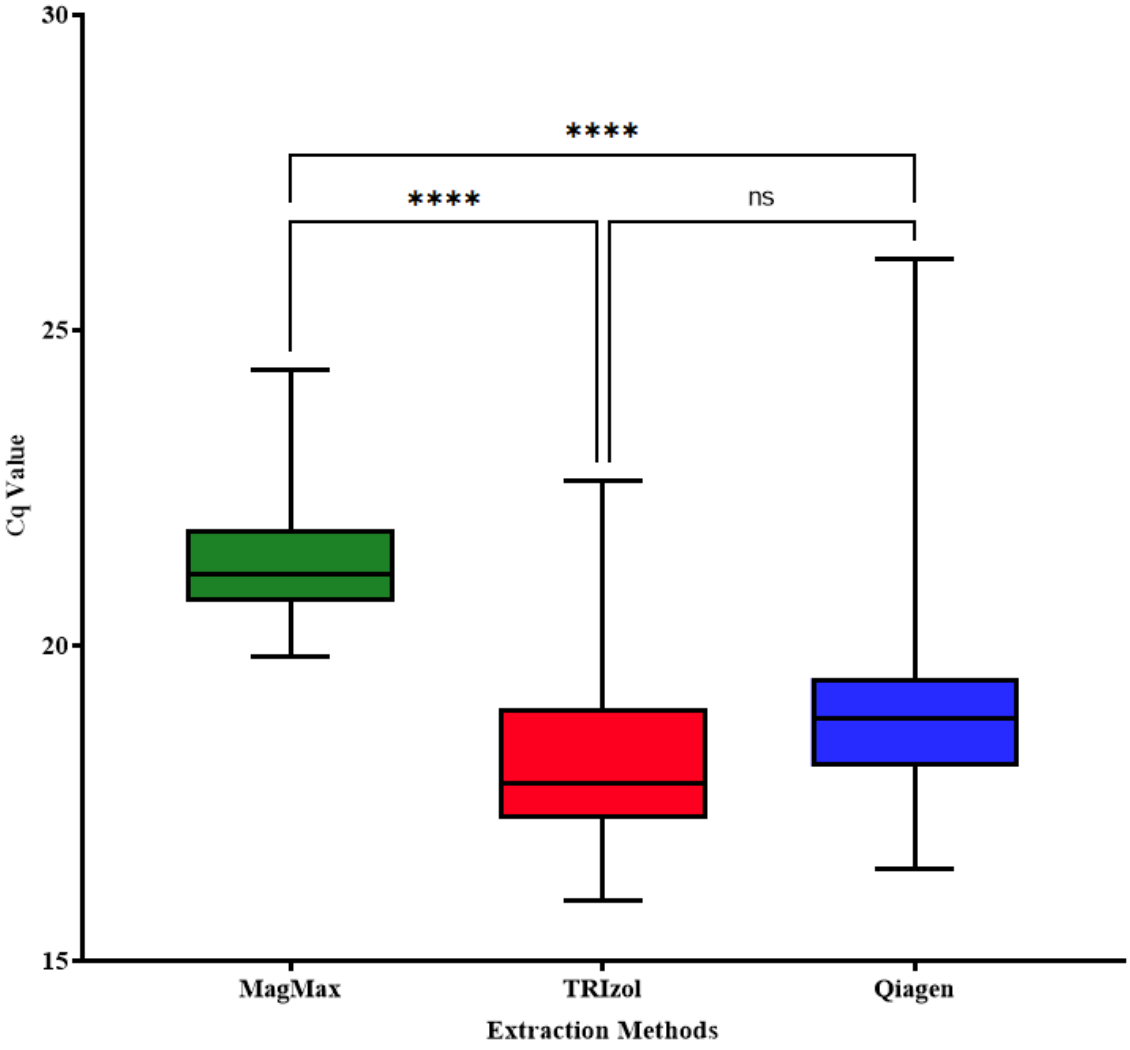

Figure 1.3 Comparison of RNA integrity evaluation using a RT-qPCR assay targeting the NAD dehydrogenase (nad5) citrus housekeeping gene between the different extraction methods: MagMax-96, TRIzol™, and Qiagen (n=43). Error bars represent the minimum and maximum values. Asterisks (*) indicate statistically significant differences based on Dunn's test of multiple comparisons ($p < 0.05$).

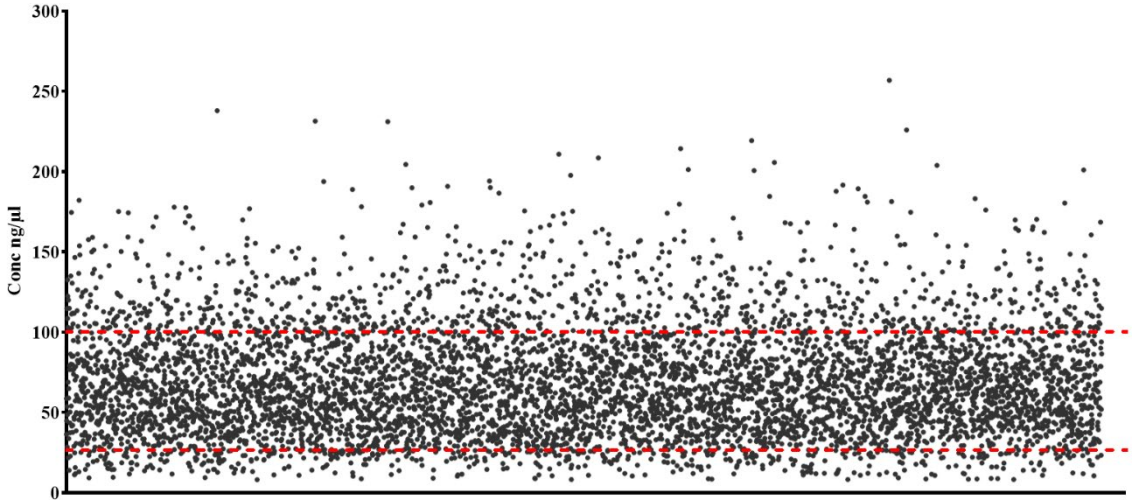

Figure 1.4- Evaluation of MagMax-96 RNA concentration on California nursery stock citrus samples required for virus and viroid pathogen testing (n= 6,461). Measurements were performed using a spectrophotometer.

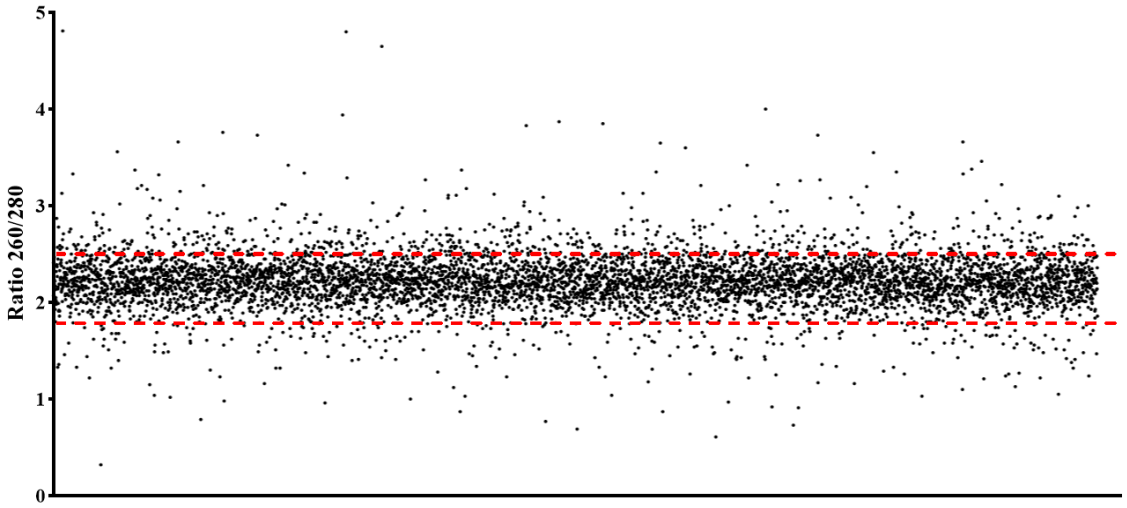

Figure 1.5- Evaluation of MagMax-96 RNA purity (260/280) on California nursery stock citrus samples required for virus and viroid pathogen testing (n= 6,461). Measurements were performed using a spectrophotometer.

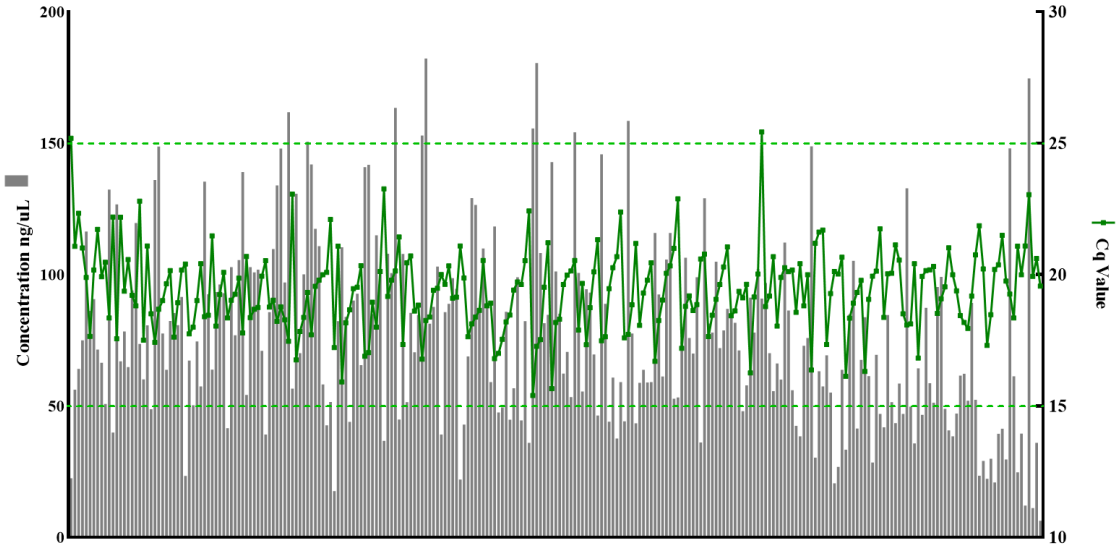

Figure 1.6- Evaluation of MagMax-96 RNA integrity on California citrus nursery stock citrus samples required for virus and viroid pathogen testing. Samples were analyzed by RT-qPCR reactions targeting the mRNA of NADH dehydrogenase citrus gene (n= 255).

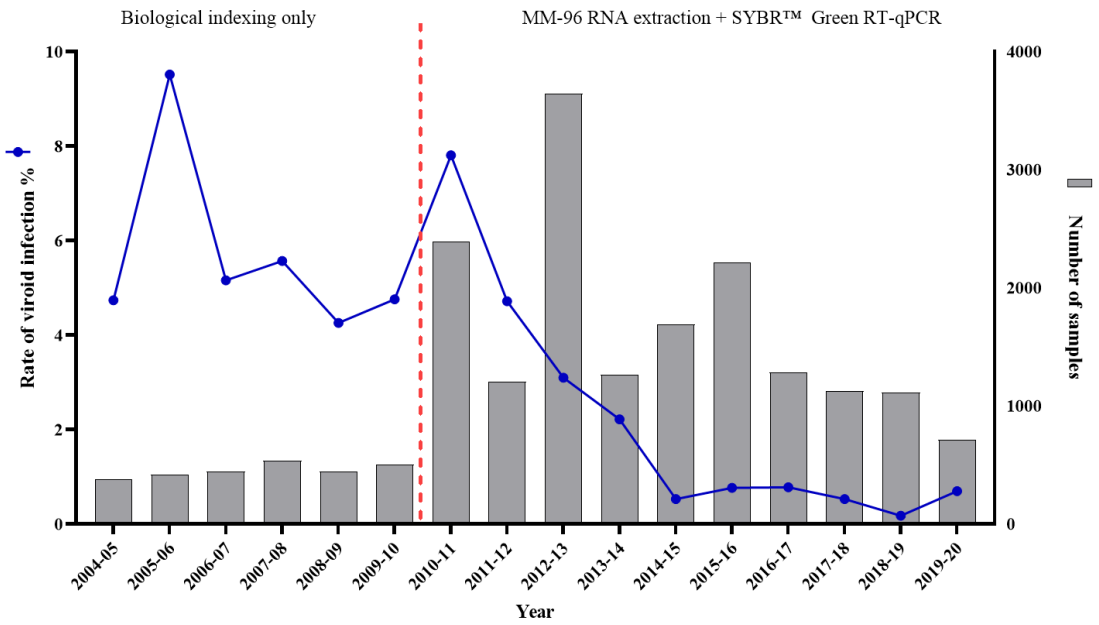

Figure 1.7- Citrus viroid infection rate and number of samples tested from 2004-05 to 2019-20. From 2004-05 to 2009-10 (n= 2,735) viroid testing was limited to greenhouse biological indexing experiments using Arizona 861-S-1 citrons (*Citrus medica* L.) indicator plants. In 2010-11, high throughput MM-96 RNA extraction and the SYBR™ Green RT-qPCR testing for citrus viroids was implemented. From 2010-11 to 2019-20, a total of 19,391 were tested using the high throughput workflow.

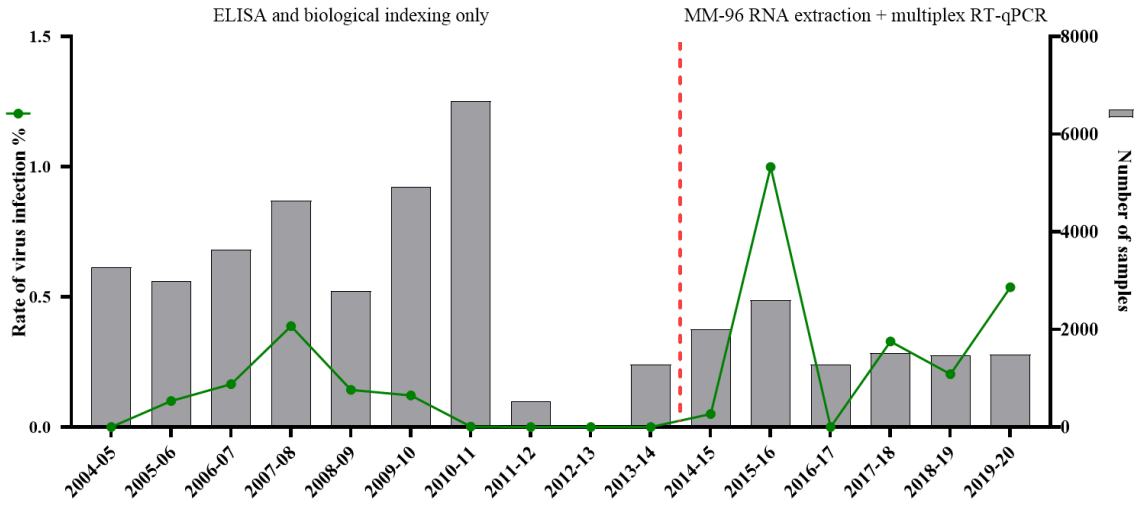

Figure 1.8- Citrus virus infection rate and number of samples tested from 2004-05 to 2019-20. From 2004-05 to 2011-12 (n=30,734), the primary detection methods for citrus tristeza virus (CTV) was enzyme-linked immunosorbent assay (ELISA) and citrus psorosis virus (CPsV) was biological indexing using Dweet tangor (*Citrus reticulata* Blanco). Since 2014-15 (n= 10,375), high throughput MM-96 RNA extraction and multiplex RT-qPCR for CTV, CPsV and citrus leaf blotch virus (CLBV) has been implemented. In 2011-12, only biological indexing testing data was performed for CPsV and no testing data was found for CTV with ELISA. In addition, no virus testing was performed in 2012-13.

REFERENCES

1. Bar-Joseph, M., Garnsey, S. M., Gonsalves, D., Moscovitz, M., Purcifull, D. E., Clark, M. F., et al. (1979). The use of enzyme-linked immunosorbent assay for detection of citrus tristeza virus. *Phytopathology* 69, 190–194.

2. Bertolini, E., Moreno, A., Capote, N., Olmos, A., de Luis, A., Vidal, E., et al. (2008). Quantitative detection of Citrus tristeza virus in plant tissues and single aphids by real-time RT-PCR. *Eur. J. Plant Pathol.* 120, 177–188.

3. Bostock, R. M., Thomas, C. S., Hoenisch, R. W., Golino, D. A., and Vidalakis, G. (2014). Plant health: How diagnostic networks and interagency partnerships protect plant systems from pests and pathogens. *Calif. Agric.* 68, 117–124.

4. Bustin, S. A., Benes, V., Garson, J. A., Hellemans, J., Huggett, J., Kubista, M., et al. (2009). The MIQE guidelines: minimum information for publication of quantitative real-time PCR experiments. *Clin. Chem.* 55, 611–622.

5. de Noronha Fonseca, M. E., Marcellino, L. H., and Gander, E. (1996). A rapid and sensitive dot-blot hybridization assay for the detection of citrus exocortis viroid in Citrus medica with digoxigenin-labelled RNA probes. *J. Virol. Methods* 57, 203–207.

6. Gambino, G., Perrone, I., and Gribaudo, I. (2008). A Rapid and effective method for RNA extraction from different tissues of grapevine and other woody plants. *Phytochem. Anal.* 19, 520–525.

7. Garnsey, S. M., Civerolo, E. L., Gumpf, D. J., Paul, C., Hilf, M. E., Lee, R. F., et al. (2005). Biological Characterization of an International Collection of Citrus tristeza virus (CTV) Isolates. *International Organization of Citrus Virologists Conference Proceedings (1957-2010)* 16.

8. Garnsey, S. M., Permar, T. A., Cambra, M., and Henderson, C. T. (1993). Direct tissue blot immunoassay (DTBIA) for detection of citrus tristeza virus (CTV). in *International Organization of Citrus Virologists Conference Proceedings (1957-2010)*

9. Gergerich, R. C., Welliver, R. A., Osterbauer, N. K., Kamenidou, S., Martin, R. R., Golino, D. A., et al. (2015). Safeguarding Fruit Crops in the Age of Agricultural Globalization. *Plant Dis.* 99, 176–187.

10. Glasel, J. A. (1995). Validity of nucleic acid purities monitored by 260nm/280nm absorbance ratios. *Biotechniques* 18, 62–63.

11. Li, R., Mock, R., Huang, Q., Abad, J., Hartung, J., and Kinard, G. (2008). A reliable and inexpensive method of nucleic acid extraction for the PCR-based detection of diverse plant pathogens. *J. Virol. Methods* 154, 48–55.

12. Loconsole, G., Saponari, M., and Savino, V. (2010). Development of real-time PCR based assays for simultaneous and improved detection of citrus viruses. *Eur. J. Plant Pathol.* 128, 251–259.

13. Manchester, K. L. (1996). Use of UV methods for measurement of protein and nucleic acid concentrations. *Biotechniques* 20, 968–970.

14. Newbury, H. J., and Possingham, J. V. (1977). Factors affecting the extraction of intact ribonucleic Acid from plant tissues containing interfering phenolic compounds. *Plant Physiol.* 60, 543–547.

15. Osman, F., Dang, T., Bodaghi, S., and Vidalakis, G. (2017). One-step multiplex RT-qPCR detects three citrus viroids from different genera in a wide range of hosts. *J. Virol. Methods* 245, 40–52.

16. Osman, F., Hodzic, E., Kwon, S.-J., Wang, J., and Vidalakis, G. (2015). Development and validation of a multiplex reverse transcription quantitative PCR (RT-qPCR) assay for the rapid detection of Citrus tristeza virus, Citrus psorosis virus, and Citrus leaf blotch virus. *J. Virol. Methods* 220, 64–75.

17. Osman, F., Olineka, T., Hodzic, E., Golino, D., and Rowhani, A. (2012). Comparative procedures for sample processing and quantitative PCR detection of grapevine viruses. *J. Virol. Methods* 179, 303–310.

18. Pagliaccia, D., Bodaghi, S., Chen, X., Stevenson, D., Deyett, E., De Francesco, A., et al. (2020). Two food waste by-products selectively stimulate beneficial resident citrus host-associated microbes in a zero-runoff indoor plant production system. Front. Sustain. Food Syst. 4 :593568.

19. Palacio-Bielsa, A., Foissac, X., and Duran-Vila, N. (1999). Indexing of Citrus Viroids by Imprint Hybridisation. *Eur. J. Plant Pathol.* 105, 897–903.

20. Papayiannis, L. C. (2014). Diagnostic real-time RT-PCR for the simultaneous detection of Citrus exocortis viroid and Hop stunt viroid. *J. Virol. Methods* 196, 93–99.

21. Porebski, S., Grant Bailey, L., and Baum, B. R. (1997). Modification of a CTAB DNA extraction protocol for plants containing high polysaccharide and polyphenol components. *Plant Mol. Biol. Rep.* 15, 8–15.

22. Rivera-Bustamante, R. F., Gin, R., and Semancik, J. S. (1986). Enhanced resolution of circular and linear molecular forms of viroid and viroid-like RNA by electrophoresis in a discontinuous-pH system. *Anal. Biochem.* 156, 91–95.

23. Rizza, S., Nobile, G., Tessitori, M., and Catara, A. (2009). Real time RT-PCR assay for quantitative detection of Citrus viroid III in plant tissues. *Plant*.

24. Roistacher, C. N. (1991). *Graft-transmissible Diseases of Citrus: Handbook for Detection and Diagnosis*. Food & Agriculture Org.

25. Roy, A., Fayad, A., Barthe, G., and Brlansky, R. H. (2005). A multiplex polymerase chain reaction method for reliable, sensitive and simultaneous detection of multiple viruses in citrus trees. J. Virol. Methods. 129:47–55.

26. Ruiz-Ruiz, S., Ambrós, S., Vives, M. del C., Navarro, L., Moreno, P., and Guerri, J. (2009). Detection and quantitation of Citrus leaf blotch virus by TaqMan real-time RT-PCR. *J. Virol. Methods* 160, 57–62.

27. Salzman, R. A., Fujita, T., Zhu-Salzman, K., Hasegawa, P. M., and Bressan, R. A. (1999). An Improved RNA Isolation Method for Plant Tissues Containing High Levels of Phenolic Compounds or Carbohydrates. *Plant Mol. Biol. Rep.* 17, 11–17.

28. Saponari, M., Manjunath, K., and Yokomi, R. K. (2008). Quantitative detection of Citrus tristeza virus in citrus and aphids by real-time reverse transcription-PCR (TaqMan®). *J. Virol. Methods* 147, 43–53.

29. Schrader, C., Schielke, A., Ellerbroek, L., and Johne, R. (2012). PCR inhibitors - occurrence, properties and removal. *J. Appl. Microbiol.* 113, 1014–1026.

30. Sipahioglu, H. M., Usta, M., and Ocak, M. (2006). Use of dried high-phenolic laden host leaves for virus and viroid preservation and detection by PCR methods. *J. Virol. Methods* 137, 120–124.

31. Sun, N., Deng, C., Zhao, X., Zhou, Q., Ge, G., Liu, Y., et al. (2014). Extraction of total nucleic acid based on silica-coated magnetic particles for RT-qPCR detection of plant RNA virus/viroid. J. Virol. Methods. 196:204–211.

32. Vidalakis, G., and Wang, J. (2013). Molecular method for universal detection of citrus viroids. United States patent US 2013/0115591 A1, May 9, 2013.

33. Vives, M. C., Velázquez, K., Pina, J. A., Moreno, P., Guerri, J., and Navarro, L. (2013). Identification of a new enamovirus associated with citrus vein enation disease by deep sequencing of small RNAs. Phytopathology. 103:1077–1086.

34. Wang, J., Bozan, O., Kwon, S.-J., Dang, T., Rucker, T., Yokomi, R. K., et al. (2013). Past and future of a century old Citrus tristeza virus collection: a California citrus germplasm tale. *Front. Microbiol.* 4. doi:10.3389/fmicb.2013.00366.

35. Wilkins, T. A., and Smart, L. B. (1996). *Isolation of RNA from plant tissue*. Wiley-Liss, Inc., New York.

36. Yokomi, R. K., Saponari, M., and Sieburth, P. J. (2010). Rapid differentiation and identification of potential severe strains of Citrus tristeza virus by real-time reverse transcription-polymerase chain reaction assays. *Phytopathology* 100, 319–327.

Chapter II

Detection and identification of invasive citrus pathogens using high-throughput RNA extraction and sequencing

Note: the contents of this chapter are adapted from Dang et. al. (2018). First report of Citrus viroid V naturally infecting grapefruit and calamondin trees in California. Plant Dis. 102:2055 and Dang et al. (2020). First report of Citrus leaf blotch virus infecting bears lime tree in California. Plant Dis. 104:3088.

ABSTRACT

Citrus is an important commodity in California (CA) that is under constant threat from both endemic and exotic citrus pathogens. There are safeguards in place to curtail the spread of citrus pathogens, such as regulatory testing of citrus propagative materials, field surveys, and proper introduction of citrus varieties. With the advancements of diagnostic tools, new high throughput RNA extraction and polymerase chain reaction (PCR) methods has increased efficiency which increased the capacity and frequency of molecular diagnostics. In this study, we performed large scale reverse transcription quantitative PCR (RT-qPCR) testing of nursery stock trees and field trees throughout California. We discovered the first natural occurrences of citrus viroid V (CVd-V) and citrus leaf blotch virus (CLBV) in nursery stock trees and a field tree, in CA respectively. Biological indexing and Sanger sequencing confirmed the presence and identity of CVd-V in redblush grapefruit and variegated calamondin trees. High throughput sequencing

confirmed the presence of CLBV and identified two other endemic citrus pathogens, citrus vein enation virus and citrus exocortis viroid, from a bearrs lime tree. This discovery of CVd-V and CLBV in CA has put a greater emphasis on the need for routine regulatory testing of citrus propagative materials and field surveys to exclude and isolate dangerous pathogens from establishing in the state.

INTRODUCTION

Citrus is an important commodity of California (CA) that is currently valued at $3.4 billion dollars with an estimated economic impact of $7.1 billion (Babcock, 2018). Because of the massive value of the industry, it must be protected from the constant threat of endemic and exotic pathogens. With the spread of deadly citrus disease such as Huanglongbing and other diverse citrus pathogens that can devastate the citrus industry, thus it is imperative to have access to pathogen free citrus propagative materials (Gottwald, 2010; da Graça et al., 2016). The state of CA requires nursery stock trees to be peroidically tested for citrus pathogens under the "QC 1388, Permit for Polymerase Chain Reaction (PCR) Protocol for Virus Testing in Citrus Nursery Stock Pest Cleanliness Program" and "QC 1354, Permit for PCR Protocol For Viroid Testing In Citrus Nursery Stock Pest Cleanliness Program". These programs have successfully excluded the unwanted pathogens before they can establish in CA. Examples of this is the discovery of the first natural infections of citrus viroid V (CVd-V) and Citrus leaf blotch virus (CLBV) by the Citrus Clonal Protection Program in CA.

Citrus viroid V (CVd-V) is an *Apscaviroid* with a GC-rich genome and size of 293 to 294 nucleotides (nt). It has been previously reported in citrus growing regions such as Spain, Nepal, Columbia, Tunisia, Japan, China, Pakistan, and parts of the United States (Serra et al., 2008b; Cao et al., 2010, 2012; Ito and Ohta, 2010; Hamdi et al., 2015). Previous studies have shown that CVd-V has a restricted host range and induces mild symptoms on plant indicator S-1 Etrog citron with mild stunting of the plant and small lesions and cracking on the stems (Serra et al., 2008a). When CVd-V is co-infected with either citrus bent leaf viroid (CBLVd) or citrus dwarfing viroid (CDVd), the synergistic effect caused severe stunting, leaf epinasty, and stem cracking can be observed on S-1 Etrog citron plant indicator (Serra et al., 2008a). CVd-V alone does not cause obvious symptoms in field or commercial trees, however citrus trees can harbor multiple viroids and the synergistic behavior between CVd-V and CBLVd or CDVd could potentially cause problems if CVd-V is introduced into an area that with existing CDVd and CBLVd infection. This puts an importance on routine testing and use of clean propagated source materials to prevent the spread of citrus viroids and other pathogens.

Citrus leaf blotch virus (CLBV syn. Dweet mottle virus) is a *Citrivirus* that is a member of the *Betaflexiviridae* family (Hajeri et al., 2010). The virus is composed of a single-stranded, positive-sense RNA with a length of 8,747 nt and three open reading frames (Vives et al., 2001; Ruiz-Ruiz et al., 2009). CLBV is primarily graft transmitted by using virus infected propagative material and it can also be transmitted in some citrus species by seed at low rates (Guerri et al., 2004). CLBV can cause chlorotic leaf blotching in Dweet tangor (*Citrus reticulata* × *C. sinensis*) and stem pitting in Etrog citron (*C.*

medica L.) (Navarro et al., 1984; Galipienso et al., 2000). In severe instances, bud union crease symptoms can develop between the scion and the trifoliate hybrid rootstocks such as Troyer citrange (*C. sinensis* (L.) Osb. × *C. trifoliata*) or citrumelo (*C. paradisi* Macf. × *C. trifoliata*) (Galipienso et al., 2004; Guardo et al., 2007) which can lead to a decline of a tree. This can be a problem because of the wide scale use of trifoliate and trifoliate hybrid rootstocks in the citrus industry due to the tristeza-tolerant characteristics (Moreno et al., 2008). CLBV has a wide host range and has been found in non-citrus hosts such as kiwi (*Actinidia* spp.) (Liu et al., 2019) mulberries (*Morus* spp.) (Xuan et al., 2020), sweet cherry (*Prunus avium*) (Wang et al., 2016) , peony (*Paeonia lactiflora*) (Gress et al., 2017), rehmannia (*Rehmannia glutinosa*) and tobacco (*Nicotiana benthamiana*) (Agüero et al., 2013; Wang et al., 2016; Gress et al., 2017; Liu et al., 2019; Xuan et al., 2020). CLBV has been discovered in several countries such as Australia, Japan, China, Spain, Corsica, and the United States (Vives et al., 2002; Hajeri et al., 2010; Cao et al., 2017).

This study was built on the results from optimizing and verifying high throughput extraction technology from Chapter 1 of this thesis. Here we utilized the MagMax-96 (MM-96) protocol to extract quality RNA for large-scale PCR testing of citrus samples. The MM-96 extraction technology has resolved several throughput issues and it has allowed programs such as the Citrus Clonal Protection Program (CCPP) to test thousands of citrus samples from various sources per year for the detection of citrus viruses and viroids. In addition, the use of HTS in this study for pathogen verification has set the foundation for the application of this technology as a citrus diagnostic tool to complement

existing methods. The results have led to the detection and identification of the first natural infection of CVd-V in nursery stock trees and CLBV from a field survey in CA.

MATERIALS AND METHODS

Plant material and sample collection for citrus virus and viroid pathogen testing

Citrus samples for regulatory pathogen testing under the mandatory California (CA) §3701 Citrus Nursery Stock Pest Cleanliness Program were collected by the California Department of Agriculture (CDFA) from various nurseries throughout the state (from October 2016 to March 2017). The CA field survey for citrus viruses and viroids were collected in 20 different counties under the Citrus Research Board project 5300-181 (from July 2017 to January 2018) (CDFA permit 3096; USDA P526P-16-00352). All stem samples were collected around the entire canopy of the tree. Between sampling of each tree, the pruners were sanitized with 10% household bleach solution (0.5% sodium hypochlorite) and dried with a paper towel to avoid cross contamination. Stem samples were packaged into a resealable bag, placed on an ice chest, shipped overnight to the CCPP and immediately stored in 4°C until further processing no later than14 days from collection.

Sample handling and preparation

For all stem samples, the phloem rich bark tissue was peeled using a disposable single edge razor blade. The peeled bark tissue was finely chopped into small pieces (4 to 5 mm) on small disposable chipboards, and 250 mg of small bark tissue pieces were placed

into a 2 mL safe-lock tube (Eppendorf, Hamburg, Germany). Between each sample, the chipboards were disposed and the bench working area was sanitized with 10% household bleach followed by application of 70% ethanol to remove any residual sodium hypochlorite. One tube was prepared for all regulatory pathogen testing and field survey samples. Sample tubes were barcoded, kept in ice during processing, sanitized externally by dipping in a series of 10% household bleach and water baths and placed in a -80°C freezer for at least two hours prior to lyophilization for 24 to 26 hours in a FreeZone® Triad™ 74000 freeze-dryer (Labconco®, Kansas City, MO). After lyophilization, a single sterile 4-mm stainless steel grinding ball was added into each sample tube and stored at -80°C until tissue pulverization and RNA extraction.

Tissue pulverization and high throughput RNA extraction

Sample tubes were placed into stainless steel Cryo-Blocks (SPEX SamplePrep, Metuchen, NJ) and chilled with liquid nitrogen using the Cryo-Station (SPEX SamplePrep) for 20 minutes. The samples were ground into fine powder using a Geno/Grinder® 2010 (SPEX SamplePrep) at 1680 RPM for 20 seconds, twice. RNA was extracted using the MagMAX™ Express-96 Deep Well Magnetic Particle Processor (Thermo Fisher Scientific, Waltham, MA) instrument utilizing the MagMAX™ 96 Viral RNA Isolation Kit (MM-96 kit). The standard kit procedures were adjusted and optimized for the extraction of total RNA from citrus tissues as described in Chapter 1. Upon tissue pulverization, 750 µl of 4 M guanidine lysis buffer (4 M guanidine thiocyanate, 0.2 M sodium acetate pH 5.0, 2 mM EDTA, 2.5% (w/v) PVP-40 at pH 5.0) were added to each sample. Samples were homogenized using the Geno/Grinder® 2010 at 1680 rpm for 20

seconds, twice. The crude homogenized extracts were incubated at 4°C for 15 min and centrifuged at 4°C for 45 min at 17,200 x g. RNA was isolated using the default MagMAX™ protocol recommended by the manufacturer "AM1836_DW_50_V2". Two mL deep well plates were used for the MagMAX™ Express-96 and were prepared as follows; lysate plate (position 1) which consisted of 139 µl of Lysis/Binding Solution Concentrate (premixed with 40 mL of isopropanol), 22 µl of Bead Mix (10 µl of RNA Binding Beads, 10 µl of Lysis/Binding Enhancer and 2 µl of Carrier RNA), 139 µl of isopropanol, and 150 µl of the processed supernatant; first set of wash plates that consisted of 500 µl of MagMAX™ Wash Solution 1 (position 2-3); a second set of wash plates that consisted of 500 µl of MagMAX™ Wash Solution 2 (positions 4–5); the elution plate (position 6) contained of 100 µl of elution buffer; and the tip comb plate loaded with the MagMAX™ Express-96 Deep Well Tip Comb (position 7). At the end of the MagMAX run, the elution plate was placed on a magnetic rack for 5 mins to collect any residual beads. The obtained purified RNA was transferred to a microtiter plate and stored in the -80°C freezer.

PCR testing for the detection and identification of citrus viruses and viroids

Two sets of reverse transcription quantitative polymerase chain reaction (RT-qPCR) primers ("Nonapsca" and "Apsca") were previously developed and used for the universal detection of all known citrus viroids (**Table 2.1**). Reactions were performed in a 96-well unskirted PCR plate using the manufacturer's recommended protocol as follows: 7.4 µL of nuclease free water, 0.6 µL (300 nM) of forward and reverse primer, and 1 µL of RNA (25 – 100 ng) per reaction. The mixture was sealed and incubated in a thermocycler

for 5 minutes at 80°C to denature the targeted RNA. The samples were taken out of the thermocycler and immediately cooled in an ice bath for at least 5 minutes. Once cooled, 10 µL of iTaq™ Universal SYBR® Green reaction mix (Bio-Rad, Hercules, CA) and 0.25 µL reverse transcriptase enzyme were added for a total reaction volume of 20 µL. The samples were loaded into the CFX96™ Real-Time PCR machine (Bio-Rad, Hercules, CA) with the following conditions: reverse transcription at 50°C for 30 mins, 95°C for 5 mins, 95°C for 10 sec, 61°C ("Nonapsca")/62°C ("Apsca") for 30 sec for 35 cycles, 95°C for 1 min, 55°C for 1 min, and melting curve analysis from 55 to 95°C with 0.5°C increments for 10 sec (Vidalakis and Wang, 2013; Chambers et al., 2018). To further identify the exact citrus viroid from positive "Nonapsca" or "Apsca" results, RT-PCR (Wang et al., 2013) reactions was performed using Qiagen OneStep RT-PCR Kit (Valencia, CA) in a total of 20 µL. One µL of RNA template, 2.6 µL RNase-free water, and 1.2 µL of forward and reverse primers (final concentration of 0.6 µM). The mixture was incubated in a thermocycler for 5 minutes at 80°C. The samples were taken out of the thermocycler and immediately cooled in an ice bath for at least 5 minutes. Once cooled, 10 µL of 5x Qiagen OneStep RT-PCR Buffer, 2 µL of the Qiagen OneStep RT-PCR Enzyme Mix, and 2 µL of 10 mM dNTP (final concentration of 400 µM) were added to the reaction mixture. The mixture was loaded into the ProFlex PCR instrument (Thermo Fisher, Waltham, MA) with the following conditions: 50°C for 30 mins, 95°C for 15 mins, 94°C for 1 min, 60°C for 30 secs, 72°C for 1 min for 30 cycles and 72°C for 10 mins. The amplicon was analyzed on a 1.5% TAE agarose gel with 120V for 30 minutes, stained with ethidium bromide and visualized under UV light with the ChemiDoc Imaging System (Bio-Rad, Hercules, CA).

Multiplex RT-qPCR assay was used to detect citrus tristeza virus (CTV), citrus leaf blotch virus (CLBV), and citrus psorosis virus (CPsV) (Osman et al., 2015) (**Table 2.1**). The assay was carried out in 12 µL reactions using the QuantiFast Multiplex RT-PCR kit (Qiagen, Valencia, CA), 0.045 µL of nuclease free water, 6.25 µL of 2x QuantiFast RT Master Mix, 0.58 µL primer and probe mix, 0.125 µL QuantiFast RT mix and 5 µL total RNA. The samples were loaded into the QuantStudio 12K Flex Real-Time PCR machine (Thermo Fisher, Waltham, MA) with the following conditions: 50◦C for 20 min, 95◦C for 5 mins, 95◦C for 15 secs, and 60◦C for 1 min for 40 cycles. All RT-qPCR reactions had the appropriate positive and negative controls in ordinance with the MIQE guidelines (Bustin et al., 2009).

Verification of CVd-V through biological indexing, cloning, and Sanger sequencing

All samples tested positive for CVd-V were recollected by CDFA from the original sources and RNA was re-extracted from phloem rich bark tissue using TRIzol™. The CVd-V positive samples were graft-inoculated on to 'Etrog' citron Arizona 861-S-1 (*Citrus medica* L.) seedlings with 2 blind buds for each citron. The inoculum was checked for survival two weeks after inoculation and the plants were maintained under greenhouse conditions (27 to 41°C) until viroid symptoms appeared.

RT-PCR was performed with overlapping CVd-V specific primers to generate a full-length genome (Wang et al., 2013) in both positive samples and indicator S-1 citrons. The amplicon was analyzed on a 1.5% TAE agarose gel with 120V for 30 minutes. The product was excised and cleaned with QIAquick Gel Extraction Kit (Qiagen, Valencia, CA) using the manufacturers recommended protocol and cloned into PGEM®-T Easy

Vector (Promega, Madison, WI). The plasmids were transformed into 25 µl of NEB 5-alpha (DH5-α) competent cells (New England Biolabs, Ipswich, MA) The cell mixtures were carefully mixed by flicking the tube 4 to 5 times and incubated on ice for 30 minutes. Cells were heat shocked at exactly 42°C for exactly 30 seconds, immediately placed on ice for 5 minutes, and 950 µl of room temperature SOC media was added into the cell mixture. Samples were placed in a shaking incubator at 37°C for 60 minutes at 250 rpm. Fifty µl of the sample were plated onto LB agar plates with ampicillin (100 µg/mL) and X-Gal solution and then placed into an incubator overnight at 37°C. Recombinant colonies were randomly chosen and placed into liquid LB culture. The liquid LB culture was placed into a shaking incubator at 37°C overnight at 250 rpm. The plasmids were extracted using QIAprep Spin Miniprep Kit (Qiagen, Valencia, CA) using the manufacturer's recommended protocol. The quality of the plasmids were assessed with a spectrophotometer and were submitted to UC Riverside Institute for Integrative Genome Biology (IIGB) Core Facility for Sanger sequencing using the 3730x/DNA Analyzer Instrument (Thermo Fisher, Waltham, MA) with SP6 and T7. Secondary structure prediction was performed using MFOLD at 37°C with default parameters (Zuker, 2003). The full length CVd-V sequences were deposited into GenBank under ascensions: MF477857 to MF477876.

RNA extraction of CLBV-BL for high throughput sequencing

CLBV positive stem sample was recollected from the original field source for high throughput sequencing analysis. Phloem rich bark tissue was peeled using a

disposable single edge razor blade. The peeled bark tissue was finely chopped into small pieces (4 to 5 mm) on small disposable chipboards, and 100 mg of small bark tissue pieces were pulverized in mortar and pestle with liquid nitrogen. The pulverized tissue was transferred into a standard 1.5 mL microcentrifuge. The RNA was extracted using TRIzol™ using the manufacturer's recommended protocol adjusted for citrus tissues. One mL of TRIzol™ reagent was added to the pulverized tissues. Samples were homogenized with a vortex for 20 seconds, centrifuged at 4°C for 5 minutes at 12,000 x g and the supernatant was then transferred to a new 1.5 mL microcentrifuge tube. Two-hundred µL of chloroform were added and the samples were incubated at room temperature for 3 minutes. Samples were centrifuged for 15 minutes at 12,000 x g at 4°C. The aqueous phase was transferred to a new 1.5 mL microcentrifuge tube and 500 µL of isopropanol were added to each sample. Samples were then incubated at room temperature for 10 minutes and subsequently centrifuged at 4°C for 10 minutes at 12,000 x g. The supernatant was discarded, and 1 mL of 75% ethanol was added. The samples were vortexed briefly and centrifuged at 4°C for 5 minutes at 7,500 x g. Ethanol was discarded and the pellet was left to air dry for 30 minutes to 1 hour. The RNA pellet was resuspended in 100 µL of UltraPure™ DNase/RNase-free distilled water (Thermo Fisher Scientific, Waltham, MA). The extracted RNA was aliquoted into three 1.5 mL screw cap microcentrifuge tubes and stored at -80°C until further use.

Depletion of host ribosomal RNA

Plant ribosomal depletion was performed on the HTS samples using the Illumina Ribo-Zero rRNA Removal Kit for plants (San Diego, CA) following the manufacturer’s

recommended protocol. For the ribosomal depletion, RNA samples were first adjusted to 1 µg in a total of 10 µL, then 5 µL of RBB and 5 µL of RRM-P was added to the reaction. The samples were incubated in the ProFlex thermal cycler (Thermo Fisher, Waltham, MA) at 68°C for 5 mins. Afterwards, 35 µL of RRB was added, incubated at room temperature, placed on a magnetic stand, and transferred to a new tube. Sample was cleaned with 99 µL of AMPure XP Beads (Beckman Coulter, Brea, CA), incubated at room temperature for 15 mins, placed on a magnetic stand until the liquid is clear, and discarded all of the supernatant from each tube. Sample was washed using 200 µl of freshly prepared 70% EtOH and air-dried on the magnetic stand. Once dried, 11 µL of ELB was added to each tube, incubated at room temperature until the liquid was clear, and transferred 8.5 µl supernatant to a new tube. Subsequently, 8.5 µl of EPH was added and then incubated in the ProFlex thermal cycler at 94°C for 8 minutes.

HTS library preparation and data analysis

HTS library was prepared using the Illumina TruSeq Stranded Total RNA kit (San Diego, CA) using the manufacturer's recommended protocol. The first strand cDNA synthesis was prepared by adding 8 µL FSA and SuperScript II mixture (ratio: 1 µL of SuperScript II 9 µL of FSA) to each tube of the rRNA depleted samples. The mixture was placed into the thermal cycler with the following conditions: 25°C for 10 mins, 42°C for 15 mins, and 70°C for 15 mins.

The second strand cDNA synthesis was performed by adding 5 µl diluted CTE (1:50) and 20 µL SMM to the first strand cDNA mixture and incubated at 16°C for 1 hour.

The cDNA was purified by adding 90 µL AMPure XP beads and incubated at room temperature for 15 minutes and placed on a magnetic stand and waited until the liquid was clear (~5 minutes). The supernatant was removed and washed twice by adding 200 µL fresh 80% EtOH to each tube. The sample was air-dried on the magnetic stand for 15 minutes and 17.5 µL RSB was added to the lobind tube. The eluted sample was placed on a magnetic stand until the liquid was clear. Fifteen µL of the elute was transferred to a new tube with 2.5 µL diluted CTA (1:100) and 12.5 µL ATL for the adenlation of 3' ends. The mixture was placed into the ProFlex thermal cycler with the following conditions: 37°C for 30 mins and 70°C for 5 mins. Adapters were ligated to the adenlated mixtures by adding 2.5 µL of diluted CTL (1:100), 2.5 µL LIG, and 2.5 µL of the RNA adapter. The mixture was incubated in the ProFlex thermal cycler at 30°C for 10 mins. The reaction was immediately removed and 5 µL STL was added to each tube. The ligated fragments were cleaned by adding 42 µL of AMPure XP beads, incubated at room temperature for 15 minutes and washed two times with 200 µL of freshly prepared 80% EtOH for 30 seconds. The sample was air-dried on the magnetic stand and 52.5 µL of RSB was added. Fifty µL of supernatant was recovered and a second cleaning was performed by adding 50 µL AMPure XP beads. The sample was incubated at room temperature for 15 minutes and washed two times with 200 µL freshly prepared 80% EtOH for 30 seconds. The sample was air-dried on the magnetic stand and 22.5 µL of RSB was added. Twenty µL of supernatant was recovered and used for PCR enrichment of DNA fragments. Twenty-five µL of PMM and 5 µL of PPC were added. The sample was placed into the ProFlex thermal cycler with the following conditions: 98°C for 30 seconds, 98°C for 10 seconds, 60°C for

30 seconds, 72°C for 30 seconds for 15 cycles, and 72°C for 5 minutes. The amplified DNA was cleaned by adding 50 µL of AMPure XP beads, incubated at room temperature for 15 minutes, and placed on a magnetic stand until the liquid was clear. The sample was washed twice, with 200 µL fresh 80% EtOH to each tube, air-dried on the magnetic stand for 15 minutes, and 32.5 µL of RSB was added. The sample was placed on a magnetic stand until the liquid was clear and 30 µL of supernatant was aliquoted into 3 screw top tubes and stored in -20°C.

The Agilent 2100 Bioanalyzer (Santa Clara, CA) was used to ensure the final library product was approximately 260 bp. The finalized sample was submitted to UC Riverside IIGB Core Facility for sequencing using the Illumina NextSeq500 platform with paired end reads (2 × 75 bp). Low-quality Illumina reads were filtered with Fastp (Chen et al., 2018) using the default settings. After quality control, Bowtie2 version 2.3.4.1 (Langmead et al., 2009) was used to align CLBV reference genome (NC_003877) guided alignment. Reads that mapped to the CLBV reference genome were assembled using Trinity version 2.8.5 (Grabherr et al., 2011). BLASTn (Altschul et al., 1990; Madden et al., 1996) was performed to confirm the identity of the assembled contig. 5′ and 3′ RACE was performed to produce the full-length virus sequence (MT038390).

To verify the presence of other citrus pathogens, a *de novo* assembly was performed. First, host reads were removed using Bowtie2 by mapping the reads to the reference citrus genome (*Citrus sinensis*, GCA_000317415.1). The reads that did not map to the citrus genome were then assembled using Trinity, and finally BLASTn was performed to identify all contigs.

RESULTS

Detection and identification of CVd V with RT-qPCR and RT-PCR

The initial CA nursery testing results from 2016-2017 using SYBR® Green RT-qPCR universal viroid detection primers identified 17 out of 2,449 as being samples positive for citrus viroids. Of the 17 samples, 8 were identified as "Apsca" viroids (CBLVd, CDVd, CVd-V, CVd-VI , or CVd-VII) and 9 were identified as "Nonapsca" (CEVd, HSVd, or CBCVd) (**Table 2.1-2.2**). I identified two samples, red blush grapefruit (RG) (*Citrus paradisi* Macfadyen) and variegated calamondin (VG) (*C. madurensis* Lour.) that had a melting temperature that was consistent with CVd-V (87.5°C) (Vidalakis and Wang, 2013) (**Table 2.2**). To validate the results, CVd-V specific RT-PCR primers were used and a 294 bp amplicon was detected in the two tested samples (Wang et al., 2013) (**Figure 2.1**).

Characterization of CVd-V from RG and VC positive samples

Full length sequences of CVd-V were obtained from Sanger sequencing from the RT-PCR amplicons and secondary structure prediction using MFOLD was performed on viroids from the the RG and VC samples. The predicted structures showed hallmark structures that were consistent with CVd-V (**Figures 2.2A - 2.2C**). An alignment of CVdV-RG and CVdV-VC showed that the two viroids were 98.64% similar with nucleotide changes at positions 69, 224, 225, and 251. The BLASTn results revealed that the RG isolate (MF477857 to MF477866) had the highest similarity with the KM isolate from Pakistan (99.66%) (JQ348924), with a single nucleotide change from A to U at position 65 (**Table 2.3A**). The VC isolate (MF477867 to MF477876) showed the highest

similarity with the MO isolate (99.32%) from Pakistan (JQ348925), with two nucleotide changes from G to A at position 69 and A to U at position 251 (**Table 2.3B**).

Verification of CVd-V with biological indexing

CVdV-RG and VC samples were grafted into Arizona 861-S-1 citron plant indicators. By 8 months post inoculation, all inoculated citrons had developed mild stunting, leaf bending and epinasty, and midvein necrosis symptoms which was consistent with viroid infection (**Figure 2.3A to C**). RT-PCR was performed on the symptomatic citron plants and CVd-V was detected and re-isolated from the inoculated S-1 citrons.

Detection of CLBV from a field tree in CA

The CCPP received and tested 1,169 samples from citrus trees that were surveyed in 20 different California counties for virus and viroid. Using RT-qPCR we identified one sample originating from a nonsymptomatic Bearss lime (BL) (*Citrus latifolia* Tan.), which tested positive for CLBV, citrus vein enation virus (CVEV), and citrus exocortis viroid (CEVd) (**Table 2.1**). HTS was performed to verify the RT-qPCR results. HTS generated a total of 81,806,700 reads, after quality control and low-quality reads were filtered. CLBV reference genome (NC_003877) guided alignment using Bowtie2 produced 135,574 reads that mapped to the CLBV genome. The Bowtie2 mapped reads were assembled with Trinity and generated an assembled contig of 8,713 nt. BLASTn results showed that the CLBV-BL isolate had the highest (98.8%) identity to the NZ-G18 (EU857539) isolate from *Citrus limon* in New Zealand and covered 99% of the genome (**Table 2.4**). Both 5′ and 3′ RACE were performed to produce the full-length CLBV sequence (8,743 nt) and

the CLBV sequence was deposited under GenBank accession number: MT038390 (**Table 2.4**).

Identification of other pathogens using HTS

Reference genome guided alignment using Bowtie2 was performed and produced 237,669 and 3,337 reads that mapped to CVEV and CEVd, respectively. The mapped reads were assembled with Trinity and generated assembled contigs of 5,948 nt and 369 nt. BLASTn results from the assembled reads confirmed the presence of CVEV and CEVd. CVEV-BL showed 97.6% similarity to PCJ (LC433634) isolated from *C. trifoliata* in Korea (**Table 2.4**). CEVd-BL was identical to the TL5 (EU564172) isolated from *C. latifolia* Tanaka in Peru. (**Table 2.4**). *De novo* assembly performed with Trinity, on nonhost reads generated from Bowtie2 removing the reads mapped to citrus genomes as references, resulting in no other known citrus pathogens being identified in the BL sample.

DISCUSSION

The advances in diagnostic tools has allowed for high throughput screening of thousands of samples in a timely manner. In this study I utilized a streamlined high throughput extraction and RT-qPCR diagnostic workflow on citrus samples which led to the discovery of the first natural occurrences of CVd-V and CLBV in CA. I used a combination of traditional molecular and biological assays to validate the CVd-V RG and VC positive results. For the CLBV-BL sample, HTS was utilized to verify the initial RT-qPCR positive results.

CVd-V was first reported in Spain (Serra et al., 2008b) and has been detected in samples from various locations including a source from UCR but the source of the UCR field material was not previously recorded (Serra et al., 2008a). This study identified the first natural occurrence of CVd-V in CA and corroborates the CVd-V variant report from the UCR source (Serra et al. 2008). The discovery of CVd-V in nursery sources highlights the importance of routine regulatory testing of propagative materials to prevent viroid infected citrus germplasm source trees from spreading into the commercial citrus setting. Although the CVd-V does not express obvious pathogenic symptoms on its own under field conditions, it is important to exclude it from the tree propagation process because it can interact with other citrus viroids and have synergistic behavior that results in enhanced symptoms (Serra et al., 2008a). As a result of this study the infected RG and VC nursery sources have been destroyed to prevent contamination of other plants. The exact mechanism on how the viroid infected the CA nursery tree is unclear, however this study demonstrated the importance of the systems approach of testing, implementation of phytosanitary measures such as use of sanitized pruning and grafting tools and use of citrus propagating materials from pathogen-free sources.

CLBV has been found throughout citrus growing regions however, this study demonstrated the first occurrence of CLBV in CA outside a citrus germplasm program (Vives et al., 2002; Hajeri et al., 2010; Cao et al., 2017). More specifically, the only reference to CLBV in CA comes from the 1956 Citrus Variety Improvement Program, the forerunner of CCPP. The virus was intercepted during a biological indexing using Dweet tangor (*C. reticulata* × *C. sinensis*) of a Florida citrus variety introduction in 1968 (Hajeri

et al. 2010). IN this study, the CLBV-BL isolate was detected in a tree grown in a CA residential area, not a commercial setting, indicating the importance for the access of pathogen free and tested budwood available for both residential and industry settings. The discovery of the virus and this study was the basis of CDFA's a pest rating of and evaluation of the potential risks associated with the CLBV for CA (https://blogs.cdfa.ca.gov/Section3162/?p=5126). CLBV and other related graft or seed-transmissible agents are capable of causing bud union crease on the commercial citrange rootstocks, therefore it is important to prevent them from establishing in CA (Galipienso et al. 2000). Although CVEV and CEVd were also discovered in the BL sample, this virus and viroid have been endemic and known to occur in CA, are managed by the use of pathogen-tested propagative materials, and they are not causing any significant adverse effects on citrus production (Wallace, 1978).

The novel CVd-V and CLBV cases in CA highlight the importance of the continuity of comprehensive citrus testing programs (germplasm production and field surveys) that include a combination of complementary biological indexing and molecular assays (Gergerich et al. 2015). The application and adoption of PCR based assays in diagnostics has played an critical role in disease management programs monitoring the sanitary status of germplasm and propagative materials, nursery stock and certification, and commercial plantings of citrus and other agriculturally significant crops (Bostock et al., 2014; Gergerich et al., 2015; Osman et al., 2015; Fuchs et al., 2021). The original discovery of both the CVd-V and CLBV in this study show the importance of reliable high throughput diagnostic tools that can help exclude potentially dangerous pathogens from

becoming permanently established in CA, or any other citrus producing area. In addition, both viroid and virus cases emphasize the need for the use of therapies and pathogen-tested citrus materials for tree propagation, regardless of residential or commercial use, to prevent the introduction and spread of citrus pathogens.

Pathogen	Sequence (5'-3')	Reference
RT-qPCR Taqman®		
Citrus tristeza virus (CTV)		
Forward1:	TGTGTGCAGATTTCTTGACCG	
Forward2:	TGTGTGCGGATTTCTTGACTG	Osman et al. 2015
Reverse1:	TTCCCAAGCTGCCTGACATT	
Probe: TET	AAGCGAGGGGCTGAT	
Citrus psorosis virus (CPsV)		
Forward1:	TCACAAATCAGTGAGGAATTGAGC	
Forward2:	CACAAATCAGTGATGAATTGAGCC	Osman et al. 2015
Reverse1:	GCAAACCCAGCATATCTCACAG	
Reverse2:	CGCAAACCCAGCATATCTTACAG	
Probe: VIC		
Citrus leaf blotch virus (CLBV)		
Forward:	TTCAAGAACTGGATTTGAATTTGC	Osman et al. 2015
Reverse:	TGCACAGAATTGCCTCACAGT	
Probe: FAM	AAGTTGTGGATCAAGAAG	
RT-qPCR SYBR® Green		
"Apsca viroids": Citrus bent leaf viroid, Citrus dwarfing viroid, Citrus viroid V, CVd VI, CVd VII		Vidalakis & Wang 2013; Chambers et al. 2018
Forward:	GARMMWYCKTGTGGTTCCTGTGG	
Reverse:	HYVDWHGTCCGCTCGACTAGC	
"Nonapsca viroids": Citrus exocortis viroid, Hop stunt viroid, Citrus bark cracking viroid		Vidalakis & Wang 2013
Forward:	ARGGAKCCCCGGGGMAA	
Reverse:	CTSKACKCCAGWGMWCCGCGG C	
Internal control NADH dehydrogenase (nad5)		Saponari et al. 2008
Forward:	GATGCTTCTTGGGGCTTCTTGTT	
Reverse:	GCGGATCCTCGGACATATATGA	
RT-PCR		
Citrus viroid V (CVd-V)		
Forward (90-114):	GACGAAGGCCGGTGAGCAGTAAGCC	
Reverse (93-69):	CGTCGACGACGACAGGTGAGTACTC	Wang et al. 2013
Forward (237-259):	CAATAAAAYCCAGGTGGCGAG	
Reverse (241-215)	TATTGCACAGGGAGAGRRAGA	

Table 2.1 List of polymerase chain reaction (PCR) primers and probes used for the detection and characterization of citrus pathogens used in this study.

Variety		Cq	Melting Temp	Specific Viroid
Apsca				
Variegated calamondin	*C. madurensis* Lour.	29.97	87.5	CVd V
Red blush grapefruit	*C. paradisi* Macfadyen	26.97	87.5	CVd V
Bearss lime	*C. latifolia* Tanaka	24.44	84.5	CDVd
Bearss lime	*C. latifolia* Tanaka	25.28	84.5	CDVd
Bearss lime	*C. latifolia* Tanaka	27.82	84.5	CDVd
Tango mandarin	*C. reticulata* Blanco	28.92	84.5	CDVd
Tango mandarin	*C. reticulata* Blanco	26.27	84.5	CDVd
Tango mandarin	*C. reticulata* Blanco	28.06	84.5	CDVd
Nonapsca				
Navel cara cara orange	*C. sinensis* (L.) Osbeck	26.18	84.0	CEVd
Moro blood orange	*C. sinensis* (L.) Osbeck	26.92	84.0	CEVd
Star ruby grapefruit	*C. paradisi* Macfadyen	28.67	83.8	CEVd
Lisbon frost lemon	*C. limon* L. Burm.f	23.36	83.5	CEVd
Fremont mandarin	*C. reticulata* Blanco	26.89	84.0	CEVd
Navel cara cara orange	*C. sinensis* (L.) Osbeck	26.68	81.8	HSVd
Navel cara cara orange	*C. sinensis* (L.) Osbeck	26.56	81.5	HSVd
Navel cara cara orange	*C. sinensis* (L.) Osbeck	24.66	81.5	HSVd
W. Murcott Afourer mandarin	*C. reticulata* Blanco	23.52	81.5	HSVd

Table 2.2 List of positive viroid samples from the 2016-2017 California nursery testing program (17 positive out of 2,602 total samples tested). Samples were initially tested using SYBR Green reverse transcription quantitative polymerase chain reaction with universal viroid detection primers and then the specific viroids were identified using specialized primers.

Table 2.3A CVd-V: Red blush grapefruit isolate

Isolate	GenBank Accession Number	% ID	Origin	Position	Position Changes
KM	JQ348924	99.66	Pakistan	65	A > U
MO	JQ348925	99.32	Pakistan	224	C > U
				225	C > U
CVdV-Nvl	MT883224	98.30	Morocco	127	C > T
				167	G > C
				217	G > C
Citrus viroid V	EU433392	98.30	Spain	224	C > U
				225	C > U
				245	U > C
CVdV-Sls	MT883225	97.96	Morocco	202	G > A
				245	U > C
				261	G > A

Table 2.3A and 2.3B BLASTn results of the citrus viroid Vs isolated from redblush grapefruit (RG) and variegated calamondin (VC).

Table 2.3B CVd-V: Variegated calamondin isolate

Isolate	GenBank Accession Number	% ID	Origin	Position	Position Changes
MO	JQ348925	99.32	Pakistan	69	G > A
				251	A > U
KM	JQ348924	98.30	Pakistan	65	A > U
				69	G > A
				224	U > C
				225	U > C
				251	A > U
IR	GQ466068	97.28	Iran	46	A > G
				48	-U
				65	A > U
				156	A > C
				224	U > C
				225	U > C
				245	U > C
				251	A > U
CVdV-Nvl	MT883224	96.94	Morocco	30	U > A
				52	A > C
				69	G > A
				127	C > U
				167	G > C
				217	G > C
				224	U > C
				225	U > C
				251	A > U

Table 2.3A and 2.3B BLASTn results of the citrus viroid Vs isolated from redblush grapefruit (RG) and variegated calamondin (VC).

Pathogen	Genome used for alignment	Pathogen reads	Assembled length (nt)	Reference length (nt)
Citrus leaf blotch virus	NC_003877	135,574	8,713	8,747
Citrus vein enation virus	NC_021564	237,669	5958	5,983
Citrus exocortis viroid	NC_001464	3,337	369	372

Table 2.4 Alignment, assembly, and BLASTn results of citrus leaf blotch virus, citrus vein enation virus, and citrus exocortis viroid isolated from the Bearss lime (*Citrus latifolia* Tan.) sample.

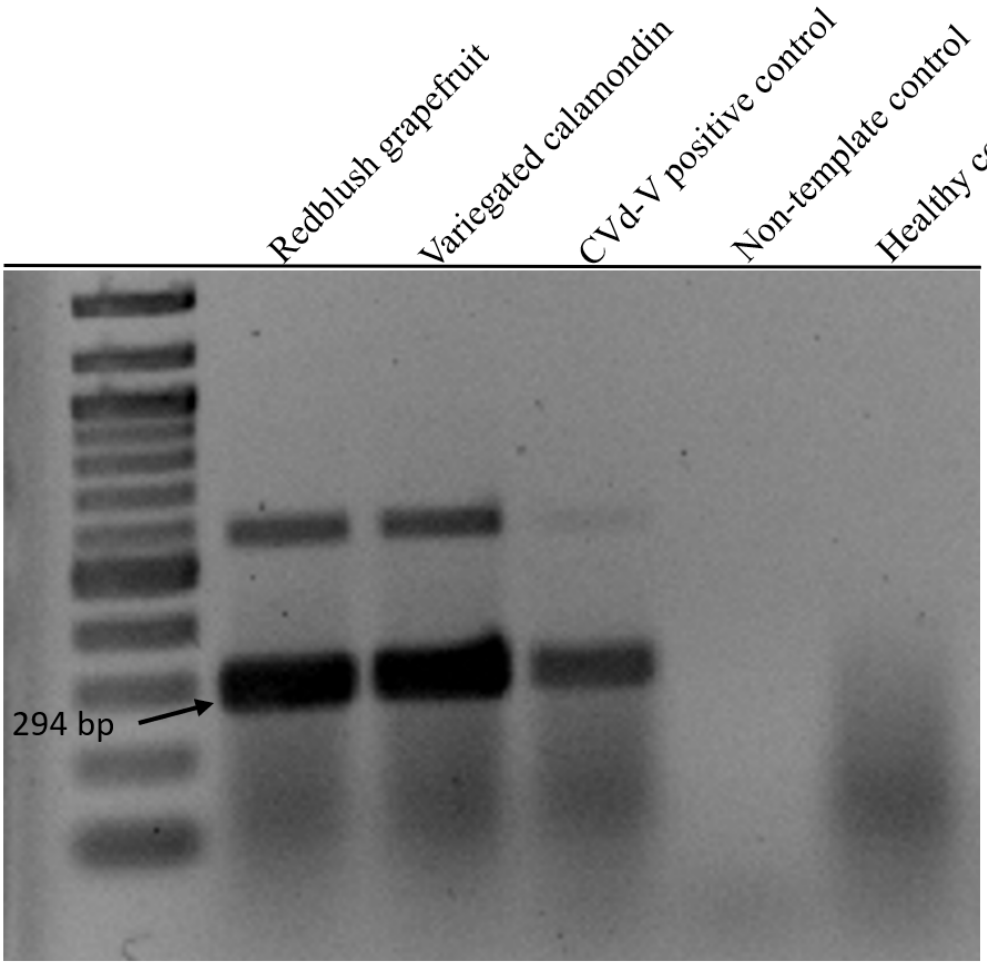

Figure 2.1 Agarose gel electrophoresis of reverse transcription polymerase chain reaction (RT-PCR) product from redblush grapefruit (RG) and variegated calamondin (VC) samples. A 294 bp band was present in samples infected with citrus viroid V (CVd-V).

Figure 2.2A

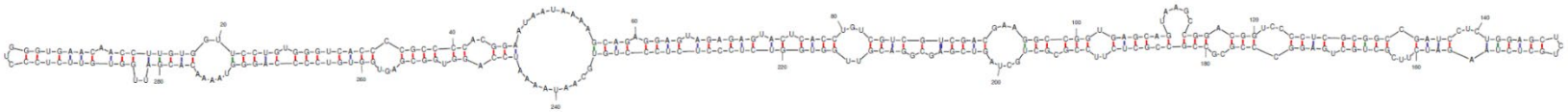

Figure 2.2B

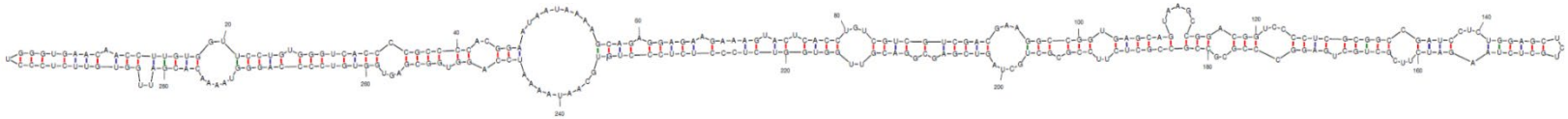

Figure 2.2C

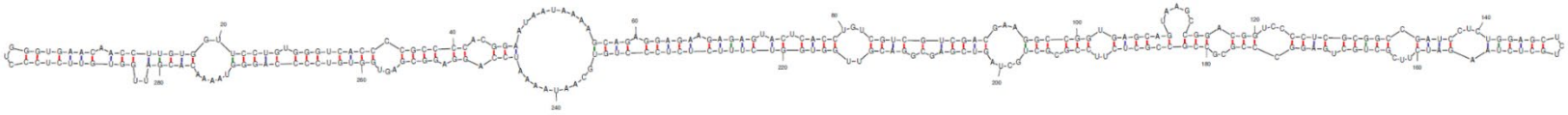

Figure 2.2A to 2.2C The nucleotide sequences and predicted structure of citrus viroid V (CVd-V), using MFOLD at 37°C, from (**A**) reference genome (NC_010165) (**B**) redblush grapefruit (RG) and (**C**) variegated calamondin (VC) samples.

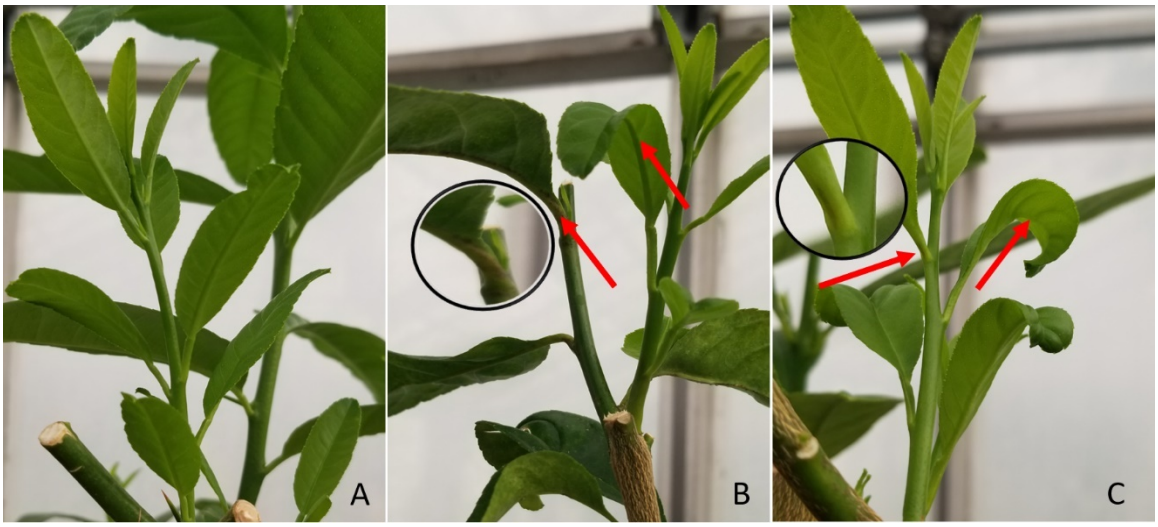

Figure 2.3 Arizona 861-S-1 citrons (*Citrus medica* L.) were inoculated with infected budwood from redblush grapefruit (RG) and variegated calamondin (VG). The healthy control (**A**) did not show viroid symptoms, while citrons inoculated with RG (**B**) and VG (**C**) exhibited mild stunting, leaf bending and epinasty, and midvein necrosis symptoms which are indicative of viroid infection.

REFERENCE

1. Agüero, J., Vives, M. C., Velázquez, K., Ruiz-Ruiz, S., Juárez, J., Navarro, L., et al. 2013. Citrus leaf blotch virus invades meristematic regions in Nicotiana benthamiana and citrus. *Mol. Plant Pathol.* 14, 610–616.

2. Altschul, S. F., Gish, W., Miller, W., Myers, E. W., and Lipman, D. J. 1990. Basic local alignment search tool. *J. Mol. Biol.* 215, 403–410.

3. Babcock, B. 2018. Economic impact of California's citrus industry. *Citrograph* 9, 36–39.

4. Bostock, R. M., Thomas, C. S., Hoenisch, R. W., Golino, D. A., and Vidalakis, G. 2014. Plant health: How diagnostic networks and interagency partnerships protect plant systems from pests and pathogens. *Calif. Agric.* 68, 117–124.

5. Bustin, S. A., Benes, V., Garson, J. A., Hellemans, J., Huggett, J., Kubista, M., et al. 2009. The MIQE guidelines: minimum information for publication of quantitative real-time PCR experiments. *Clin. Chem.* 55, 611–622.

6. Cao, M., Atta, S., Su, H., Wang, X., Wu, Q., Li, Z., et al. 2012. Molecular characterization and phylogenetic analysis of Citrus viroid V isolates from Pakistan. *Eur. J. Plant Pathol.* 135, 11–21.

7. Cao, M. J., Liu, Y. Q., Wang, X. F., Yang, F. Y., and Zhou, C. Y. 2010. First Report of Citrus bark cracking viroid and Citrus viroid V Infecting Citrus in China. *Plant Dis.* 94, 922.

8. Cao, M. J., Yu, Y.-Q., Tian, X., Yang, F. Y., Li, R. H., and Zhou, C. Y. 2017. First Report of Citrus leaf blotch virus in Lemon in China. *Plant Dis.* 101, 1561–1561.

9. Chambers, G. A., Donovan, N. J., Bodaghi, S., Jelinek, S. M., and Vidalakis, G. 2018. A novel citrus viroid found in Australia, tentatively named citrus viroid VII. *Arch. Virol.* 163, 215–218.

10. Chen, S., Zhou, Y., Chen, Y., and Gu, J. 2018. fastp: an ultra-fast all-in-one FASTQ preprocessor. *Bioinformatics* 34, i884–i890.

11. da Graça, J. V., Douhan, G. W., Halbert, S. E., Keremane, M. L., Lee, R. F., Vidalakis, G., et al. 2016. Huanglongbing: An overview of a complex pathosystem ravaging the world's citrus. *J. Integr. Plant Biol.* 58, 373–387.

12. Fuchs, M., Almeyda, C. V., Al Rwahnih, M., Atallah, S. S., Cieniewicz, E. J., Farrar, K., et al. 2021. Economic Studies Reinforce Efforts to Safeguard Specialty Crops in the United States. *Plant Dis.* 105, 14–26.

13. Galipienso, L., Carmen Vives, M., Navarro, L., Moreno, P., and Guerri, J. 2004. Detection of Citrus Leaf Blotch Virus Using Digoxigenin-Labeled cDNA Probes and RT–PCR. *Eur. J. Plant Pathol.* 110, 175–181.

14. Galipienso, L., Navarro, L., Ballester-Olmos, J. F., Pina, J. A., Moreno, P., and Guerri, J. 2000. Host range and symptomatology of a graft-transmissible pathogen causing bud union crease of citrus on trifoliate rootstocks. *Plant Pathol.* 49, 308–314.

15. Gergerich, R. C., Welliver, R. A., Osterbauer, N. K., Kamenidou, S., Martin, R. R., Golino, D. A., et al. 2015. Safeguarding Fruit Crops in the Age of Agricultural Globalization. *Plant Dis.* 99, 176–187.

16. Gottwald 2010. Current Epidemiological Understanding of Citrus Huanglongbing. *Annu. Rev. Phytopathol.* 48, 119–139.

17. Grabherr, M. G., Haas, B. J., Yassour, M., Levin, J. Z., Thompson, D. A., Amit, I., et al. 2011. Full-length transcriptome assembly from RNA-Seq data without a reference genome. *Nat. Biotechnol.* 29, 644–652.

18. Gress, J. C., Smith, S., and Tzanetakis, I. E. 2017. First Report of Citrus leaf blotch virus in Peony in the U.S.A. *Plant Dis.* 101, 637–637.

19. Guardo, M., Sorrentino, G., Marletta, T., and Caruso, A. 2007. First Report of Citrus leaf blotch virus on Kumquat in Italy. *Plant Dis.* 91, 1054.

20. Guerri, J., Pina, J. A., Vives, M. C., Navarro, L., and Moreno, P. 2004. Seed Transmission of Citrus leaf botch virus: Implications in Quarantine and Certification Programs. *Plant Dis.* 88, 906–906.

21. Hajeri, S., Ramadugu, C., Keremane, M., Vidalakis, G., and Lee, R. 2010. Nucleotide sequence and genome organization of Dweet mottle virus and its relationship to members of the family Betaflexiviridae. *Arch. Virol.* 155, 1523–1527.

22. Hamdi, I., Elleuch, A., Bessaies, N., Grubb, C. D., and Fakhfakh, H. 2015. First report of Citrus viroid V in North Africa. *J. Gen. Plant Pathol.* 81, 87–91.

23. Ito, T., and Ohta, S. (2010). First report of Citrus viroid V in Japan. *J. Gen. Plant Pathol.* 76, 348–350.

24. Langmead, B., Trapnell, C., Pop, M., and Salzberg, S. L. 2009. Ultrafast and memory-efficient alignment of short DNA sequences to the human genome. *Genome Biol.* 10, R25.

25. Liu, H., Song, S., Wu, W., Mi, W., Shen, C., Bai, B., et al. 2019. Distribution and molecular characterization of Citrus leaf blotch virus from Actinidia in Shaanxi province, China. *Eur. J. Plant Pathol.* 154, 855–862.

26. Madden, T. L., Tatusov, R. L., and Zhang, J. 1996. Applications of network BLAST server. *Methods Enzymol.* 266, 131–141.

27. Moreno, P., Ambrós, S., Albiach-Martí, M. R., Guerri, J., and Peña, L. 2008. Citrus tristeza virus: a pathogen that changed the course of the citrus industry. *Mol. Plant Pathol.* 9, 251–268.

28. Navarro, L., Pina, J. A., Ballester-Olmos, J. F., Moreno, P., and Cambra, M. 1984. A new graft transmissible disease found in Nagami kumquat. in *International Organization of Citrus Virologists Conference Proceedings (1957-2010)* (escholarship.org). Available at: https://escholarship.org/content/qt3kk581p9/qt3kk581p9.pdf.

29. Osman, F., Hodzic, E., Kwon, S.-J., Wang, J., and Vidalakis, G. 2015. Development and validation of a multiplex reverse transcription quantitative PCR (RT-qPCR) assay for the rapid detection of Citrus tristeza virus, Citrus psorosis virus, and Citrus leaf blotch virus. *J. Virol. Methods* 220, 64–75.

30. Ruiz-Ruiz, S., Ambrós, S., Vives, M. del C., Navarro, L., Moreno, P., and Guerri, J. (2009). Detection and quantitation of Citrus leaf blotch virus by TaqMan real-time RT-PCR. *J. Virol. Methods* 160, 57–62.

31. Saponari, M., Manjunath, K., and Yokomi, R. K. (2008). Quantitative detection of Citrus tristeza virus in citrus and aphids by real-time reverse transcription-PCR (TaqMan®). *J. Virol. Methods* 147, 43–53.

32. Serra, P., Barbosa, C. J., Daròs, J. A., Flores, R., and Duran-Vila, N. 2008a. Citrus viroid V: molecular characterization and synergistic interactions with other members of the genus Apscaviroid. *Virology* 370, 102–112.

33. Serra, P., Eiras, M., Bani-Hashemian, S. M., Murcia, N., Kitajima, E. W., Daròs, J. A., et al. 2008b. Citrus viroid V: occurrence, host range, diagnosis, and identification of new variants. *Phytopathology* 98, 1199–1204.

34. Vidalakis, G., and Wang, J. (2013). Molecular method for universal detection of citrus viroids. United States patent US 2013/0115591 A1, May 9, 2013.

35. Vives, M. C., Galipienso, L., Navarro, L., Moreno, P., and Guerri, J. 2001. The nucleotide sequence and genomic organization of Citrus leaf blotch virus: candidate type species for a new virus genus. *Virology* 287, 225–233.

36. Vives, M. C., Rubio, L., Galipienso, L., Navarro, L., Moreno, P., and Guerri, J. 2002. Low genetic variation between isolates of Citrus leaf blotch virus from different host species and of different geographical origins. *J. Gen. Virol.* 83, 2587–2591.

37. Wallace, J. M. (1978). Virus and viruslike diseases [of citrus]. *Citrus Industry Berkeley. University of California, Division of Agricultural Sciences*. Available at: https://agris.fao.org/agris-search/search.do?recordID=US19800539930.

38. Wang, J., Boubourakas, I. N., Voloudakis, A. E., Agorastou, T., Magripis, G., Rucker, T. L., et al. (2013). Identification and characterization of known and novel viroid variants in the Greek national citrus germplasm collection: threats to the industry. *Eur. J. Plant Pathol.* 137, 17–27.

39. Wang, J., Zhu, D., Tan, Y., Zong, X., Wei, H., and Liu, Q. 2016. First Report of Citrus leaf blotch virus in Sweet Cherry. *Plant Dis.* 100, 1027–1027.

40. Xuan, Z., Xie, J., Yu, H., Zhang, S., Li, R., and Cao, M. 2020. Mulberry (Morus alba) is a new natural host of Citrus leaf blotch virus in China. *Plant Dis.* doi:10.1094/PDIS-07-20-1580-PDN.

41. Zuker, M. (2003). Mfold web server for nucleic acid folding and hybridization prediction. *Nucleic Acids Res.* 31, 3406–3415.

Chapter III

Development of *in silico* detection assays for citrus pathogens from raw high throughput sequencing data

Note: some of the contents of this chapter are adapted from Dang, T. et al. (2021). An *In-silico* Detection of a Citrus Viroid from Raw High Throughput Sequencing Data. In: Rao, A., Lavagi-Craddock, I., Vidalakis, G., (Eds), Methods Molecular Biology, Viroids. Vol. 2316 Springer *In press*.

ABSTRACT

The cost for high-throughput sequencing (HTS) has decreased significantly and has made it possible for the application of this technology to be expanded into routine plant diagnostics. There are constraints with the use of HTS as a diagnostic tool which include the need for dedicated personnel with bioinformatics background for data analysis and the lack of a uniform raw sequences analysis pipeline that makes evaluating and validating results generated at different HTS laboratories difficult. E-probe Diagnostic for Nucleic Acid Analysis (EDNA) is an *in silico* bioinformatic tool that utilizes short curated electronic probes (e-probes) designed from pathogen specific sequences which allow users to detect and identify a single or multiple pathogens of interest from raw HTS datasets. This platform can alleviate the above mentioned problems for the use of HTS as a routine plant diagnostic tool. In this study, I provided the proof of concept for the development, validation and use of e-probes for the detection

and identification of three different types of citrus graft-transmissible pathogens, a virus, a viroid and a bacterium i.e., citrus tristeza virus (CTV), citrus exocortis viroid (CEVd), and *Candidatus* Liberibacter asiaticus (CLas). I was able to demonstrate that HTS and EDNA can be extremely sensitive and specific to the targeted pathogens and perform equally well as the current citrus pathogen detection tools such as polymerase chain reaction. Finally, I proved that the HTS and EDNA technologies can be easily integrated into existing citrus testing laboratories as in the past year the Citrus Clonal Protection Program has tested with this technology on 6 citrus introductions for federal and state quarantine release.

INTRODUCTION

Citrus is an iconic high value crop in California (CA, estimated at $3.4 billion) that is under constant threat of endemic and exotic citrus pathogens (Babcock 2018). State and federal phytosanitary regulations, quarantine programs for variety introductions , and frequent testing of tree sources for propagative materials at citrus nurseries have helped exclude pathogens from establishing and spreading in CA (Bostock et al. 2014; Gergerich et al. 2015; Fuchs et al. 2021). Many diagnostic methods have been developed for the detection of citrus pathogens. Traditional methods like biological indexing have proved reliable for detecting pathogens, however the method is low throughput, time consuming, demands highly trained and experienced personnel in the identification of symptoms, and requires large greenhouse space to maintain different species of plant indicators in order to detect a wide range of citrus pathogens (Roistacher 1991; Vidalakis et al. 2004). The transition to laboratory based methods such as enzyme-linked

immunosorbent assay (ELISA), sequential polyacrylamide gel electrophoresis (sPAGE), and polymerase chain reaction (PCR) based methods have helped streamline citrus diagnostics and have laid the foundation for the transition towards high throughput workflows (Duran-Vila et al. 1993; Cambra et al. 2000; Osman et al. 2015). With the rise in use and declining cost of high throughput sequencing (HTS), it appeared to be the most logical development for the ever evolving citrus diagnostics (Figure 3.2) is the transition to HTS based methods (Shendure and Ji 2008; Adams et al. 2009).

HTS is a powerful technology that combines molecular biology and computer science. It has been used in various applications, not just as a research tool, for gene expression studies or the *de novo* discovery of pathogens (Adams et al. 2009; Villamor et al. 2019). The technology has also gained traction and showed potential as a routine plant diagnostic tool for the detection and identification of pathogens (Al Rwahnih et al. 2015; Visser et al. 2016; Rott et al. 2017; Villamor et al. 2019; Soltani et al. 2021). In the case of citrus, the proper implementation of HTS based diagnostics can streamline laboratory processes and progressively compliment and phase out more than 20 individual laboratory tests (PCR, qPCR, ELISA, etc.) currently required for the detection of all known graft-transmissible pathogens of citrus. HTS can generate data with enough resolution to discern between different isolates of the same pathogen. HTS will allow for the reduction of plant indicators used for biological indexing that will free valuable greenhouse space. The constant declining cost of HTS, has made the technology more accessible for laboratories to implement (Shendure and Ji 2008; Adams et al. 2009).

On the other hand, one of the difficulties with implementing HTS based diagnostics is the analysis of millions of data points. HTS data analysis is time consuming, laborious, and requires dedicated personnel with high-level knowledge in bioinformatics and computer programming as well as access to expensive high-performance computing. Cut off values for diagnostic calls using a traditional bioinformatic workflow (i.e., aligning, assembling and BLASTn reads) can vary from lab to lab and in some cases can be arbitrary (Rott et al. 2017; Massart et al. 2019). Online platforms such as Virfind provide an accessible bioinformatic pipeline that can be used for pathogen identification(Ho and Tzanetakis 2014). However such analysis can be over complicated because of the different parameters that the user needs to define for the statistical cut off values as well as the excess information provided by the software and the finds in the global database searches that subsequently needs to be sorted by the user including the report of unrelated or unknown pathogens to the tested plant species i.e. non-citrus pathogens (Villamor et al. 2019).

To overcome the challenges with HTS data analysis, the E-probe Diagnostic for Nucleic Acid Analysis (EDNA) was originally developed by Oklahoma State University Institute of Biosecurity and Microbial Forensic as a user-friendly online HTS data analysis tool for diagnostic applications of specific targeted pathogens and not for the *de novo* discovery of all pathogens and pathogen like sequences in an HTS data set. EDNA is an *in silico* bioinformatic tool that utilizes short curated electronic probes (e-probes) designed from pathogen specific sequences. The e-probes allow users to detect and identify a single or multiple pathogens of interest from raw HTS datasets and ignore

irrelevant sequences such as the host or other not-targeted microbes present in the sample similarly to the use of pathogen specific primers used in a PCR reaction (Stobbe et al. 2013, 2014). EDNA can be utilized on raw HTS data generated from different sequencing platforms such as Illumina (San Diego, CA) and MinIon (Oxford Nanopore, Oxford, UK). This technology has been previously used for the detection of foodborne pathogens such as *E. coli* O157: H7 (Blagden et al. 2016), plant pathogens such as oomycetes (*Phytophthora ramorum* and *Pythium ultimum*), fungi (*Phakopsora pachyrhizi* and *Puccinia graminis*) (Espindola et al. 2015), and viruses (plum pox virus) (Stobbe et al. 2014).

In this study, I provide evidence that HTS and EDNA technologies can be utilized as a routine diagnostic tool for the detection of citrus pathogens. As a proof of concept, e-probes were developed, validated and used for the detection and identification of citrus tristeza virus (CTV), citrus exocortis viroid (CEVd), and *Candidatus* Liberibacter asiaticus (CLas) as representatives of the three different types of graft-transmissible pathogens of citrus namely a virus, a viroid and a bacterium. In order for the HTS/EDNA technology to be adopted for mainstream citrus diagnostics, the e-probes' performance (i.e., sensitivity, specificity, and reproducibility) must be evaluated against the currently used diagnostic methods. Side-by-side comparisons of HTS/EDNA and PCR assays for the detection of known graft-transmissible pathogens of citrus available in the Citrus Clonal Protection Program (CCPP) disease bank, as single and mixed infected samples.

MATERIALS AND METHOD

Tissue preparation

All samples were collected from one-year old hardened stems around the canopy of the citrus tree. A clean razor blade was used to peel the phloem rich bark tissues from the stems. The peeled samples were transferred to a mortar filled with liquid nitrogen and pulverized with a pestle into a fine powder. One-hundred mg of the powdered sample was transferred to a 2.0 mL microcentrifuge tube (Eppendorf, Hamburg, Germany) using a disposable spatula and immediately placed into -80°C until all samples were processed.

RNA extraction

RNA was extracted from the pulverized bark tissues using TRIzol™ following the manufacturer's recommended protocol adjusted for citrus tissues. More specifically, one mL of TRIzol™ reagent was added to the pulverized tissues. Samples were homogenized with a vortex for 20 seconds, centrifuged at 4°C for 5 minutes at 12,000 x g and the supernatant was transferred to a new 1.5 mL microcentrifuge tube. Two-hundred µL of chloroform were added and the samples were incubated at room temperature for 3 minutes. Samples were centrifuged for 15 minutes at 12,000 x g at 4°C. The aqueous phase was transferred to a new 1.5 mL microcentrifuge tube and 500 µL of isopropanol were added to each sample. Samples were incubated at room temperature for 10 minutes and subsequently centrifuged at 4°C for 10 minutes at 12,000 x g. The supernatant was discarded and 1 mL of 75% ethanol was added. The samples were vortexed briefly and centrifuged at 4°C for 5 minutes at 7,500 x g. Ethanol was discarded and the pellet was

left to air dry for 30 minutes to 1 hour. The RNA pellet was resuspended in 100 µL of UltraPure™ DNase/RNase-free distilled water (Thermo Fisher Scientific, Waltham, MA). The extracted RNA was aliquoted into three 1.5 mL DNA LoBind® microcentrifuge tubes (Eppendorf, Hamburg, Germany) and stored at -80°C until further use.

DNA Extraction

DNA extraction was performed using the DNeasy® Plant Mini Kit (Qiagen, Valencia, CA). Four-hundred µL of Buffer AP1 and 4 µL of RNase A was added to each pulverized bark tissue sample. The samples were mixed by tube flicking in order to prevent DNA from shearing and subsequently incubated at 65°C for 10 min. Aftwards, 130 µL of Buffer P3 were added to each sample and incubated on ice for 5 min. The sample was centrifuged for 5 min at 20,000 x g. The lysate was transferred into a QIAshredder spin column and then centrifuge for 2 min at 20,000 x g. The flow-through was transferred to a new tube and 1.5 volume of Buffer AW1 was added and gently mixed by pipetting. Six hundred fifty µL of the mixture was transferred into a DNeasy Mini spin column. The column was centrifuged for 1 min at 6,000 x g and the flow through was discarded. This step was repeated with the remaining sample. The spin column was transferred to a new 2 mL collection tube and 500 µL of Buffer AW2 was added. The column was centrifuged for 1 min at 6,000 x g at room temperature. The wash was repeated and the column was centrifuged for 2 min at 20,000 x g. The spin column was transferred to a 1.5 mL microcentrifuge tube and 100 µL of Buffer AE was added and incubated at 5 min at room temperature. The samples were centrifuged for 1 min at

6,000 x g room. The extracted DNA was aliquoted into three 1.5 mL DNA LoBind® microcentrifuge tubes (Eppendorf, Hamburg, Germany) and stored at -20°C until further use.

Depletion of host ribosomal RNA for RNA HTS

Plant ribosomal depletion was performed on the HTS samples using the Illumina Ribo-Zero rRNA Removal Kit for plants (San Diego, CA) following the manufacturer's recommended protocol. For the ribosomal depletion, RNA samples were first adjusted to 1 µg in a total of 10 µL, then 5 µL of RBB and 5 µL of RRM-P was added to the reaction. The samples were incubated in a ProFlex thermal cycler (Thermo Fisher Scientific, Waltham, MA) at 68°C for 5 mins. Afterwards, 35 µL of RRB was added, incubated at room temperature, placed on a magnetic stand, and transferred to a new tube. Sample was cleaned with 99 µL of AMPure XP Beads (Beckman Coulter, Brea, CA), incubated at room temperature for 15 mins, placed on a magnetic stand until the liquid was clear, and discarded all of the supernatant from each tube. Sample was washed using 200 µL of freshly prepared 70% EtOH and air-dried on the magnetic stand. Once dried, 11 µL of ELB was added to each tube, incubated at room temperature until the liquid was clear, and transferred 8.5 µL supernatant to a new tube. Subsequently, 8.5 µL of EPH was added and then incubated in a ProFlex thermal cycler at 94°C for 8 minutes.

HTS library preparation and data analysis

HTS library was prepared using the Illumina TruSeq Stranded Total RNA kit (San Diego, CA) using the manufacturer's recommended protocol. The first strand cDNA synthesis was prepared by adding 8 µL FSA and SuperScript II mixture (ratio: 1 µL of

SuperScript II and 9 µL of FSA) to each tube of the rRNA depleted samples. The mixture was placed into the thermal cycler with the following conditions: 25°C for 10 mins, 42°C for 15 mins, and 70°C for 15 mins.

The second strand cDNA synthesis was performed by adding 5 µL diluted CTE (1:50) and 20 µL SMM to the first strand cDNA mixture and incubated at 16°C for 1 hour. The cDNA was purified by adding 90 µL AMPure XP beads and incubated at room temperature for 15 minutes and placed on a magnetic stand and waited until the liquid was clear (~5 minutes). The supernatant was removed and washed twice by adding 200 µl fresh 80% EtOH to each tube. The sample was air-dried on the magnetic stand for 15 minutes and 17.5 µl RSB was added to the lobind tube. The eluted sample was placed on a magnetic stand until the liquid was clear. Fifteen µl of the elute was transferred to a new tube with 2.5 µl diluted CTA (1:100) and 12.5 µL ATL for the adenlation of 3' ends. The mixture was placed into a ProFlex thermal cycler with the following conditions: 37°C for 30 mins and 70°C for 5 mins. Adapters were ligated to the adenlated mixtures by adding 2.5 µL of diluted CTL (1:100), 2.5 µL LIG, and 2.5 µL of the RNA adapter. The mixture was incubated in a ProFlex thermal cycler at 30°C for 10 mins. The reaction was immediately removed and 5 µL STL was added to each tube. The ligated fragments were cleaned by adding 42 µL of AMPure XP beads, incubated at room temperature for 15 minutes and washed two times with 200 µL of freshly prepared 80% EtOH for 30 seconds. The sample was air-dried on the magnetic stand and 52.5 µL of RSB was added. Fifty µL of supernatant was recovered and a second cleaning was performed by adding 50 µL AMPure XP beads. The sample was incubated at room temperature for 15 minutes

and washed two times with 200 µL freshly prepared 80% EtOH for 30 seconds. The sample was air-dried on the magnetic stand and 22.5 µL of RSB was added. Twenty µL of supernatant was recovered and used for PCR enrichment of DNA fragments. Twenty-five µL of PMM and 5 µL of PPC were added. The sample was placed into a ProFlex thermal cycler with the following conditions: 98°C for 30 seconds, 98°C for 10 seconds, 60°C for 30 seconds, 72°C for 30 seconds for 15 cycles, and 72°C for 5 minutes. The amplified DNA was cleaned by adding 50 µL of AMPure XP beads, incubated at room temperature for 15 minutes, and placed on a magnetic stand until the liquid was clear. The sample was washed twice, with 200 µL fresh 80% EtOH to each tube, air-dried on the magnetic stand for 15 minutes, and 32.5 µL of RSB was added. The sample was placed on a magnetic stand until the liquid was clear and 30 µL of supernatant was aliquoted into 3 screw top tubes and stored at -20°C until further use.

Microbial enrichment

Samples were enriched using the NEBNext Microbiome DNA Enrichment Kit (New England Biolabs, Ipswich, MA). The enrichment beads were prepared by adding 16 µL of MBD2-Fc protein and 160 µL of Protein A Magnetic Beads each sample. The mixture was mixed using a rotating mixer for 10 minutes at room temperature and placed on the magnetic rack for 2–5 minutes. The supernatant was removed with a pipette without disturbing the beads. One ml of 1X Bind/wash Buffer was added to each tube and mixed up and down until the beads are completely homogeneous. The mixture was mixed using a rotating mixer for 3 min and 160 µL of 1X Bind/wash Buffer was added to resuspend the beads. DNA samples were adjusted to 1 µg and 160 µL of the finalized

MBD2-Fc-bound magnetic beads were mixed together. Undiluted Bind/wash Buffer (5X) was added to adjust the final concentration of the sample to 1X. The mixture was agitated on a rotating mixer for 15 minutes at room temperature and then transferred to the magnetic rack for 5 minutes. The supernatant was removed and transferred to a clean microcentrifuge tube. The samples were purified by adding 1.8x volume of AMPure XP bead and was incubated at room temperature for 5 min. The samples were placed on a magnetic stand and the supernatant was discarded. The samples were washed with 200 uL of 80% freshly prepared ethanol while in the magnetic stand and incubated at room temperature for 30 seconds. The supernatant was removed, and the wash step was repeated. The samples were air dried for 5 min on the magnetic stand and 50 µL of 1X TE was added to each sample. The elute was transferred to a new centrifuge for DNA HTS library construction.

DNA HTS library construction

HTS library was prepared using the NEBNext Ultra II FS DNA Library Prep Kit (New England Biolabs, Ipswich, MA). The first strand synthesis was performed by combining the 26 µL of the enriched DNA, 7 µL of Ultra II FS Reaction Buffer, and 2 µL NEBNext Ultra II FS Enzyme Mix. Samples were placed into a ProFlex thermal cycler (Thermo Fisher Scientific, Waltham, MA) with the following conditions: 37°C for 25 mins and 65C for 30 min. Adaptors were ligated by combining: 30 µL of the Ultra II Ligation Master Mix, 1 µL of the Ligation Enhancer NEBNext Adaptor, 2.5 µL of the Adaptor and 35 µL of the first strand reaction mixture. Samples were incubated in the

thermal cycler at 20°C for 15 minute and 3 µL of USER® Enzyme was subsequently added. The mixture was immediately incubated at 37°C for 15 min. Size selection for targets between 150 - 250 bp was performed by adding 28.5 µL 0.1x TE buffer to bring the volume up to 100 µL and 40 µL of AMPure XP beads (Beckman Coulter, Brea, CA). The samples were mixed and incubated for 5 min at room temperature. The samples were placed on the magnetic stand for 5 min and the supernatant was transferred into a new tube. A second size selection was performed by mixing 20 µL of AMPure XP beads to the supernatant and incubating the samples on the bench top for 5 minutes at room temperature. The samples were placed on the magnetic stand for 5 min and the supernatant was discarded. The samples were washed with 200 µL of 80% freshly prepared ethanol while in the magnetic stand and incubated at room temperature for 30 seconds. The supernatant was removed and the wash step was repeated. The sample beads were air dried for 5 minutes on the magnetic stand and 17 µL of 0.1x TE was added and 15 µL to a new PCR tube. PCR enrichment of samples were performed by adding 25 µL Ultra II Q5 Master Mix, 5 µL Universal PCR primer and 5 µL Index primer to the sample. The sample was placed into a ProFlex thermal cycler with the following conditions: 98°C for 30 seconds, 98°C for 10 seconds, 65°C for 75 seconds for 5 cycles, and 65°C for 5 min. The PCR reaction was cleaned by adding 45 µL AMPure XP beads and incubated the samples for 5 min at room temperature. The bead mixture was placed on a magnetic stand and the supernatant was discarded. The samples were washed twice with 200 µL of 80% freshly prepared ethanol while in the magnetic stand and incubated at room temperature for 30 seconds. The supernatant was removed, and the wash step

was repeated. The samples were air dried for 5 min and 33 µL of 0.1X TE was added. The sample was placed on a magnetic stand until the liquid was clear and 30 µL of supernatant was aliquoted into 3 screw top tubes and stored at -20°C until further use.

Assess the RNA and DNA quantity and quality with the Nanodrop™ instrument, Qubit™ and Agilent Bioanalyzer. The finalized sample was submitted to UC Riverside IIGB Core Facility for sequencing using the Illumina NextSeq500 platform with paired end reads (2 × 75 bp).

HTS data processing and analysis

Low-quality Illumina reads were filtered with Fastqc (Andrews 2010) using the default settings. After quality control, citrus host reads were removed by using Bowtie2 version 2.3.4.1 (Langmead et al. 2009) by mapping the reads to the reference citrus genome (*Citrus sinensis*, GCA_000317415). Reads that mapped to the citrus reference genome were discarded and the unmapped reads were assembled *de novo* using Trinity version 2.8.5 (Grabherr et al. 2011). BLASTn (Altschul et al. 1990; Madden et al. 1996) was performed to confirm the identity of the assembled contigs. A custom Unix shell and R script was used to filter out BLASTn results that were relevant only to citrus pathogens.

Diagnostic verification with PCR

PCR was performed for the validation of HTS and EDNA results. The list of primers and probes used in this study are summarized in **Table 3.1**. All multiplex reverse

transcription-quantitative PCRs (RT-qPCR) were performed in 12 µL reactions using the QuantiFast Multiplex RT-PCR kit (Qiagen, Valencia, CA), 0.045 µL of nuclease free water, 6.25 µL of 2x QuantiFast RT Master Mix, 0.58 µL primer and probe mix, 0.125 µL QuantiFast RT mix and 5 µL total RNA. For the detection of citrus viroids, two sets of SYBR® Green RT-qPCR primers namely "Nonapsca" and "Apsca" were previously developed for the universal detection of all known citrus viroids (Vidalakis and Wang 2013). The reaction was prepared with: 7.4 µL of nuclease free water, 0.6 µL of forward and reverse primer, and 1 µL of template. The mixture was sealed and incubated in a thermocycler for 5 minutes at 80°C to denature the targeted RNA. The samples were taken out of the thermocycler and immediately cooled in an ice bath for at least 5 minutes. Once cooled, 10 µL of iTaq™ Universal SYBR® Green reaction mix (Bio-Rad, Hercules, CA) and 0.25 µL reverse transcriptase enzyme were added for a total reaction volume of 20 µL. The samples were loaded into a CFX96™ Real-Time PCR machine (Bio-Rad, Hercules, CA) with the following conditions: reverse transcription at 50°C for 30 mins, 95°C for 5 mins, 95°C for 10 sec, 61°C for "Nonapsca" or 62°C for Apsca viroids for 30 sec for 35 cycles, 95°C for 1 min, 55°C for 1 min, and melting curve analysis from 55 to 95°C with 0.5°C increments for 10 sec (Vidalakis and Wang 2013; Chambers et al. 2018) (**Table 3.2**).

RT-PCR reactions were in a total of 20 µL: 1 µL of RNA template, 2.6 µL nuclease-free water, 1.2 µL of forward and reverse primers, 10 µL of 5x Qiagen OneStep RT-PCR Buffer, 2 µL of Qiagen OneStep RT-PCR Enzyme Mix, and 2 µL of 10 mM dNTP were added to the reaction mixture. The mixture was loaded into a ProFlex PCR

instrument (Thermo Fisher Scientific, Waltham, MA) with the following conditions: 50°C for 30 mins, 95°C for 15 mins, 94°C for 1 min, 60°C for 30 secs, 72°C for 1 min for 30 cycles and 72°C for 10 mins.

qPCR for detection of CLas was performed in 20 µL: 7.7 µL of nuclease-free water, 0.5 µL of forward and reverse primer, 10 µL of iTaq Universal Probes Supermix (Bio-Rad, Hercules, CA), 0.3 µL of probe, and 1 µL of template. The samples were loaded into aCFX96™ Real-Time PCR machine (Bio-Rad, Hercules, CA) with the following conditions: 95°C for 5 min, 95°C for 10 sec, and 58°C for 30 sec for 40 cycles. All PCRs performed had the appropriate positive and negative controls in ordinance with the MIQE guidelines (Bustin et al. 2009).

Biological indexing

Biological indexing was performed to resolve any samples that had conflicting CTV results between the PCR and the HTS/EDNA data. The suspected CTV false positive samples were graft-inoculated onto 6 Mexican limes (*Citrus aurantifolia* (Christm.) Swingle) seedlings with 2 blind buds of inoculation in each tree indicator as described by (Vidalakis et al. 2004). Known healthy and CTV positive samples were used as controls. The inoculum was checked for survival two weeks after inoculation and the plants were maintained under cool greenhouse conditions (18 to 27°C) and monitored for virus symptoms development.

E-probe design and validation

E-probes, ranging from 20 to 40 nt, were designed to target CTV, CEVd, and CLas. The pathogen target and the taxonomically near neighbors or other citrus pathogen genomes were retrieved from NCBI GenBank (**Figure 3.1**). Pathogen specific sequences were identified using the EDNA built in sequence alignment program MUMmer by comparing the target and the near neighbors sequences (Delcher et al. 2003). The similar sequences were removed while the unique sequences used for the e-probes were uploaded to NCBI for BLASTn analysis. Any hits with an e-value of 1×10^{-10} or lower and not from the target pathogen were removed from the final e-probe set (Stobbe et al. 2013, 2014). Decoy e-probes were generated from the curated e-probes by using the reverse sequence of the target e-probe. The analysis was based on a T-test comparing the scores of the target and the decoy e-probes. No significant differences between the target and decoy scores indicated the absence of the targeted pathogen (p-value > 0.5), while a significant difference indicated the presence of the targeted pathogen (p-value < 0.5) (Stobbe et al. 2013) (**Figure 3.1**). MetaSim was used to generate synthetic HTS data from the reference citrus genome (*Citrus sinensis*, GCA_000317415) and the targeted pathogens (i.e., CTV, CEVd, and CLas) for e-probe validation (Richter et al. 2008). The HTS data was generated with approximately 10 million reads per sample and spiked with a percentage of pathogen sequence reads that ranged from 0.01% to 0.0001%. The "empirical" option was utilized to generate data that was in line with Illumina sequencing lengths and error rates.

EDNA data analysis

For EDNA data analysis, the compressed raw HTS fastq files were uploaded onto the MiFi™ platform (https://bioinfo.okstate.edu/) (**Figure 3.1**).

RESULTS

E-probes development

As a proof of concept for the application of EDNA technology for the detection of citrus pathogens from raw HTS data, e-probes were designed for three different organisms that represent a range of genome sizes: virus (CTV-19Kb), viroid (CEVd-0.3Kb), and a bacterium (CLas-2.7Mb). The genome sequences used to develop the e-probes are summarized in **Table 3.2**. A total of 12 CTV, 6 CEVd, and 10 CLas genome sequences from different isolates or genotypes were used to generate the pathogen e-probes. E-probes with lengths of 20 and 30 nt were designed for CTV and CEVd, while e-probes with 40 nt in length were designed for CLas. The e-probes were curated by comparing genome sequences against other citrus pathogens and BLASTn analysis was performed to identify and retain the pathogen specific e-probes of interest. The final CTV-30 and 20 nt design, generated 860 and 1,149 e-probes respectively. E-probes for CEVd-30 and 20nt were 6 and 12, while the CLas design generated 9,005 e-probes (**Table 3.3).**

Determine the sensitivity of pathogen e-probes from simulated HTS data

Simulated data was used to test the theoretical limit of detection (LOD) for the e-probes designed for CTV, CEVd and CLas. For each simulated Illumina data set, a total number of 10 million reads were generated. Pathogen and citrus host sequences were simulated together *in silico*. The pathogen sequences were added into the dataset that ranged from 0.01 to 0.00001% of the total reads generated (**Table 3.4A - 3.4C**). The simulated data was uploaded to MiFi for analysis with the sensitivity set to 5 hits and an e-value of $1x10^{-1}$. All e-probes reliably detected the pathogen of interest at 0.01% and 0.001% pathogen reads (**Table 3.4A - 3.4C**). The CTV-30nt e-probes began showing conflicting results when the percent pathogen reads were approximately 0.0001% (15 and 23 CTV reads), defining the LOD at those levels. The CTV-20nt e-probes on the other hand were theoretically more sensitive and approached the LOD at 0.00001% pathogen reads (2 and 3 CTV reads) (**Table 3.4A**). A similar trend was observed with the CEVd-30 and CEVd-20nt e-probes where the LOD was defined at 0.00001% pathogen reads (**Table 3.4B**). The CLas-40nt e-probes LOD showed similar sensitivity to the CTV-30nt at 0.0001% (11 and 13 CLas reads) (**Table 3.4C**).

Comparison of traditional HTS analysis/EDNA and PCR based methods

All positive controls were screened with PCR for the targeted pathogen and other graft-transmissible citrus pathogens that could have been present in the sample. Results between the traditional HTS analysis and EDNA and PCR were the same between the different methods. (**Table 3.5**). Healthy controls from different varieties were tested with

the different diagnostic methods (**Table 3.6**). EDNA results remained negative indicating that e-probes were not cross reacting with the citrus host genome sequences.

There were instances where CTV reads were detected with the traditional HTS analysis and EDNA while the PCR results were negative for CTV. For these specific samples, PCR was able to detect the targeted pathogens, but not CTV. Biological indexing on Mexican lime was performed in order to resolve this discrepancy in the results. All samples inoculated to the Mexican lime plant indicators did not develop any symptoms associated with CTV. On the other hand, all negative and positive Mexican lime controls remained symptomless and developed typical CTV symptoms (i.e., vein clearing), respectively (**Table 3.7**). Mexican lime is also the plant indicator for citrus vein enation virus (CVEV). According to HTS results the CVEV sample VE 709 was presumably also infected with CTV. While enations were developed on the veins in the lower leaf surface of the Mexican lime trees inoculated with CVEV isolate VE709, no CTV symptoms were developed even after 6-month post inoculation (**Table 3.7**).

The fact that HTS analysis presumably detected CTV in all tested samples (**Table 3.7**) in combination with the lack of any biological evidence for the presence, systemic accumulation and symptom expression on the specific CTV plant indicator indicated that the discrepant HTS CTV results were most likely a result of cross contamination during the sampling extraction or library preparation. These findings indicate the importance of maintaining strict cleaning and decontamination protocols at the laboratory areas and

equipment that process samples that will be analyzed by HTS (Massart et al. 2014; Adams et al. 2018; Osman et al. 2021).

DISCUSSION

HTS has become a popular molecular tool and the decreasing cost has made it possible for its application to be expanded into plant diagnostics. In this study I showed that the combination of HTS and EDNA platforms perform equally well compared to the validated, regulatorily approved and currently widely used diagnostics assays such as PCR (**Table 3.5-3.6**). As with any pathogen detection technology there are limitations with HTS and EDNA, as it is not a “one shoe fits all" method.

For example, HTS is extremely sensitive and can be prone to cross-contamination false positive results (**Table 3.7**). This places a greater importance on the need to implement laboratory operation protocols that are stricter compared to protocols for handling and preparing samples for PCR based diagnostics (Borst et al. 2004). Samples should be handled with extreme care and implement strict cleaning and decontamination protocol in order to reduce the chances for cross-contamination false positives. In addition, this places an importance on the need to progressively incorporate HTS as a complementary diagnostic tool in a lab or a program and retain the validated PCR and bioindexing based diagnostic methods. This can continue until large numbers of samples under different “real life” circumstances (i.e., not controlled experiments with greenhouse-maintained pathogen isolates or *in silico* simulations etc.) have been tested with HTS with comparable results with PCR or bioindexing. At such a point, the PCR

and bioindexing based assays can be scaled down and be used on a limited basis to support HTS and EDNA as needed to resolve any questionable results that may arise. EDNA is a dynamic platform that allows for the continued expansion of the citrus pathogen e-probes library as new pathogens are discovered or new isolates and variants of the known ones are characterized and sequenced.

EDNA allows for the design of e-probes via a crowd sourced model where experts in their respective fields are designing e-probes based on the sequence data available not only on public databases but on data available only to their laboratories. EDNA simplifies and streamline the HTS data analysis process without the need of dedicated highly trained bioinformatic personnel to analyze the millions of the data points resulting in some cases to arbitrary and non-comparable results for the same samples among different laboratories (Rott et al. 2017). The EDNA platform allows for the standardization in HTS data analysis and can be a starting point for quality assurance and accreditation for laboratories using HTS as a diagnostic tool in order to make pathogen detection results comparable and reliable utilizing the standard approach of proficiency tests (a.k.a., ring tests) among different HTS/EDNA laboratories (Soltani et al. 2021). Finally, EDNA is not limited to Illumina, but can be used with other sequencing platforms such as the Oxford Nanopore MinION (Liefting et al. 2021; Phannareth et al. 2021). This level of integration allows greater flexibility for laboratories and does not require dependence on sequencing facilities or one specific sequence technology.

In this chapter, I demonstrated that the HTS/EDNA technology is applicable and shows promise as a routine citrus pathogen detection tool. However, before it becomes mainstream widely adopted by citrus diagnostic laboratories and quarantine or survey programs it will require regulatory approval. The regulatory approval process will require more comprehensive studies that will demonstrate that HTS/EDNA can work equally well or better than the current regulatory approved diagnostic assays for each of the targeted pathogens. Based on the experience of the current study, a key element for the successful implementation and regulatory approval of the HTS/EDNA technologies is the development of sophisticated statistical models that will constantly fine-tune the EDNA protocols on their capacity to decipher the quantitative results of the multiple e-probes detection hits as they scout the millions of HTS sequence data point for their targeted pathogens.

HTS/EDNA based diagnostics is a new technology that will undergo great scrutiny and evaluation from multiple laboratories and scientists in the near future. However, once it is proven to perform accurately and reliably and is approved by the regulatory agencies, the technology has the potential to be incorporated seamlessly to existing citrus testing laboratories and programs (e.g., germplasm and quarantine introductory programs) and truly transform their operations since diagnostics is one of their most important functional pillars (Gergerich et al. 2015; Fuchs et al. 2021).

Pathogen	Reference
RT-qPCR Taqman®	
Citrus tristeza virus (CTV)	
Citrus psorosis virus (CPsV)	Osman et al. 2015
Citrus leaf blotch virus (CLBV)	
Citrus bent leaf viroid (CBLVd)	
Hop stunt viroid (HSVd)	Osman et al 2017
Citrus exocortis viroid (CEVd)	
RT-qPCR SYBR® Green	
Citrus bent leaf viroid, Citrus dwarfing viroid, Citrus viroid V, CVd VI, CVd VII	Vidalakis and Wang 2013
Citrus exocortis viroid, Hop stunt viroid, Citrus bark cracking viroid	
RT-PCR	
Citrus virus A (CiVA)/ Citrus concave gum associated virus (CCGaV)	Navarro et al. 2018
Citrus vein enation virus (CVEV)	Vives et al. 2013
Citrus tatter leaf virus (CTLV)	Roy et al. 2005
Citrus varigated virus (CVV)	Roy et al. 2005
qPCR	
Candidatus Liberibacter asiaticus (CLas)	Li et al. 2008

Table 3.1 Summary of polymerase chain reaction (PCR) primers and probes used in this study.

Pathogen	Genotype/Isolate	Accession #
Citrus tristeza virus	B165	EU076703
	T30	AF260651
	T30	EU937520
	T30	KC517489_FS701
	T30	KC517490_FL278
	T30	KC517491_FS703
	T30	KU578007
	T36	EU937521
	T36	KC517485_FS674
	T36	KC517487_FS701
	T36	KC517487_FS703
	VT	EU937519
		NC001661
Citrus exocortis viroid	AD	AB054592
	-	J02053
	AZN-4	KX156933
	Australia	M34917
	-	M308682
	Reference	NC001464
Candidatus Liberibacter asiaticus	SGCA5	GCA_001430705
	TX2351	GCA_001969535
	HHCA	GCA_000724755
	Psy5	GCA_000023765
	gxpsy	GCF_000346595
	A5	GCF_000590865
	Ishi-1	GCF_000829355
	FL17	GCF_000820625
	YCPsy	GCF_001296945
	JXGC	GCF_002216815
C. Liberibacter americanus		NC022793
C. Liberibacter africanus		NZ_CP004021

Table 3.2 List of genome sequences used to develop the citrus tristeza virus (CTV), citrus exocortis viroid (CEVd) and *Candidatus* Liberibacter asiaticus (CLas) e-probes.

Target pathogen	Genome size (bp)	E-probe length (nt)	Number of e-probes generated
Citrus tristeza virus	~20,000	30	860
		20	1,149
Citrus exocortis viroid	~372	30	6
		20	12
Candidatus Liberibacter asiaticus	~1,200,000	40	9,005

Table 3.3 The e-probe lengths and number of e-probes generated for citrus tristeza virus (CTV), citrus exocortis viroid (CEVd), and *Candidatus* Liberibacter asiaticus (*C*Las).

Table 3.4A		CTV- 30 nt			CTV- 20nt		
Number of CTV reads	**Approximate percent pathogen reads**	**E-probe score**	**P-value**	**Diagnostic results**	**E-probe score**	**P-value**	**Diagnostic results**
1783	0.01	575	8.10E-184	Positive	566	2.33E-141	Positive
1683		576	1.19E-177	Positive	559	1.94E-133	Positive
161	0.001	255	9.52E-47	Positive	203	6.72E-35	Positive
173		226	1.30E-29	Positive	141	3.13E-20	Positive
23	0.0001	58	3.16E-03	Positive	59	7.89E-08	Positive
15		5	0.876	Negative	46	8.07E-04	Positive
3	0.00001	6	0.953	Negative	19	0.087	Negative
2		10	0.383	Negative	32	5.90E-04	Positive
0	0		0.5	Negative		0.5	Negative

Table 3.4A-3.4C Sensitivity results for citrus tristeza virus (CTV), citrus exocortis viroid (CEVd) and *Candidatus* Liberibacter asiaticus (CLas) analyzed with simulated Illumina data generated from MetaSim software from Richter et al. 2008.

Table 3.4B		CEVd- 30 nt			CEVd- 20nt		
Number of CEVd reads	**Approximate percent pathogen reads**	**E-probe score**	**P-value**	**Diagnostic results**	**E-probe score**	**P-value**	**Diagnostic results**
2590	0.01	8	9.62E-05	Positive	15	2.61E-07	Positive
2558		8	4.10E-04	Positive	15	1.91E-07	Positive
220	0.001	8	3.73E-04	Positive	15	1.73E-07	Positive
273		9	2.81E-04	Positive	14	2.70E-07	Positive
27	0.0001	8	7.26E-04	Positive	8	7.88E-03	Positive
39		8	1.44E-04	Positive	14	9.17E-07	Positive
3	0.00001	3	1.98E-01	Positive	2	5.80E-02	Positive
3		3	0.5	Negative	2	0.5	Negative
0	0		0.5	Negative		0.5	Negative

Table 3.4A-3.4C Sensitivity results for citrus tristeza virus (CTV), citrus exocortis viroid (CEVd) and *Candidatus* Liberibacter asiaticus (CLas) analyzed with simulated Illumina data generated from MetaSim software from Richter et al. 2008.

Table 3.4C

Number of CLas reads	Approximate percent pathogen reads	E-probe score	P-value	Diagnostic results
1015	0.01	237	6.02E-48	Positive
1089		237	6.02E-48	Positive
121	0.001	80	2.35E-11	Positive
102		74	5.71E-12	Positive
13	0.0001	12	0.092	Negative
11		12	0.040	Positive
8	0.00001	11	0.129	Negative
9		3	0.500	Negative
0	0		0.500	Negative

Table 3.4A-3.4C Sensitivity results for citrus tristeza virus (CTV), citrus exocortis viroid (CEVd) and *Candidatus* Liberibacter asiaticus (CLas) analyzed with simulated Illumina data generated from MetaSim software from Richter et al. 2008.

Table 3.5

Samples	Pathogen	PCR Results	Traditional HTS analysis	EDNA
IPPN443	CTV	CTV	CTV	CTV
IPPN459	CTV	CTV	CTV	CTV
IPPN465	CTV	CTV	CTV	CTV
IPPN467	CTV	CTV	CTV	CTV
IPPN468	CTV	CTV	CTV	CTV
IPPN495	CTV	CTV	CTV	CTV
B121	CTV	CTV	CTV	CTV
14D-19-2	CTV Viroids	CTV Viroids	CTV CEVd	CTV CEVd
14D-19-3	CPsV CTV Viroids	CPsV CTV Viroids	CTV CEVd	CTV CEVd
14D-19-4	CPsV CTV Viroids	CPsV CTV Viroids	CTV CEVd	CTV CEVd
14D-20-1	CPsV CTV Viroids	CPsV CTV Viroids	CTV CEVd	CTV CEVd
14D-20-2	CPsV CTV Viroids	CPsV CTV Viroids	CTV CEVd	CTV CEVd
14D-21-1	CPsV CTV Viroids	CPsV CTV Viroids	CTV CEVd	CTV CEVd
14D-21-2	CPsV CTV Viroids	CPsV CTV Viroids	CTV CEVd	CTV CEVd
14D-21-3	CPsV CTV Viroids	CPsV CTV Viroids	CTV CEVd	CTV CEVd
P213	CPsV CTV	CPsV CTV	CTV	CTV
CVV2	CVV CEVd	CVV CEVd	CVV CEVd	CEVd
CLBV-CA	CEVd CLBV CVEV	CEVd	CEVd	CEVd
China7	CLas	CLas	CLas	CLas

Table 3.5 Continued

Samples	Pathogen	PCR Results	Traditional HTS analysis	EDNA
744	CLas	CLas	CLas	CLas
FL-Val	CLas	CLas	CLas	CLas
FL-Dancy	CLas	CLas	CLas	CLas
FL-Lemon	CLas	CLas	CLas	CLas
773	CLas	CLas	CLas	CLas
782	CLas	CLas	CLas	CLas
VI840	Healthy	NEG	NEG	NEG
VI853	Healthy	NEG	NEG	NEG
VI854B	Healthy	NEG	NEG	NEG

Table 3.5 Comparison between polymerase chain reaction (PCR), traditional high-throughput sequencing (HTS) analysis and e-probe diagnostics nucleic acid analysis (EDNA) technologies.

Variety		Biological indexing	qPCR Results	HTS Results	EDNA
Mexican Lime	*Citrus aurantifolia*	(-)	(-)	(-)	(-)
Chandler Pummelo	*C.grandis* (L.) Osb.	(-)	(-)	(-)	(-)
S-1 Citron	*C. medica* L.	(-)	(-)	(-)	(-)
Page Mandarin	*C. reticulata* Blanco	(-)	(-)	(-)	(-)
Campbell Nucellar Valencia	*C. sinesis* (L.) Osbeck	(-)	(-)	(-)	(-)
Parent Washington Navel	*C. sinesis* (L.) Osbeck	(-)	(-)	(-)	(-)
Melogold Grapefruit	*C. paradisi* Macfadyen	(-)	(-)	(-)	(-)
Nagami Kumquat	*Fortunella margarita* (Lour.) Swing.	(-)	(-)	(-)	(-)
W. Murcott Afourer Mandarin	*C. reticulata* Blanco	(-)	(-)	(-)	(-)

Table 3.6 List of known healthy controls used to validate high throughput sequencing (HTS) and E-probe diagnostic nucleic acid analysis (EDNA)

Isolate	Experiment #	Pathogen	PCR Results	Traditional HTS analysis	EDNA	Biological Indexing
CG301	3347-1	Citrus virus A (CiVA)	CiVA	CiVA [CTV]	[CTV]	0/4
CTLV100	1703-1	Citrus tatter leaf virus (CTLV)	CTLV	CTLV [CTV]	[CTV]	0/6
K-1	3069-2	Citrus leaf blotch virus (CLBV)	CLBV	CLBV [CTV]	[CTV]	0/5
P205	3347-8	Citrus psorosis virus (CPsV)	CPsV	CPsV [CTV]	[CTV]	0/5
P212	3347-11	CPsV	CPsV, Viroids	CPsV, Viroids [CTV]	[CTV]	0/4
P215	3347-14	CPsV	CPsV, Viroids	CPsV [CTV]	[CTV]	0/5
P250	3347-15	CPsV	CPsV	CPsV [CTV]	[CTV]	0/5
IV402	2923-10	Citrus varigated virus (CVV)	CVV	CVV [CTV]	[CTV]	0/5
IPPN122	2986-48	Mixed	CTLV, Viroids	CTLV, Viroids [CTV]	[CTV]	0/6
VE709**	3273-16	Citrus vein enation virus (CVEV)	CVEV	CVEV [CTV]	[CTV]	0/4
3207-8	3207-8	Viroids	Viroids	Viroids [CTV]	[CTV]	0/6
Controls						
Healthy		-				0/6
SY554	3347-34	CTV+	CTV+	CTV+	CTV+	6/6

Table 3.7 List of samples with conflicting results among the different pathogen detection assays used in this study and the comparison between polymerase chain reaction (PCR), traditional high-throughput sequencing (HTS) analysis, e-probe diagnostic nucleic acid analysis (EDNA) technologies, and biological indexing. Note: **Mexican lime (*Citrus aurantifolia*) is the biological indicator for CTV and citrus vein enation virus (CVEV). CVEV symptoms developed in 4/4 trees while CTV symptoms were not present (0/4).

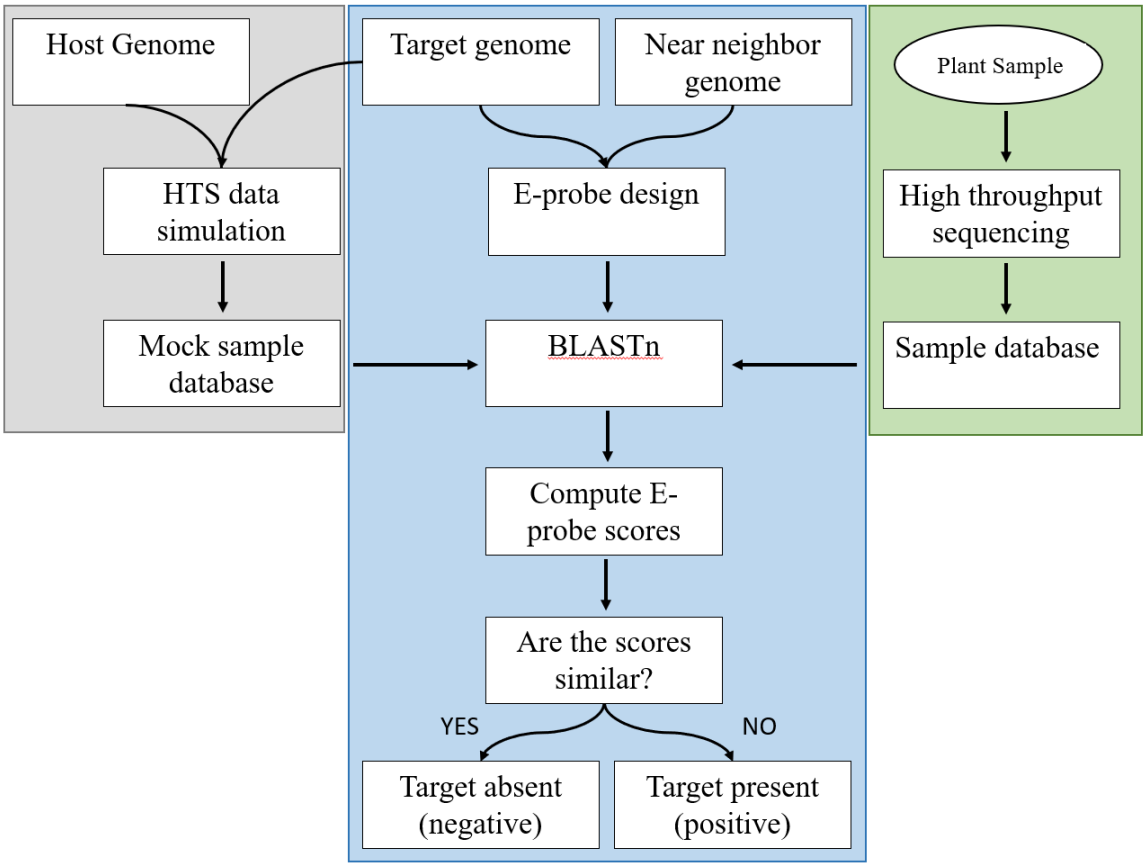

Figure 3.1 Workflow of e-probes the design and application of the EDNA for diagnostic results for citrus tissues.

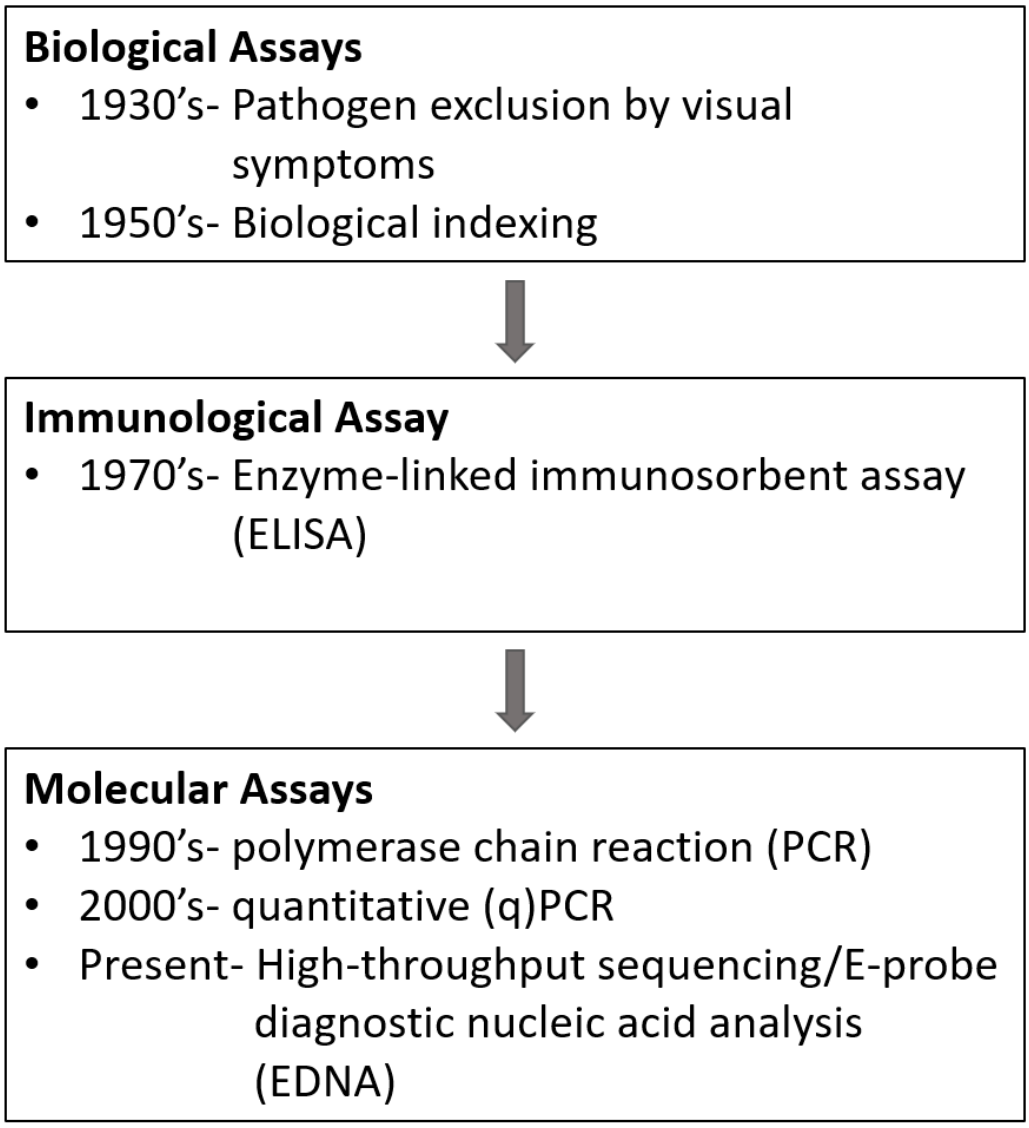

Figure 3.2 The evolution of citrus diagnostics at the Citrus Clonal Protection Program from 1930's, observe visual symptoms, to present day implementation of high throughput sequencing (HTS)/e-probe diagnostic nucleic acid analysis (EDNA).

REFERENCE

1. Adams, I. P., Glover, R. H., Monger, W. A., Mumford, R., Jackeviciene, E., Navalinskiene, M., et al. 2009. Next-generation sequencing and metagenomic analysis: a universal diagnostic tool in plant virology. Mol. Plant Pathol. 10:537–545.

2. Andrews S. 2010. FastQC: a quality control tool for high throughput sequence data.

3. Al Rwahnih, M., Daubert, S., Golino, D., Islas, C., and Rowhani, A. 2015. Comparison of Next-Generation Sequencing Versus Biological Indexing for the Optimal Detection of Viral Pathogens in Grapevine. Phytopathology. :PHYTO–06–14–0165–R.

4. Altschul, S. F., Gish, W., Miller, W., Myers, E. W., and Lipman, D. J. 1990. Basic local alignment search tool. J. Mol. Biol. 215:403–410.

5. Babcock, B. 2018. Economic impact of California's citrus industry. Citrograph. 9:36–39.

6. Blagden, T., Schneider, W., Melcher, U., Daniels, J., and Fletcher, J. 2016. Adaptation and Validation of E-Probe Diagnostic Nucleic Acid Analysis for Detection of Escherichia coli O157:H7 in Metagenomic Data from Complex Food Matrices. J. Food Prot. 79:574–581.

7. Borst, A., Box, A. T. A., and Fluit, A. C. 2004. False-positive results and contamination in nucleic acid amplification assays: suggestions for a prevent and destroy strategy. Eur. J. Clin. Microbiol. Infect. Dis. 23:289–299.

8. Bostock, R., Thomas, C., Hoenisch, R., Golino, D., and Vidalakis, G. 2014. EXCLUDING PESTS AND PATHOGENS: Plant health: How diagnostic networks and interagency partnerships protect plant systems from pests and pathogens. Calif. Agric. 68:117–124.

9. Bustin, S. A., Benes, V., Garson, J. A., Hellemans, J., Huggett, J., Kubista, M., et al. 2009. The MIQE guidelines: minimum information for publication of quantitative real-time PCR experiments. Clin. Chem. 55:611–622.

10. Cambra, M., Gorris, M. T., Román, M. P., Terrada, E., Garnsey, S. M., Camarasa, E., et al. 2000. Routine detection of citrus tristeza virus by direct immunoprinting-ELISA method using specific monoclonal and recombinant antibodies. In *Proc. 14th Conf. IOCV*, escholarship.org, p. 34–41.

11. Chambers, G. A., Donovan, N. J., Bodaghi, S., Jelinek, S. M., and Vidalakis, G. 2018. A novel citrus viroid found in Australia, tentatively named citrus viroid VII. Arch. Virol. 163:215–218.

12. Delcher, A. L., Salzberg, S. L., and Phillippy, A. M. 2003. Using MUMmer to identify similar regions in large sequence sets. Curr. Protoc. Bioinformatics. Chapter 10:Unit 10.3.

13. Duran-Vila, N., Pina, J. A., and Navarro, L. 1993. IImproved Indexing of Citrus Viroids. International Organization of Citrus Virologists Conference Proceedings (1957-2010). 12 Available at: https://escholarship.org/uc/item/2gr565m0.

14. Espindola, A., Schneider, W., Hoyt, P. R., Marek, S. M., and Garzon, C. 2015. A new approach for detecting fungal and oomycete plant pathogens in next generation sequencing metagenome data utilising electronic probes. Int. J. Data Min. Bioinform. 12:115–128.

15. Fuchs, M., Almeyda, C. V., Al Rwahnih, M., Atallah, S. S., Cieniewicz, E. J., Farrar, K., et al. 2021. Economic Studies Reinforce Efforts to Safeguard Specialty Crops in the United States. Plant Dis. 105:14–26.

16. Gergerich, R. C., Welliver, R. A., Osterbauer, N. K., Kamenidou, S., Martin, R. R., Golino, D. A., et al. 2015. Safeguarding Fruit Crops in the Age of Agricultural Globalization. Plant Dis. 99:176–187.

17. Grabherr, M. G., Haas, B. J., Yassour, M., Levin, J. Z., Thompson, D. A., Amit, I., et al. 2011. Full-length transcriptome assembly from RNA-Seq data without a reference genome. Nat. Biotechnol. 29:644–652.

18. Ho, T., and Tzanetakis, I. E. 2014. Development of a virus detection and discovery pipeline using next generation sequencing. Virology. 471-473:54–60.

19. Langmead, B., Trapnell, C., Pop, M., and Salzberg, S. L. 2009. Ultrafast and memory-efficient alignment of short DNA sequences to the human genome. Genome Biol. 10:R25.

20. Li, W., Hartung, J. S., and Levy, L. 2007. Evaluation of DNA Amplification Methods for Improved Detection of "Candidatus Liberibacter Species" Associated with Citrus Huanglongbing. Plant Dis. 91:51–58.

21. Liefting, L. W., Waite, D. W., and Thompson, J. R. 2021. Application of Oxford Nanopore Technology to Plant Virus Detection. Viruses. 13:1424.

22. Madden, T. L., Tatusov, R. L., and Zhang, J. 1996. Applications of network BLAST server. Methods Enzymol. 266:131–141.

23. Massart, S., Chiumenti, M., De Jonghe, K., Glover, R., Haegeman, A., Koloniuk, I., et al. 2019. Virus Detection by High-Throughput Sequencing of Small RNAs: Large-Scale Performance Testing of Sequence Analysis Strategies. Phytopathology. 109:488–497.

24. Navarro, B., Zicca, S., Minutolo, M., Saponari, M., Alioto, D., and Di Serio, F. 2018. A Negative-Stranded RNA Virus Infecting Citrus Trees: The Second Member of a New Genus Within the Order Bunyavirales. Front. Microbiol. 9:2340.

25. Osman, F., Hodzic, E., Kwon, S.-J., Wang, J., and Vidalakis, G. 2015. Development and validation of a multiplex reverse transcription quantitative PCR (RT-qPCR) assay for the rapid detection of Citrus tristeza virus, Citrus psorosis virus, and Citrus leaf blotch virus. J. Virol. Methods. 220:64–75.

26. Osman, F., Dang, T., Bodaghi, S., and Vidalakis, G. 2017. One-step multiplex RT-qPCR detects three citrus viroids from different genera in a wide range of hosts. J. Virol. Methods. 245:40–52.

27. Osman, F., Vidalakis, G., 2021. Real-Time Detection of Viroids Using Singleplex and Multiplex Quantitative Polymerase Chain Reaction. Viroids: Methods and Protocols. Rao, A., Lavagi-Craddock, I., Vidalakis, G. Eds. Springer Nature, Switzerland AG.

28. Phannareth, T., Nunziata, S. O., Stulberg, M. J., Galvez, M. E., and Rivera, Y. 2021. Comparison of nanopore sequencing protocols and real-time analysis for phytopathogen diagnostics. Plant Health Prog. 22:31–36.

29. Richter, D. C., Ott, F., Auch, A. F., Schmid, R., and Huson, D. H. 2008. MetaSim: a sequencing simulator for genomics and metagenomics. PLoS One. 3:e3373.

30. Roistacher, C. N. 1991. *Graft-transmissible Diseases of Citrus: Handbook for Detection and Diagnosis*. Food & Agriculture Org.

31. Rott, M., Xiang, Y., Boyes, I., Belton, M., Saeed, H., Kesanakurti, P., et al. 2017. Application of Next Generation Sequencing for Diagnostic Testing of Tree Fruit Viruses and Viroids. Plant Dis. 101:1489–1499.

32. Roy, A., Fayad, A., Barthe, G., and Brlansky, R. H. 2005. A multiplex polymerase chain reaction method for reliable, sensitive and simultaneous detection of multiple viruses in citrus trees. J. Virol. Methods. 129:47–55.

33. Shendure, J., and Ji, H. 2008. Next-generation DNA sequencing. Nat. Biotechnol. 26:1135–1145.

34. Soltani, N., Stevens, K. A., Klaassen, V., Hwang, M.-S., Golino, D. A., and Al Rwahnih, M. 2021. Quality Assessment and Validation of High-Throughput Sequencing for Grapevine Virus Diagnostics. Viruses. 13 Available at: http://dx.doi.org/10.3390/v13061130.

35. Stobbe, A. H., Daniels, J., Espindola, A. S., Verma, R., Melcher, U., Ochoa-Corona, F., et al. 2013. E-probe Diagnostic Nucleic acid Analysis (EDNA): a theoretical approach for handling of next generation sequencing data for diagnostics. J. Microbiol. Methods. 94:356–366.

36. Stobbe, A. H., Schneider, W. L., Hoyt, P. R., and Melcher, U. 2014. Screening metagenomic data for viruses using the e-probe diagnostic nucleic acid assay. Phytopathology. 104:1125–1129.

37. Vidalakis, G., Garnsey, S. M., Bash, J. A., Greer, G. D., and Gumpf, D. J. 2004. Efficacy of Bioindexing for Graft-Transmissible Citrus Pathogens in Mixed Infections. Plant Dis. 88:1328–1334.

38. Vidalakis, G., and Wang, J. 2013. Molecular method for universal detection of citrus viroids. US Patent US20130115591.

39. Villamor, D. E. V., Ho, T., Al Rwahnih, M., Martin, R. R., and Tzanetakis, I. E. 2019. High Throughput Sequencing For Plant Virus Detection and Discovery. Phytopathology. 109:716–725.

40. Visser, M., Bester, R., Burger, J. T., and Maree, H. J. 2016. Next-generation sequencing for virus detection: covering all the bases. Virol. J. 13:85.

41. Vives, M. C., Velázquez, K., Pina, J. A., Moreno, P., Guerri, J., and Navarro, L. 2013. Identification of a new enamovirus associated with citrus vein enation disease by deep sequencing of small RNAs. Phytopathology. 103:1077–1086.

Chapter IV

Identification and characterization of plant microRNAs of pathogen infected dwarfed citrus trees using high throughput sequencing

Note: the contents of this chapter are adapted from Dang et. al. (2021) Front Microbio. 12. 980.

ABSTRACT

Citrus dwarfing viroid (CDVd) induces stunting on sweet orange trees (*Citrus sinensis* (L.) Osbeck), propagated on trifoliate orange rootstock (*C. trifoliata* (L.), syn. *Poncirus trifoliata* (L.) Raf.). MicroRNAs (miRNAs) are a class of non-coding small RNAs (sRNAs) that play important roles in the regulation of tree gene expression. To identify miRNAs in dwarfed citrus trees, grown in high-density plantings, and their response to CDVd infection, sRNA high throughput sequencing was performed on CDVd-infected and non-infected controls. A total of 1,290 and 628 miRNAs were identified in stem and root tissues, respectively, and among those, 60 were conserved in each of these two tissue types. Three conserved miRNAs (csi-miR479, csi-miR171b and csi-miR156) were significantly downregulated (adjusted p-value <0.05) in the stems of CDVd-infected trees compared to the non-infected controls. The three stem downregulated miRNAs are known to be involved in various physiological and developmental processes some of which may be related to the characteristic dwarfed phenotype displayed by CDVd-infected *C. sinensis* on *C. trifoliata* rootstock field trees. Only one miRNA (csi-miR535) was

significantly downregulated in CDVd-infected roots and it was predicted to target genes controlling a wide range of cellular functions. Reverse transcription quantitative polymerase chain reaction analysis performed on selected miRNA targets validated the negative correlation between the expression levels of these targets and their corresponding miRNAs in CDVd-infected trees. The results indicate that CDVd-responsive plant miRNAs play a role in regulating important citrus growth and developmental processes that may participate in the cellular changes leading to the observed citrus dwarf phenotype. Most importantly, the observed lack of a differential induction and regulation of defense genes via the small RNA pathway in response to CDVd infection strongly concurs with the hypothesis that some viroids might be better considered as RNA elements modifying tree performance rather than infectious agents inducing a specific disease syndrome.

INTRODUCTION

Small RNAs (sRNAs) can be divided into several categories, which include small-interfering (si)RNAs, *trans*-acting (ta)-siRNAs, microRNAs, natural-antisense siRNAs (nat-siRNAs), and Piwi-interacting RNAs (piwi-RNAs) (Borges and Martienssen, 2015; Czech et al., 2018; Zhu et al., 2018; Treiber et al., 2019). One of the major components of endogenous plant sRNAs are microRNAs (miRNAs). miRNAs have essential functions in plant development and are involved in regulating a myriad of plant processes such as leaf, root, stem and floral organ morphogenesis and development, biosynthesis, metabolism, homeostasis, vegetative to reproductive growth transition, senescence, signal transduction and response to biotic and abiotic stress. The biogenesis of miRNA occurs by the

transcription of plant *MIR* genes that have independent transcriptional units with their own regulatory promoters (RNA polymerase II). The primary transcripts (pri-miRNA) form double stranded stem loop structures and are processed by Dicer into precursor miRNAs (pre-miRNAs). The pre-miRNAs (miRNA/miRNA* duplex) is exported into the cytosol and one strand of the duplex is degraded. The remaining mature single stranded miRNA, typically 21-24 nucleotides (nt) in length, is incorporated into the Argonaute protein to form the RNA-induced silencing complex (RISC) which targets complementary RNAs to the miRNA guide strand. Once the activated miRNA-RISC complex finds the complementary plant mRNA, it silences the target via RNA degradation or translational repression (Wang et al., 2019) (**Figure 4.1A**).

Viroid derived sRNAs (vdsRNA) are products of the RNA interference (RNAi) basal plant antiviral defense response (Navarro et al., 2012; Dadami et al., 2013, 2017; Eamens et al., 2014; Adkar-Purushothama et al., 2015, 2017; Reis et al., 2015). Viroids, subviral (246-401nt), highly structured, autonomously replicating RNA plant pathogenic agents, trigger RNAi during their replication due to the formation of double stranded intermediate RNAs (Flores et al., 2009; Dadami et al., 2017). Similar to plant endogenous sRNAs, vdsRNAs are 21-22nt and 24nt in length and have been detected in plants infected by several different viroids (Navarro et al., 2009; Bolduc et al., 2010; Diermann et al., 2010; Tsushima et al., 2011). vdsRNAs play an important role in viroid-mediated biological and pathogenic activities by guiding the RISC-mediated cleavage of host RNAs (**Figure 4.1B**) (Wassenegger et al., 1994; Itaya et al., 2007; Navarro et al., 2012; Dadami et al., 2013, 2017; Eamens et al., 2014; Adkar-Purushothama et al., 2015, 2017; Reis et al.,

2015; Flores et al., 2017). Viroid infection might cause symptoms through the action of vdsRNAs which alter the expression levels of plant miRNAs, which in turn affects the expression levels of the plant mRNA targets of those plant miRNAs. It was reported that potato spindle tuber viroid (PSTVd) infection of tomato affects host miRNA production (Diermann et al., 2010) and host mRNA production (Wang et al., 2011; Owens et al., 2012). More recently, citrus bark cracking viroid infection was shown to affect plant miRNA regulation of plant transcription factors regulating leaf, cone and root growth and development of hop plants (Mishra et al., 2016).

The *Citrus* genus (family *Rutaceae*), includes several cultivars of high economic value including oranges, mandarins, grapefruits and lemons (2018-19 US citrus crop packinghouse-door equivalent $3.35 billion) (USDA-NASS, 8/2019). Citrus flavors and aromas are among the most recognizable and preferred worldwide. In addition, citrus fruits are a rich source of vitamins, antioxidants, minerals and dietary fiber essential for overall nutritional wellbeing (Van Duyn and Pivonka, 2000; Yao et al., 2004). Citrus trees are produced by grafting a desired scion variety onto a suitable rootstock species that then are planted in commercial citrus orchards. Tree spacing in citrus orchards has varied depending upon the cultivated species and a variety of factors such as soil type, climatic conditions and available farming equipment (Platt, 1973; Tucker and Wheaton, 1978). The historical global trend of citrus orchard spacing has been towards higher tree densities to maintain yield on the reduced available agricultural land and to increase economic returns. However, high-density citrus plantings cannot be achieved in the

absence of dwarf citrus trees (Boswell and Others, 1970; Platt, 1973; Tucker and Wheaton, 1978).

Citrus dwarfing viroid (CDVd) infection of navel orange trees (*Citrus sinensis* (L.) Osb.) propagated on trifoliate orange (*C. trifoliata* (L.), syn. *Poncirus trifoliata* (L.) Raf.) rootstock has been previously reported to reduce canopy volume by approximately 50% (**Figure 4.1B**) (Vidalakis et al., 2011) and >20% reduction in the apical growth of individual shoots within the tree canopy (Lavagi-Craddock et al., 2020). Understanding the molecular mechanism of the CDVd-induced citrus tree size reduction, will be most valuable as it could provide information on how to systematically produce dwarf trees for high density plantings without the use of a graft-transmissible viroid agent. Based on the current understanding of viroid infection and RNAi pathways (Ding, 2009; Gómez et al., 2009; Owens and Hammond, 2009; Dadami et al., 2017), we hypothesized how CDVd infection may lead to the observed citrus dwarfed phenotype (**Figure 4.1B**).

To date, very few studies exist of miRNAs in citrus and even fewer in navel orange trees (Lu et al., 2015; Ma et al., 2016; Liang et al., 2017; Xie et al., 2017; Huang et al., 2019) and to the best of my knowledge, there are no published studies on citrus miRNAs in response to viroid infection of citrus field trees. To explore the effect of CDVd-infection on citrus miRNAs and gain insight into the symptom development mechanism leading to the dwarfed phenotype observed in field plantings, I analyzed the effect of CDVd infection using a high through sequencing (HTS) approach. The

increasing number of miRNAs deposited in the miRBase database (Kozomara and Griffiths-Jones, 2014; Kozomara et al., 2019) from a wide range of species (< 200), including *C. sinensis,* enables the discovery of novel miRNAs and their responses to pathogen infection, which may account for the observed species specific reactions and symptom development. Many plant miRNAs are conserved (Axtell and Bartel, 2005) but some are species specific (Moxon et al., 2008) and expressed at lower levels, thus making HTS the ideal approach to discover them and study their expression profiles (Jagadeeswaran et al., 2010; Motameny et al., 2010). miRNAs from different plant species such as maize (Zhang et al., 2009), potato (Zhang et al., 2013), peanut (Zhang et al., 2017), barley (Ferdous et al., 2017), soybean (Zhang et al., 2008), and hop (Mishra et al., 2016), have been identified using HTS approaches.

In this study, I analyzed sRNA libraries prepared from field grown CDVd-infected navel orange and non-infected control trees to characterize miRNAs in the *C. sinensis* (stems) and *C. trifoliata* (roots) and their expression profile in response to CDVd infection. This work provides valuable information at the molecular level and establishes the foundational framework that is necessary to dissect the subcellular mechanisms responsible for the observed citrus dwarf phenotype in the field.

MATERIAL AND METHODS

Plant material and RNA isolation

Plant material (stems and roots) was collected in January 2016 from six 18-year-old ‘Parent Washington’ navel (*C. sinensis* (L.) Osbeck) on ‘Rich 16-6’ trifoliate orange

(*C. trifoliata* (L.)*,* syn. *Poncirus trifoliata* (L.) Raf) rootstock infected (n= 3) and non-infected (n= 3) with CDVd, respectively. Trees were planted in an East-West running orchard located at the University of California (UC), Agriculture and Natural Resources, Lindcove Research and Extension Center (Exeter, CA, USA). CDVd-infected trees were planted at high density (3 x 6.7 m), whereas non-infected control trees were spaced at standard density (6.1 x 6.7 m).

Stem and root samples were processed in the field and immediately frozen in liquid nitrogen. For each tree, eight stem samples from around the canopy were collected. Leaves and petioles were removed, the stems were roughly chopped into approximately 0.5-1 cm pieces, placed into 50 ml conical tubes, and flash frozen. Root samples were collected from around the tree, at approximately 1 m away from the trunk and 20 cm deep, near the irrigation emitters, using a corer. The roots from eight core soil samples were washed thoroughly with water, gently blotted dry with paper towels, chopped into 0.5-1 cm pieces, placed into 50 ml conical tubes, and flash frozen. In between each sample collection and processing, cutting tools and working surfaces were sanitized with 10% bleach solution (0.5-1% sodium hypochlorite) and rinsed with water and new sterile disposable plasticware and razor blades were used. Samples were transported into the Citrus Clonal Protection Program (CCPP), Citrus Diagnostic Therapy and Research Laboratory at the UC Riverside (Riverside, CA, USA) on dry ice and stored at -80°C until analysis.

Total RNA was isolated using the Invitrogen™ TRIzol™ (Thermo Fisher Scientific, Waltham, MA, USA) reagent. For each sample, 300 mg of frozen tissue were

ground in liquid nitrogen with mortar and pestle. The ground material was transferred to a 5 ml Eppendorf tube and 3 ml of TRIzol™ reagent was added immediately. RNA extraction was performed according to the manufacturer's instructions and scaled to the appropriate volumes. The eluted RNA was aliquoted into four 1.5 ml microcentrifuge tubes to prevent freezing-thawing cycles during downstream analysis. The RNA concentration and quality was assessed with a spectrophotometer and the Agilent 2100 Bioanalyzer (Agilent, Santa Clara, CA, USA) using the Plant RNA Nano assay (RIN values were between 7.9 and 8.6).

The presence or absence of CDVd in each sample was confirmed by reverse transcription quantitative polymerase chain reaction (RT-qPCR) using a CCPP developed and validated assay (F: 5'-AAC TTA CCT GTC GTC GTC-3'; R: 5'-CGT GTT TTA CCC TGG A GG-3'; Probe (FAM): 5'-CTC CGC TAG TCG GAA AGA CTC CGC-3'). The assay was performed using the iTaq™ Universal Probes One-Step Kit (Bio-Rad, Hercules, CA, USA) in 20 µL reactions with 10 µL of iTaq universal probe reaction mix, 0.5 µL of reverse transcriptase, 0.6 µL of forward primer (300 nM final concentration), 1.2 µL reverse primer (600 nM final concentration), 0.4 µL of probe (200 nM final concentration), 1 µL of RNA template, and 6.3 µL of water. The RT-qPCR was performed in the Bio-Rad CFX-96 (Hercules, CA, USA) and the reaction conditions were as follows: 30 min at 50°C, 5 min at 95°C, followed by 45 cycles of 10 sec 95°C, 30 sec at 59°C.

High throughput sequencing, sRNA library preparation and sequencing analysis to identify conserved and novel miRNAs and their predicted targets

The sRNA libraries were prepared using the Illumina TruSeq Small RNA Kit (San Diego, CA, USA) following the manufacturer's recommended protocol. The libraries were sequenced using an Illumina HiSeq™ 2500 instrument with single-end 50 bp reads (SeqMatic, Fremont, CA, USA). Raw reads were trimmed to remove low quality bases and adapters using cutadapt v. 1.15 (Martin, 2011) to generate clean sRNAs reads ranging from 18 to 28 nt in length.

The clean reads were then filtered for rRNA, tRNA, snRNA, snoRNA, repeat sequences and other ncRNAs, using Rfam v.13.0 (Kalvari et al., 2018) with default parameters. The remaining reads were mapped to known miRNAs from the miRBase database (release 21, June 2014) to identify conserved miRNAs (Kozomara and Griffiths-Jones, 2011, 2014). The reads were further analyzed to predict potential novel miRNAs using miR-PREFer v. 0.24 using default parameters (Lei and Sun, 2014).

The conserved and novel miRNA sequences were analyzed against *C. sinensis* mRNA transcripts and *C. trifoliata* coding sequences (CDS) using psRNATarget v. 2.0 (Dai et al., 2018) to predict potential miRNA-mRNA interactions. DESeq2 v. 1.18 (Love et al., 2014) was used for the differential expression analyses of the miRNAs. The annotated mRNA targets were identified using the Blast2Go (Götz et al., 2008) tool within the OmicsBox software suite v. 1.4.11 (Cambridge, MA). Figures were created using GraphPad Prism v. 9.0 (San Diego, CA).

Expression analysis of citrus miRNAs and miRNA target genes using RT-qPCR

To validate the expression levels of conserved and novel miRNAs, custom stem-loop RT-qPCR assays (catalog number: 4398987) were designed by ThermoFisher Scientific (Waltham, MA, USA) based on the sequences provided in **Table 4.1**. For the relative expression quantification, U6 spliceosomal RNA was used as an internal control gene to normalize the efficiency between the target and internal control using the comparative Cq method (Schmittgen and Livak, 2008; Kou et al., 2012). The assay was carried out based on the manufacturer's recommended protocol and all samples were standardized to the same concentration to ensure equal representation. The reverse transcription reactions were performed in a total volume of 15 µL with the TaqMan™ MicroRNA Reverse Transcription Kit (Thermo Fisher, Carlsbad, MA, USA) which contained 0.15 µL of 100 mM dNTP, 1 µL of MultiScribe Reverse transcriptase, 1.5 µL of 10x RT Buffer, 0.19 µL of RNase Inhibitor, 4.16 µL of nuclease-free water, 5 µL of total RNA, and 3 µL of 5x RT primer. The reverse transcription reactions were performed with the ProFlex PCR System (Thermo Fisher, Carlsbad, MA, USA) as follows: 16°C for 30 min, 42°C for 30 min, 85°C for 5 min, and 4°C hold. The endpoint qPCR was performed in triplicates, according to the MIQE guidelines (Bustin et al., 2009), on a QuantStudio 12K Flex Real-Time PCR System (Thermo Fisher, Carlsbad, MA, USA) with the TaqMan™ Fast Advanced Master Mix (Thermo Fisher, Carlsbad, MA, USA) in a total of 20 µL reactions which included: 10 µL of master mix, 7.67 µL of nuclease-free water, 1 µL of TaqMan™ Small RNA Assay, 1.33 µL of the cDNA

template. The endpoint PCR conditions were as follows: 50°C for 2 min, 95°C for 20 sec, followed by 40 cycles of 95°C for 1 sec, and 60°C for 20 sec.

To verify the relative expression levels of the miRNA target genes, primers for the predicted target genes of miRNAs, were designed for RT-qPCR (**Table 4.2**). Actin2 was used as an internal control gene to determine the relative abundance of the target mRNA expression levels by the comparative Cq method (Schmittgen and Livak, 2008; Mafra et al., 2012). Reverse transcription was performed using the Invitrogen™ SuperScript™ II Reverse Transcriptase (RT) (Carlsbad, MA, USA). The reaction was performed using the manufacturer's recommended protocol as follows: 1µL of olig(dT) (500 µg/mL), 1 µL of dNTP (10 mM), 2 µL of total RNA and 8 µL of nuclease-free water. The mixture was incubated for 5 min at 65°C and subsequently chilled on ice. The reaction was prepared with 4 µL of 5x First-Strand Buffer, 2 µL of 0.1M DTT, and 1 µL of RNaseOUT (40 units/uL) and then incubated for 2 min at 42°C. Finally, 1 µL of SuperScript™ II RT (200 units) was added and the reaction was incubated at 42°C for 50 min followed by 70°C for 15 min. Downstream qPCR was also performed in triplicates, according to the MIQE guidelines, using the iTaq Universal SYBR Supermix (Bio-Rad, Hercules, CA, USA): 10 µL of iTaq Universal SYBR Supermix,1 µL of cDNA, 0.6 µL of each forward and reverse primers and 7.8 µL of nuclease-free water. The qPCR was performed on the Bio-Rad CFX-96 (Hercules, CA, USA) with the following conditions: 95°C for 1 min, followed by 40 cycles of 95°C for 10 sec, and 60°C for 15 sec.

RESULTS

High throughput sequencing and characterization of potential citrus miRNAs

To characterize citrus miRNAs and their expression profile in response to CDVd infection, we prepared and analyzed two sRNA libraries from stems and root samples of CDVd-infected and non-infected controls of navel orange citrus trees on trifoliate orange rootstock. The Illumina sequencing generated 16,008,944 reads for the non-infected stems and 6,524,898 reads for the non-infected roots. For the CDVd-infected trees, 13,764,218 reads were generated from the stems, and 5,864,614 reads from the roots. Removal of low-quality reads, adapter sequences and selection for 18-28 nt reads resulted in 6,742,931 reads from non-infected stems and 2,030,419 reads from the roots. For the CDVd-infected samples, 5,733,421 stem and 1,873,309 root reads were identified (**Table 4.3**).

From the non-infected trees, 8.1% of the stem and 6.1% of the root were classified as miRNAs. Similarly, for the CDVd-infected stems and roots, 7.2% and 5.8% of the reads, respectively, were classified as miRNAs. The unique unannotated sequences in both the non-infected and CDVd-infected stems represented at least 90% of the total reads while for the roots they represented over 82% (**Table 4.3)**. The total unique miRNA reads for both non-infected and CDVd-infected stems represented 0.05% of the reads, while both non-infected and CVd-infected roots represented 0.0006% of the reads (**Table 4.3)**.

The most common size among the total mapped miRNAs sequences ranged between 20 to 24 nt in length, with 21-nt being the predominant miRNA class (**Figure**

4.2) across different treatments and tissue types. This is consistent with plant antiviral RNAi responses and DCL-mediated processing of dsRNA producing 21nt siRNAs.

Identification of conserved miRNAs and their expression profiles

The miRNA sequencing from non-infected control and CDVd-infected stems and roots identified 60 unique conserved miRNAs that ranged from 20 to 24 nt (**Tables 4.6 & 4.7**). Based on differential expression analysis, four conserved miRNAs (3 in the stems and 1 in the roots) were found to be significantly altered in response to CDVd-infection (P-value and adjusted P-value <0.05) (**Table 4.4**). Our results indicated that different members of the three miRNA families of interest had different expression levels between the non-infected and the CDVd-infected trees. The conserved miRNA families in the stems included csi-miR156, csi-miR171b, and csi-miR479, while csi-miR535 was the only conserved miRNA found in the roots. The conserved stem miRNAs were moderately more abundant compared to the conserved root miRNAs (**Table 4.4**). All four conserved miRNAs had higher expression levels in the non-infected control than the CDVd-infected trees (**Table 4.4**).

Five miRNA families present in both stem and root tissues were identified: miR166, miR171b, miR399, miR477, and miR482. In stems, the highest represented miRNA families were miR166, and miR399, with 5 members each, followed by miR171b with 4 members, miR396, miR477, and miR482 with 3 members and the remaining 40 miRNAs were represented by a single member (**Table 4.6**). In the roots, two miRNA families (miR166 and miR399) were represented by 5 members, five

miRNA families (miR167, miR172, miR396, miR477, and miR482) were represented by 3 members, two miRNA families (miR530 and miR171b) contained 2 members, and the remaining 40 root miRNA families were represented by a single member (**Table 4.7**).

Stem-loop RT-qPCR analysis was performed on the four conserved miRNAs in root and stem tissues (csi-miR479, csi-miR156, csi-miR171b, and csi-miR535) from non-infected and CDVd-infected trees to determine their abundance. The expression levels of the four conserved miRNAs were significantly altered as a result of CDVd infection. In the stems, csi-miR479's expression decreased 3.55-fold and csi-miR171b had a fold decrease of 2.24, while csi-miR156 had the smallest negative fold change (0.11) (**Figure 4.3**). In the roots, csi-miR535's expression decreased 1.12-fold (**Figure 4.3**). The results obtained from the RT-qPCR analysis (**Figure 4.3**) were consistent with the HTS read frequencies (**Table 4.4**) indicating a strong correlation between the RT-qPCR analysis and read frequencies obtained through small sRNA sequencing.

Identification of novel miRNAs and their expression profiles

The lengths of the predicted novel miRNAs from stems and roots ranged between 19 and 24 nt.A total of 646 stem and 108 root novel miRNAs were identified. No novel root miRNAs had significant differential expression levels. On the other hand, three novel stem miRNAs (csi-miRNA-75, csi-miRNA-114, and csi-miRNA-435) had significantly different expression levels in response to CDVd infection (P-value and adjusted P-value <0.05). All three novel stem miRNAs had higher expression levels in the non-infected trees than in the CDVd-infected trees (**Table 4.5**).

Stem-loop RT-qPCR was performed to confirm the HTS read frequency results of the identified novel miRNAs in response to CDVd-infection. csi-miRNA-114 showed the largest expression fold change (-9.23), while csi-miRNA-75 and csi-miRNA-435 showed similar fold changes (-1.44 and -1.22, respectively) (**Figure 4.4**). These results also support the reliability of RT-qPCR and HTS read frequencies (**Table 4.5**) as measurements of the expression levels of miRNAs.

Citrus miRNA-target prediction and functional analysis

To understand the function of the identified citrus miRNAs, host target genes were analyzed using the psRNATarget program by cross referencing the results against the *C. sinensis* genome for the stems (ref: GCF_000317415.1) and the *C. trifoliata* CDS for the roots (Kawahara et al., 2020). For both conserved and novel stem miRNAs, 83.1% of the miRNA targets were predicted to be regulated by cleavage and 16.9% by translational inhibition. Similarly, in the roots, 86.4% of the miRNA targets were predicted to be regulated by cleavage and 13.6% by translational inhibition.

Based on the extent of sequence complementarity between miRNAs and their targets, a total of 5,542 potential targets were predicted for the conserved and novel stem and root miRNAs (conserved: stem 63 and root 64; novel: stem 647 and root 109). Of the 5,542 potential miRNA target genes, 494 and 3,926 were targets of the conserved and novel stem miRNAs while 495 and 627 were targets of the conserved and novel root miRNAs, respectively.

The conserved stem and root miRNAs (miR479, mi171b, miR156, and miR535) analyzed in this study were associated with 10 different groups of target genes. (i) Uridine diphosphate (UDP)-glucose flavonoid glucosyltransferase (orange1.1g033614m) is involved in the process of conjugating hormones, stabilizing secondary metabolites, solubility, transport, and regulating bioavailability of compounds for other metabolic process in *Arabidopsis thaliana* (Vogt and Jones, 2000; Offen et al., 2006). Flavonoid glycosylation reactions depend on UDP sugars as donors (Liu et al., 2018) and have been shown to play an important role in flavonoid modification that can affect the taste characteristics of citrus (Owens and McIntosh, 2009); (ii) DEAD/DEAH box helicase (orange1.1g028826m; orange1.1g026925m) are enzymes involved in molecular mechanisms such as RNA splicing, ribosome assembly, transcription initiation and nuclear export (Macovei et al., 2012). In addition, the DEAD/DEAH box helicase are important in regulatory events such as organ maturation and cellular growth and differentiation (Macovei et al., 2012); (iii) Glutathione s-transferase (orange1.1g033674m) enzyme that functions to catalyze the conjugation of glutathione (GSH) that can help protect the cell from toxins such as herbicides. In addition, the enzyme may function to protect the cellular lipid from oxidative damage (Bartling et al., 1993); (iv) The squamosa promoter-binding protein-like transcription factor family (orange1.1g011651m; orange1.1g032310m; orange1.1g008776m) plays a critical role in plant growth and development such as plant phase transition, flower and fruit development and plant architecture (Chen et al., 2010b); (v) RHOMBOID-like protein 1 (P_trifoliata_00066_mRNA_51.1) contains proteolytic activity and high substrate

specificity that catalyzes intramembrane proteolysis in the Golgi apparatus (Kanaoka et al., 2005); (vi) Scarecrow-like protein 26 (orange1.1g011012m), from *Arabidopsis thaliana*, has been shown to be important in plant growth and development and belongs to the GIBBERELLIC-ACID INSENSITIVE, REPRESSOR of GAI and SCARECROW (GRAS) family of plant specific transcription factors (Lee et al., 2008; Ma et al., 2014); (vii) The no apical meristem (NAM) protein (orange1.1g037150m) protein is required for plant development that controls boundary functions and lateral organ separations, which is critical for proper leaf and flower patterning (Cheng et al., 2012); (viii) Xyloglucan endotransglucosylase protein 23 (P_trifoliata_00148_mRNA_25.1; P_trifoliata_00148_mRNA_20.1) is required for loosening the cell wall during expansion and cutting and rejoining the xyloglucans that hold the adjacent cellulose microfibrils (Van Sandt et al., 2007); (ix) protein kinase family protein (orange1.1g003605m; orange1.1g000757m); and (x) oxidoreductase (orange1.1g019665m).

The novel stem miRNAs (csi-miRNA-75, csi-miRNA-114, and csi-miR435) showing differential expression levels in response to CDVd infection were associated with target genes including (i) squamosa promoter-binding like proteins (orange1.1g030599m, orange1.1g029650m, orange1.1g021420m, orange1.1g017256m, orange1.1g016971m, orange1.1g032310m orange1.1g046416m, orange1.1g011662m, orange1.1g010865m, and orange1.1g010591m; target of csi-miRNA-75); (ii) plastid-lipid associated protein (PAP, orange1.1g030218m, orange1.1g025746m, orange1.1g030180m, and orange1.1g020639m; csi-miRNA-114) which are structures

that contain lipids and proteins that sequester the overaccumulation of carotenoids during flower development and fruit ripening (Moriguchi et al., 1998; Leitner-Dagan et al., 2006); and (iii) vacuolar protein sorting-associated proteins (orange1.1g021304m and orange1.1g017530m ; target of csi-miR435), which direct protein cargo from the Golgi apparatus to the vacuoles (Xiang et al., 2013) and have been shown to be important in plant development (Cai et al., 2014).

Clusters of orthologous groups (COG) functional classification of the targets of conserved and novel miRNAs revealed that the highest proportion of the genes were associated with (i) the nucleus (21% conserved and 11% novel); (ii) the integral component of membrane (14% conserved and 22% novel); and (iii) ATP binding (11% conserved and 10% novel) (**Figure 4.5A, B**).

Other miRNA targets shared by the conserved and novel miRNAs include (i) ADP binding (9% conserved and 2% novel); (ii) cytoplasm (4% conserved and 6% novel); (iii) DNA-binding transcription factor activity (3% conserved and 1% novel); (vi) oxidation-reduction processes (7% conserved and 4% novel); (v) plasma membrane (6% conserved and 1% novel); (vi) protein phosphorylation (2% conserved and 4% novel); and (vii) regulation of transcription (14% conserved and 3% novel) (**Figure 4.5A, B**).

The data were further annotated based on ontological definitions of the gene ontology (GO) terms, which categorized the predicted targets of the conserved miRNAs differentially expressed in response to CDVd infection into various biological, molecular and cellular processes (**Figure 4.6A**). Under the biological process, the predicted targets

of conserved miRNA responsive to CDVd infection were subcategorized to (i) metabolic process; (ii) cellular process; (iii) biological regulation; and (iv) regulation of biological processes. The number of sequences associated with these four biological process subcategories had similar values in the stems and roots with the exception of the metabolic process that was higher in the roots (**Figure 4.6A**). For the molecular process, the majority of the predicted target genes of conserved miRNAs responsive to CDVd infection in the roots were subcategorized to catalytic activity while the targets in the stems were mostly subcategorized to binding. Targets belonging to the cellular components category were subcategorized to (i) cellular anatomical entity; and (ii) intracellular subcategories (**Figure 4.6A**).

The targets of the predicted novel miRNAs displaying significant differential expression in response to CDVd infection (csi-miRNA-75, csi-miRNA-114, and csi-miRNA-435) were categorized to (i) biological process; (ii) molecular process; and (iii) cellular components. The cellular components subcategories (i) cellular anatomical entity; and (ii) intracellular contained most of the sequences (**Figure 4.6B**).

Expression profiles and experimental validation of miRNA target transcripts

The expression levels of eight predicted mRNA targets of the conserved CDVd-responsive miRNAs were determined via RT-qPCR. The results indicate that the expression of the miRNA target genes correlates negatively with the expression of their corresponding miRNA (**Figure 4.7**), thus confirming the relationship between CDVd-infection and altered expression levels of specific miRNA targets. Targets of miRNAs

belonging to the same miRNA family showed variable results. For example, orange1.1g011651m (Figure 7, bar #5), orange1.1g032310m (Figure 7, bar #6), and orange1.1g008776m (Figure 7, bar #7), which are all targets of different members of the csi-miR156 family, were not uniform and showed fold-change differences.

DISCUSSION

Citrus production exceeded 157.9 million tons in over 9.8 million hectares worldwide for 2019 (http://www.fao.org/faostat/en/#data/QC), while in California alone the citrus industry is valued at $3.4 billion dollars with an estimated total economic impact of $7.1 billion (Babcock, 2018). Global decrease in farmland availability, increasing land, water and labor costs, and the continued spread of the deadly Huanglongbing (HLB) disease of citrus, make it imperative to develop tools that allow for high-density citrus plantings for maximization of yields and economic returns per land surface unit. In addition, these factors have forced the citrus industry towards the implementation of novel cultivation practices that would allow for mechanized citrus production under protective structures (Gottwald, 2010; Vidalakis et al., 2011; Lambin, 2012; Verburg et al., 2013; da Graça et al., 2016). The observation that CDVd significantly reduced *C. sinensis* canopy volume on *C. trifoliata* rootstock (Semancik et al., 1997; Vidalakis et al., 2011); by reducing vegetative growth (Lavagi-Craddock et al., 2020) indicated that CDVd may be used as a possible tool for high-density plantings of citrus, and provided key information on the possible biological mechanism through which CDVd affects specific rootstock-scion combinations to reduce tree canopy volume (Vidalakis et al., 2011). Furthermore,

understanding the detailed molecular regulatory mechanisms that lead to a reduction in tree canopy volume in response to CDVd infection would provide the necessary knowledge to produce reduced-size citrus trees without the need of a -graft-transmissible viroid agent.

sRNAs play an essential regulatory role in cellular and plant development functions including antiviral host responses and potentially viroid pathogenesis (Borges and Martienssen, 2015; Dadami et al., 2017; Flores et al., 2017; Czech et al., 2018; Zhu et al., 2018; Treiber et al., 2019; Wang et al., 2019). Two models have been proposed to explain the involvement of RNAi in the pathogenic process induced by viroid infections and both involve vdsRNAs. In the first model, vdsRNAs may act as miRNAs, downregulating the expression of physiologically important host genes, thus inducing disease associated symptoms. vdsRNAs are expected to contain significant identity to a region of the host genome for this model to work and resistance of viroids to RNAi is a feature of the viroid genome (Wang et al., 2004). In the second model, disease symptoms caused by the nucleus replicating pospiviroids might result from the incorporation of viroid replication intermediates into the trans-acting small interfering RNA (ta-siRNA) biogenesis pathway. The nucleolus is a ta-siRNA free zone, and mature viroid forms produced in the nucleolus are resistant to degradation. In contrast, (vd)ta-siRNA produced in the nucleus from replication intermediates can then translocate to the cytoplasm where they guide the cleavage of target host mRNA leading to observed symptoms (Gómez et al., 2009). Both models involve viroid secondary structures as a key element that can therefore be interpreted as the evolutionary compromise between the need to interact with host factors and the necessity to survive RNAi. Regardless of whether vdsRNAs are produced

according to the first or second model, it is also important to point out that rather than acting directly on host mRNA, vdsRNAs may affect host mRNA targets genes via host miRNAs as previously described (Mishra et al., 2016; Dadami et al., 2017).

Plant disease resistance gene families are typically very large with thousands of members and are commonly considered the putative targets of sRNAs (Chen et al., 2010a), thus making the study of sRNAs in response to viroid infection a valid approach to investigate the biological mechanisms associated with symptoms. The systematic profiling of sRNAs in CDVd-infected trees, using HTS technologies, was the next logical step to gain insight into the function and regulatory mechanisms of miRNAs through which CDVd may reduce tree canopy size. In this study, I identified conserved and novel miRNAs in citrus and their response to CDVd infection. Consistent with the distribution patterns of sRNAs in other plant species, most sRNAs from both the CDVd-infected and non-infected libraries were found in the 21nt and 24nt classes (Jia et al., 2014; Gao et al., 2015; Mishra et al., 2016; Farooq et al., 2017; Zhang et al., 2018). CDVd-infected stems produced higher frequencies of the 21-nt class than their non-infected counterparts, indicating a CDVd induction of the 21-nt class since the other sRNA classes remained at comparable levels with the non-infected libraries. The increased abundance of the 21-nt class of small RNAs in response to viroid infection observed here is in agreement with previous reports for viral (viroid and virus) infections (Minoia et al., 2014; Zavallo et al., 2015).

All identified differentially expressed conserved and novel miRNAs, in this study, displayed overall reduced expression levels in response to CDVd-infection (**Figures 4.3**

and 4.4). Several evolutionary deeply-conserved miRNAs have been shown to retain homologous targets across plant phyla (Axtell et al., 2007) and these include miR156 (stem), miR535 (roots) and miR171b (stem), which represent three out of the four conserved miRNA with differential expression levels in response to CDVd infection identified in this study. In agreement with previous studies, miR156 was shown here to direct the cleavage of SBP box genes (squamosa-promoter binding-like protein) (Cardon et al., 1999; Rhoades et al., 2002; Wu and Poethig, 2006; Xie et al., 2006; Gandikota et al., 2007; Riese et al., 2007) (**Figure 4.7**). Members of this transcription factor family are known to play important roles in flower and fruit development, plant architecture, and in the transitions from juvenile to adult stages and to flowering (Yu et al., 2012). Even though miR535 is also known to target squamosa promoter-binding-like protein 3 (Shi et al., 2017; Zhou et al., 2020), this study identified RHOMBOID-like protein 1 as the target of miR535 in the roots. In Arabidopsis, a RHOMBOID-like protein was identified, providing evidence for the existence of regulated intramembrane proteolysis (RIP), a fundamental mechanism for controlling a wide range of cellular functions, in plants (Kanaoka et al., 2005). miR171b directs the cleavage of GRAS domain transcription factor genes (Ma et al., 2014). However, in this study, I found that miR171b's target, a probable glutathione-S-transferase, was altered in response to CDVd infection. Glutathione-S-transferases are ubiquitous and multifunctional enzymes encoded by large gene families that can be highly induced by biotic stress including bacterial, fungal and viral infection (Gullner et al., 2018). I found that the less conserved miR479 cleaves the UDP-glucose flavonoid glucosyl-transferase (Vogt and Jones, 2000; Offen et al., 2006) and DEAD/DEAH box helicases (Macovei et

al., 2012) both of which may be related to the observed dwarf phenotype. The predicted target genes of the novel miRNAs identified in this study (csi-miRNA-75, csi-miRNA-114, and csi-miRNA-435) include proteins involved in various miRNA plant developmental aspects, thus suggesting that CDVd-infection affects a wide range of biological functions via different miRNAs. In addition, the GO distribution analysis performed in this study, identified targets of conserved and novel CDVd-responsive miRNAs involved in various processes (**Figure 4.6A, B**). Taken together, our findings might suggest that CDVd-infection could lead to developmental reprogramming and growth alterations of citrus trees, leading to the observed symptoms of reduced vegetative growth and overall smaller tree size. Future transcriptome studies could provide additional evidence to elucidate the molecular details in support of this hypothesis.

In this study, the miRNA profile of roots (trifoliate orange, *C. trifoliata*) in response to CDVd infection was not altered to the same extent as the stem (navel orange, *C. sinensis*) miRNA profile. Although CDVd-derived sRNAs were detected in the roots, the trifoliate orange rootstock does not display major symptoms in response to CDVd infection (Vidalakis et al., 2004; Vernière et al., 2006; Murcia et al., 2009). This observation is consistent with the findings that the striking dwarfed citrus tree phenotype caused by CDVd infection results from the reduced vegetative growth of the stems, supporting the hypothesis that the molecular mechanisms responsible for this reprogramming must be primarily active in the stems.

Finally, the term “Transmissible small nuclear ribonucleic acids” (TsnRNAs) was coined to identify those viroids that do not express a disease syndrome, but rather act as modifying agents of tree performance that result in desirable agronomic traits with potential economic advantages (Semancik et al., 1997; Semancik, 2003). In our study, I did not observe a global induction and regulation of defense genes via the sRNA pathway in response to CDVd infection, a finding that consistent with the hypothesis that some viroid species might be better considered as RNAs modifying cellular functions and plant performance rather than infectious agents inducing a specific disease. This idea is also in agreement with the original 1946 concept behind the term “viroid” as described by Dr. Edgar Altenburg, “*Now, it is conceivable that there exist ultra-microscopic organisms which are akin to viruses but which are useful symbionts, and that these symbionts occur universally within the cells of larger organisms. We might call these supposed symbionts viroids” (Altenburg, 1946)*.

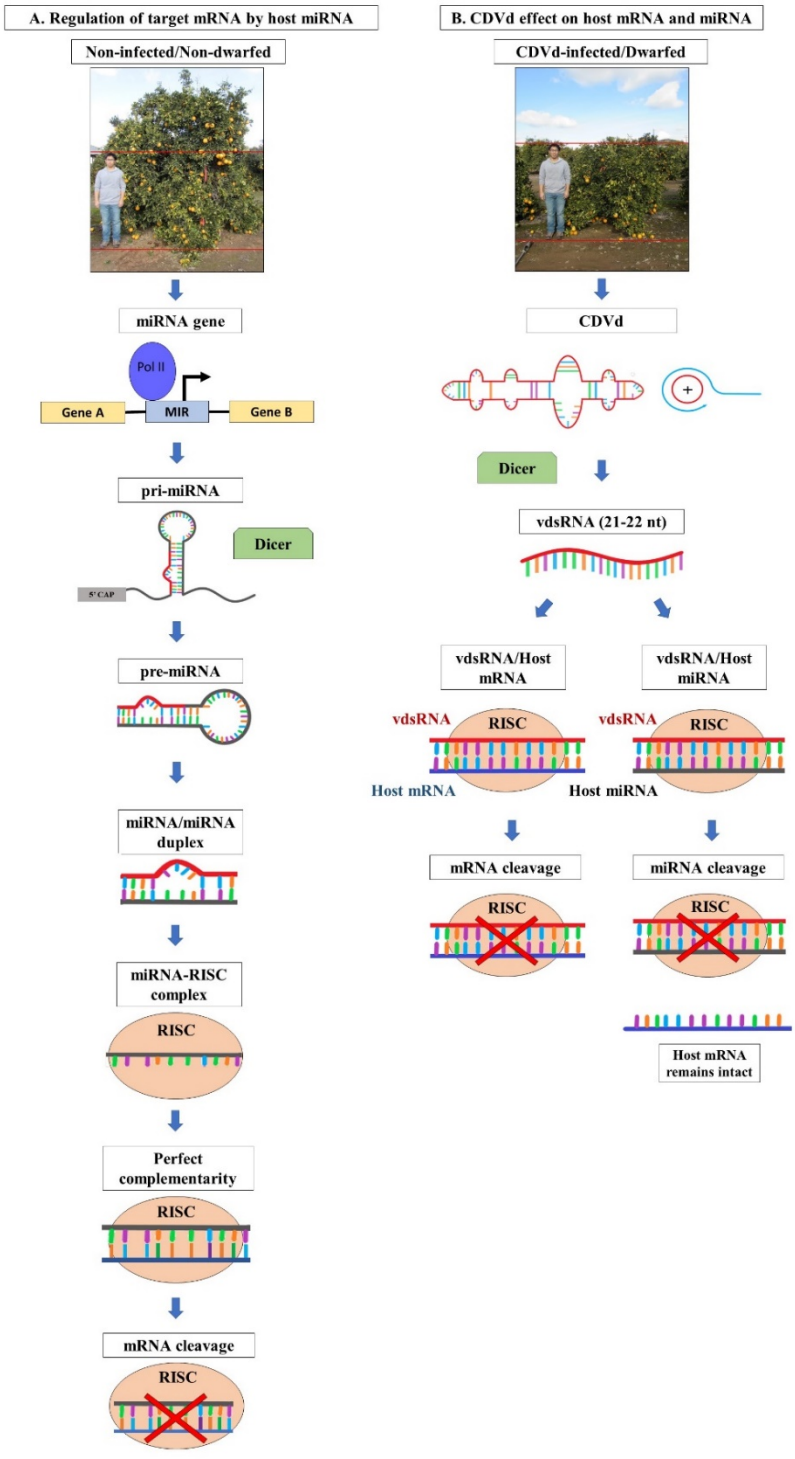
A. Regulation of target mRNA by host miRNA
Non-infected/Non-dwarfed
miRNA gene
Pol II
Gene A
MIR
Gene B
pri-miRNA
Dicer
5'CAP
pre-miRNA
miRNA/miRNA duplex
miRNA-RISC complex
RISC
Perfect complementarity
RISC
mRNA cleavage
RISC
B. CDVd effect on host mRNA and miRNA
CDVd-infected/Dwarfed
CDVd
Dicer
vdsRNA (21-22 nt)
vdsRNA/Host mRNA
vdsRNA/Host miRNA
vdsRNA
RISC
Host mRNA
vdsRNA
RISC
Host miRNA
mRNA cleavage
RISC
miRNA cleavage
RISC
Host mRNA remains intact

Figure 4.1 Citrus phenotypes and schematic representation of **(A)** host microRNA (miRNA)-based gene expression regulatory pathway. The host contains miRNA genes which are transcribed by RNA polymerase II to form RNA stem loop primary transcripts (pri-miRNA). The pri-miRNA is processed into precursor miRNA (pre-miRNA) by Dicer. One strand of the miRNA/miRNA duplex is degraded, and the mature miRNA loaded on to Argonaute protein to form the RNA-induced silencing complex (RISC). The miRNA guide the miRNA-RISC complex to the complementary sequence which result in the mRNA cleavage for the RNA degradation or translational repression. **(B)** The hypothesized schematic of the effects of citrus dwarfing viroid (CDVd) on the expression of host target genes. The viroid enter the host which trigger RNAi response. The viroid is cleaved by Dicer to form viroid derived sRNAs (vdsRNA) (21-22nt). The vdsRNA is loaded into Argonaute protein to form the vdsRNA-RISC complex. The vdsRNA guide the activated vdsRNA-RISC complex to complementary sequences and cleave the host mRNA or miRNA. The cleaved miRNA will alter the expression of level of plant miRNA, as a result affects the expression level of plant mRNA target of those plant miRNAs.

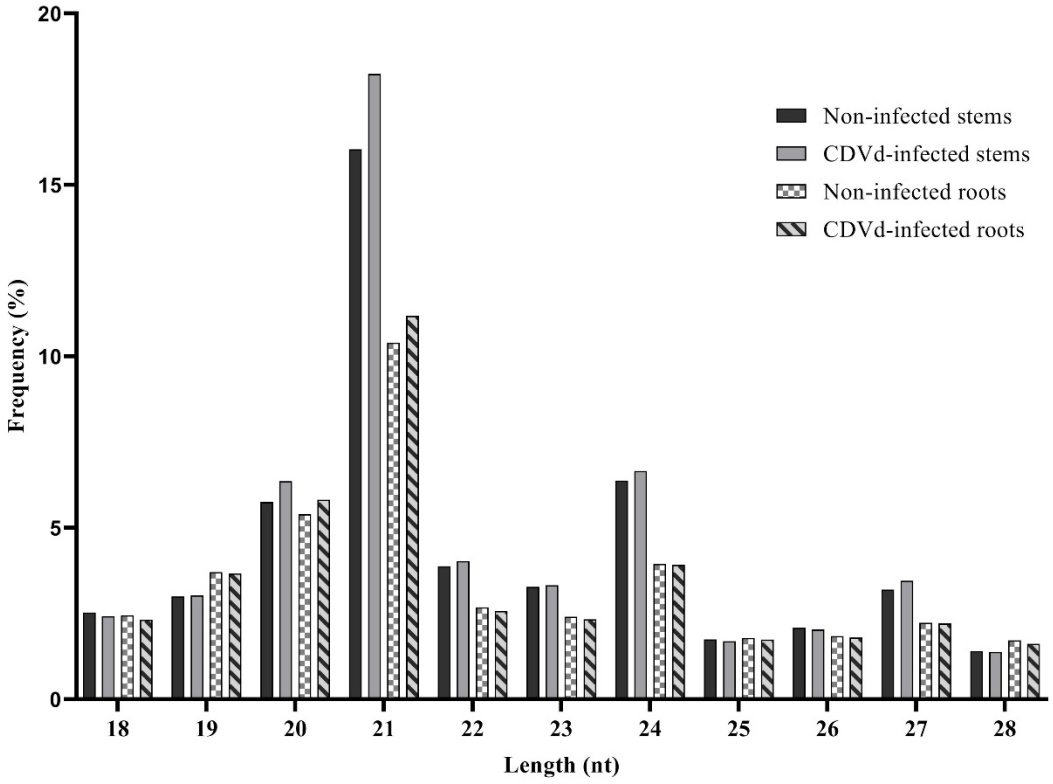

Figure 4.2 Length distribution of small RNAs in citrus dwarfing viroid (CDVd)-infected and non-infected citrus trees.

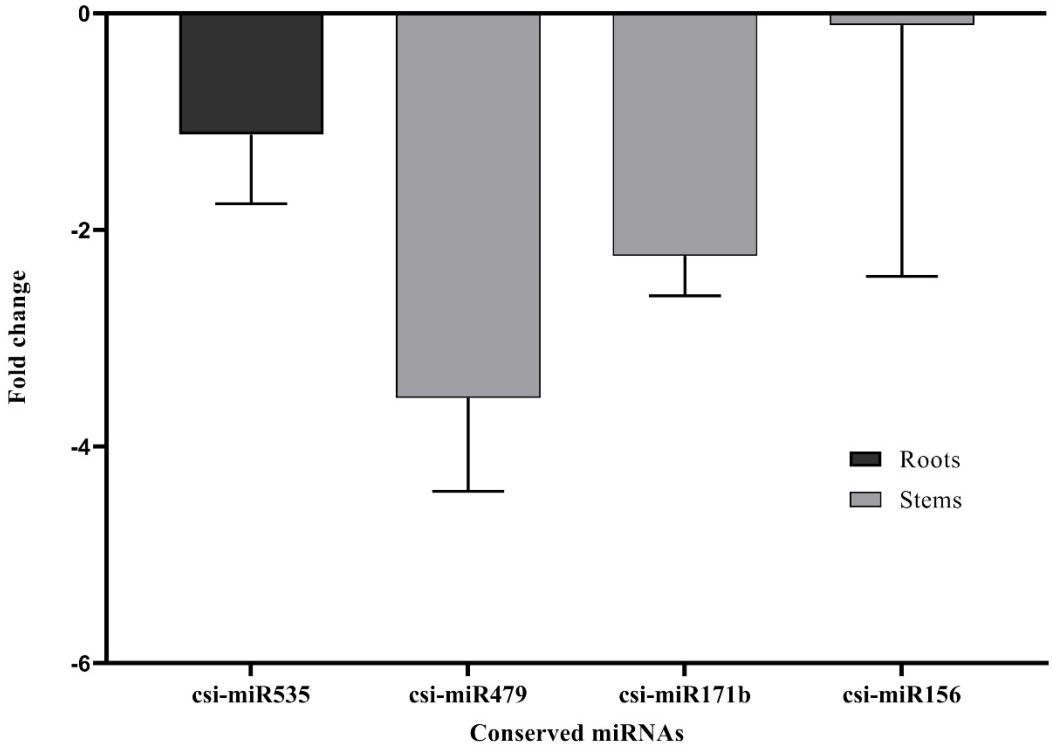

Figure 4.3 Differential expression analysis of four identified conserved microRNAs (miRNAs) in response to citrus dwarfing viroid (CDVd) infection. The relative abundance of each analyzed miRNA in CDVd-infected and non-infected trees was determined using the comparative Cq method by normalization to the U6 spliceosomal RNA. Conserved miRNAs with a significant change (P-value and adjusted P-value <0.05) were differentially expressed. The bar graph shows the $\log_2$ fold change of expression levels of the miRNAs in CDVd-infected samples relative to non-infected samples in stem and root tissues.

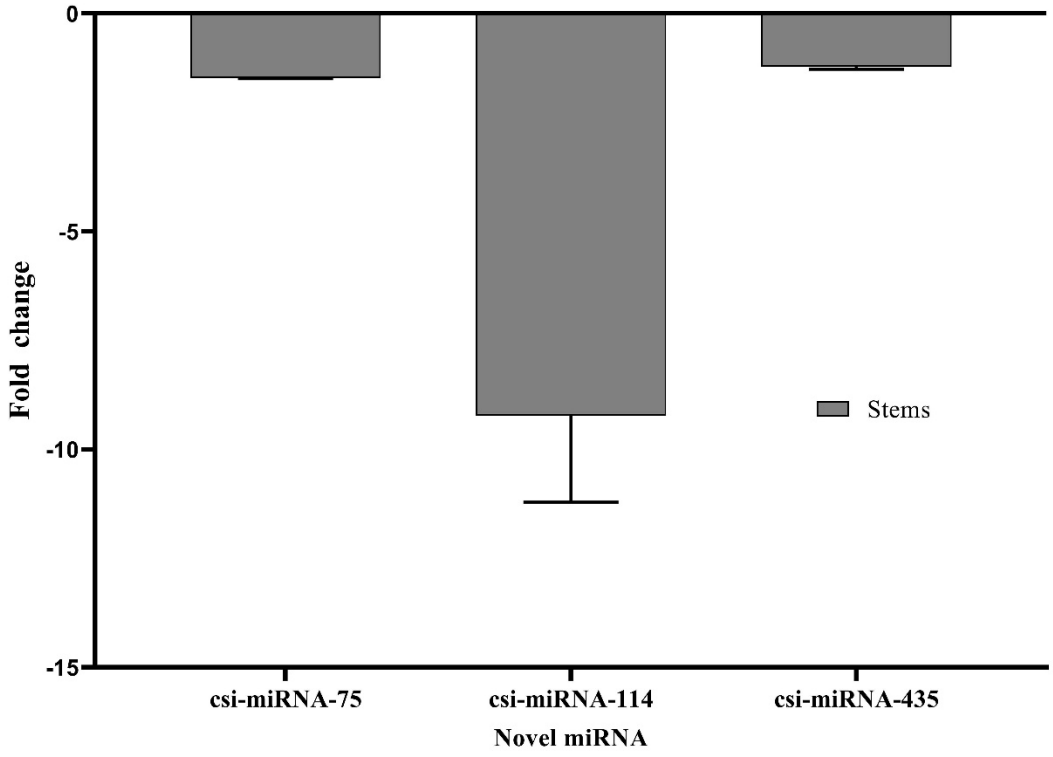

Figure 4.4 Differential expression analysis of three predicted novel microRNAs (miRNAs) in response to citrus dwarfing viroid (CDVd) infection. The relative abundance of each analyzed miRNA in CDVd-infected compared to non-infected trees was determined using the comparative Cq method by normalization to the U6 spliceosomal RNA (U6). Novel miRNAs with significant fold changes (P-value and adjusted P-value <0.05) were differentially expressed. The bar graph shows $\log_2$ fold changes in expression levels of miRNAs in CDVd-infected samples relative to non-infected samples from stems.

Figure 4.5A

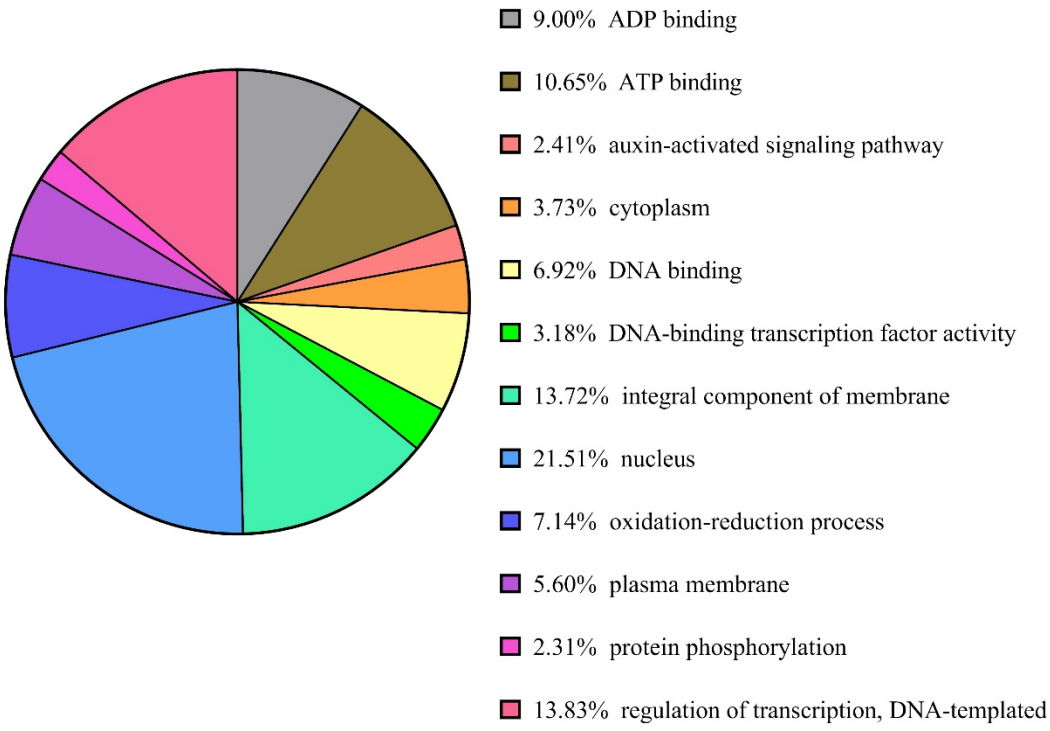
9.00% ADP binding
10.65% ATP binding
2.41% auxin-activated signaling pathway
3.73% cytoplasm
6.92% DNA binding
3.18% DNA-binding transcription factor activity
13.72% integral component of membrane
21.51% nucleus
7.14% oxidation-reduction process
5.60% plasma membrane
2.31% protein phosphorylation
13.83% regulation of transcription, DNA-templated

Figure 4.5B

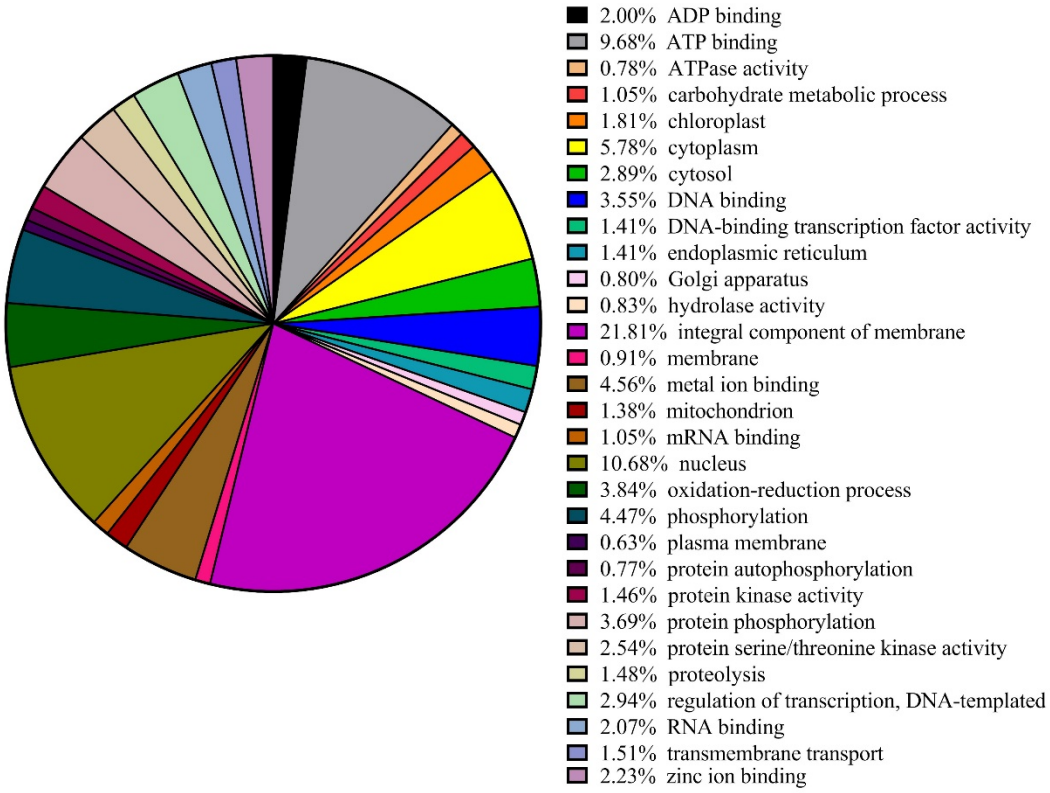

Figure 4.5 Clusters of orthologous groups **(**COG) functional classification of predicted target genes of conserved **(A)** and novel **(B**) CDVd-responsive miRNAs. The bar graph shows the number of sequences and distribution in different functional categories of the predicted miRNA targets at gene ontology (GO) level 2.

Figure 4.6A

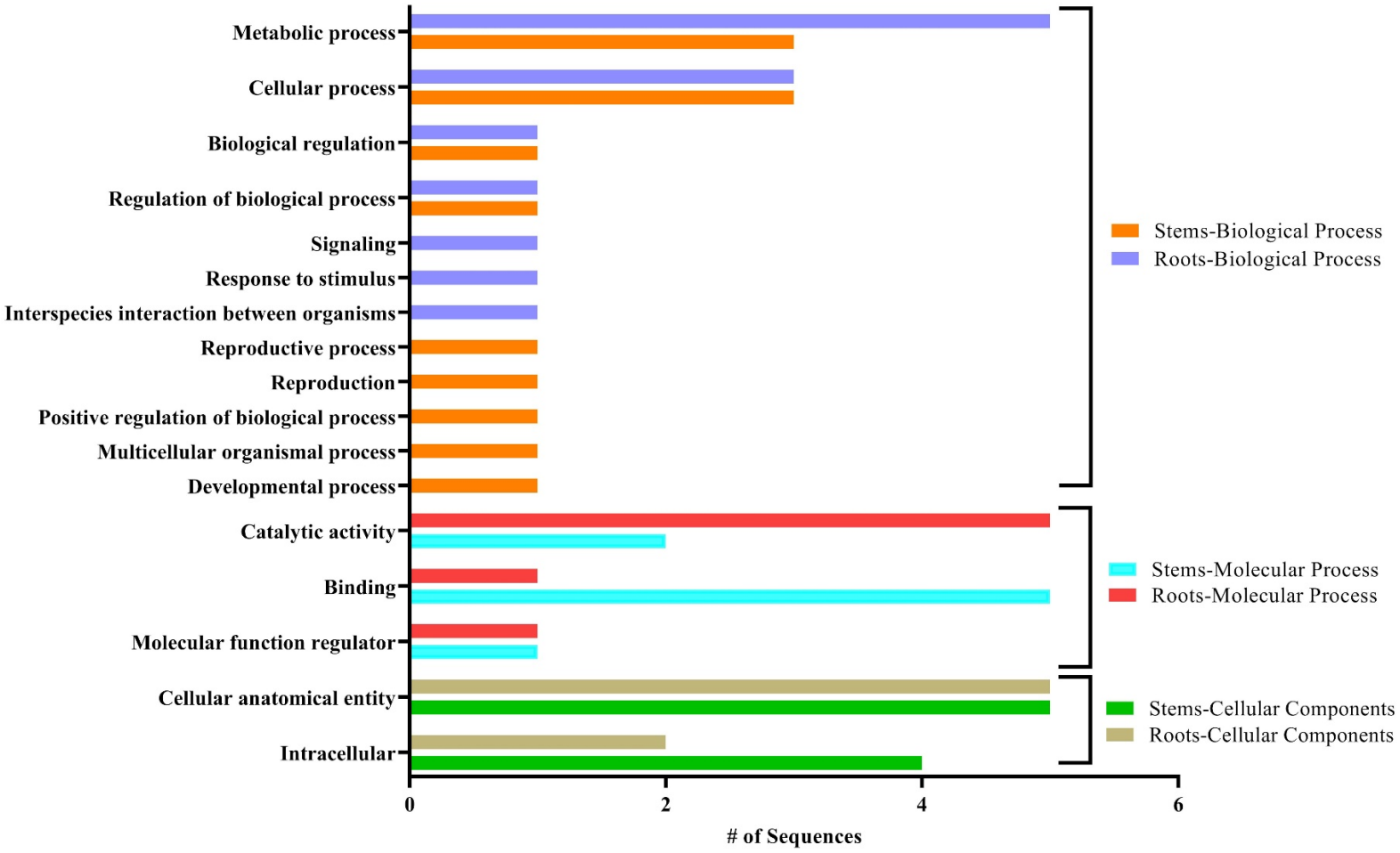
Metabolic process
Cellular process
Biological regulation
Regulation of biological process
Signaling
Response to stimulus
Interspecies interaction between organisms
Reproductive process
Reproduction
Positive regulation of biological process
Multicellular organismal process
Developmental process
Catalytic activity
Binding
Molecular function regulator
Cellular anatomical entity
Intracellular
0
2
4
6
# of Sequences
Stems-Biological Process
Roots-Biological Process
Stems-Molecular Process
Roots-Molecular Process
Stems-Cellular Components
Roots-Cellular Components

Figure 4.6B

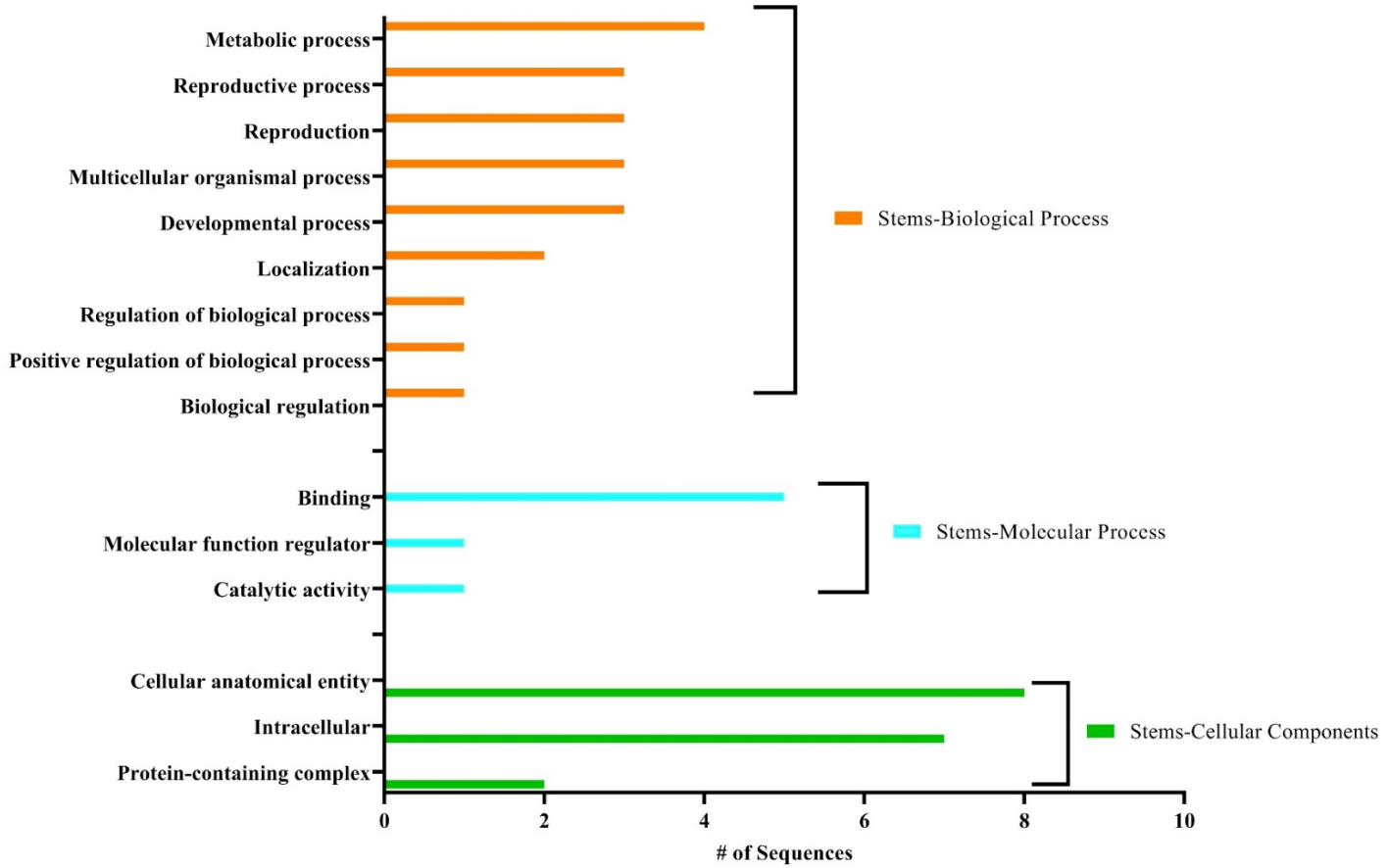

Figure 4.6 Cluster orthologous groups (COG) function calcification of predicted citrus target genes of (**A**) conserved and (**B**) novel miRNAs.

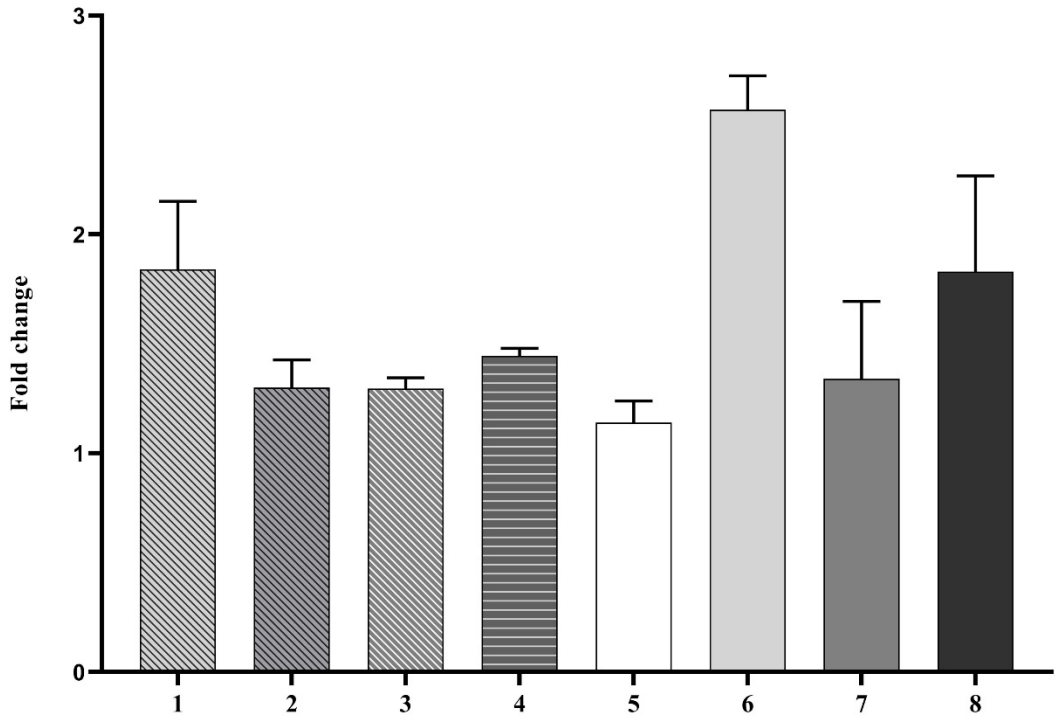
Fold change
3
2
1
0
1
2
3
4
5
6
7
8

Figure 4.7 Differential expression profile of selected microRNA (miRNA) target genes. The relative gene expression was evaluated by the comparative Cq method using actin2 as a reference gene. The bar graph shows $\log_2$ fold changes of expression levels of target genes in citrus dwarfing viroid (CDVd)-infected stems and roots relative to non-infected tissues. The predicted target genes used in the analysis were (1) UDP-glucose flavonoid glucosyl-transferase (orange1.1g033614m, target of csi-miR479-1-stem); (2) DEAD/DEAH box helicase (orange1.1g028826m, target of csi-miR479-2-stem); (3) DEAD/DEAH box helicase (orange1.1g026925m, target of csi-miR479-3-stem); (4) glutathione S-transferase (orange1.1g033674m, target of csi-miR171b-stem); (5) squamosa promoter binding protein-like 2 (orange1.1g011651m, target of csi-miR156-1-stem); (6) squamosa promoter binding protein-like 3 (orange1.1g032310m, target of csi-miR156-2-stem); (7) squamosa promoter-binding protein-like transcription factor family protein (orange1.1g008776m, target of csi-miR156-3-stem); (8) RHOMBOID-like protein, P_trifoliata_00066_mRNA_51.1, target of csi-miR535-root).

miRNA	Family	Target genes (5'-3')
MIR156	csi-mR156	UGACAGAAGAGAGUGAGCAC
MIR171	csi-mR479	UGUGAUAUUGGUUCGGCUCAUC
MIR535	csi-mR535	UGACAAUGAGAGAGAGCACAC
MIR171	csi-mR171b	CGAGCCGAAUCAAUAUCACUC
-	miRNA-precursor_435	GUCCCUCUCACAGCUACAGUACCC
-	miRNA-precursor_114	UUGGGCUCUCUUCCUCUCAUG
-	miRNA-precursor_75	GUGACAGAAGAGAGUGAGCAC

Table 4.1- List of conserved and novel miRNA sequences submitted for stem-loop RT-qPCR design.

miRNA	Accession	Target genes	Forward Primer-Sequence (5'-3')	Reverse Primer-Sequence (5'-3')	Reference
miR479-set1	orange1.1g033614m	UDP-glucose flavonoid glucosyl-transferase	CACCATCTACAGCGATACCAACC	CCACCCAGGTCAATGTTTTAGCAC	This study
miR479-set4	orange1.1g028826m	DEAD/DEAH box helicase	GTCTATGCTTCTTGTGGGAGGTGT	AGCCTGTCAGCCTCATCTAGAAC	This study
miR479-set5	orange1.1g026925m		GTTCTAGATGAGGCTGACAGGCT	CTTCAACCCTCACAGGATTCCTCA	This study
miR171b-set2	orange1.1g033674m	Glutathione S-transferase, C-terminal domain	CAGGAGGCAGCTAAGAAGGAGTT	AGCTATGAACTTGGGGCACTCAG	Ma et al. 2016
miR156-set9	orange1.1g011651m	Squamosa promoter binding protein-like 2	CGTGATGATTCCAATGGGCTCT	GACTTGTACTCGTGGGGTGCTG	This study
	orange1.1g011635m				
	orange1.1g011646m				
	orange1.1g013094m				
	orange1.1g011637m				
	orange1.1g011662m				
miR156-set10	orange1.1g032310m	Squamosa promoter binding protein-like 3	GCCAAGGCTCCTGTTGTTCG	CGGCAACTCCTTTTGGTGTCA	This study
miR156-set2	orange1.1g008776m	Squamosa promoter-binding protein-like (SBP domain) transcription factor family protein	CATAGAGAAGCTCCTGGGAACCAA	GTGGACTCATCTTCCCCAAAAGAC	Ma et al. 2016
miR535-set4	P_trifoliata_00066_mRNA_51.1	RHOMBOID-like protein 1	CAGTAGCCAAGGTGGTAACTCAAC	CCAAAACCAGAAAGGACGTAGAGG	Ma et al. 2016

Table 4.2- Specific primers used for RT-qPCR relative quantification of miRNA target genes.

	Non-infected stem		CDVd-infected stem	
	Reads	**Unique Sequences**	**Reads**	**Unique Sequences**
Raw reads	16,008,944	N/A	13,764,218	N/A
Clean reads (18-28 nt sRNA)	6,742,931 (100%)	1,453,586 (100%)	5,733,421 (100%)	1,214,014 (100%)
miRNA	545,243 (8.1%)	683 (0.05%)	412,526 (7.2%)	607 (0.05%)
rRNA, tRNA, snRNA, snoRNA	3,220,307 (47.8%)	115,180 (7.9%)	2,880,237 (50.2%)	109,817 (9.05%)
Unannotated	2,977,381 (44.2%)	1,336,138 (91.9%)	2,440,659 (42.6%)	1,102,588 (90.8%)

	Non-infected root		CDVd-infected root	
	Reads	**Unique Sequences**	**Reads**	**Unique Sequences**
Raw Reads	6,524,898	NA	5,864,614	NA
Clean Reads (18-28 nt sRNA)	2,030,419 (100%)	515,978 (100%)	1,873,309 (100%)	468,357 (100%)
miRNA	125,224 (6.1%)	313 (0.00061%)	108,262 (5.8%)	315 (0.0007%)
rRNA, tRNA, snRNA, snoRNA	1,027,218 (50.5%)	87,435 (16.9%)	984,550 (52.5%)	81,988 (17.5%)
Unannotated	877,976 (43.2%)	427,990 (82.9%)	780,496 (41.6%)	385,868 (82.4%)

Table 4.3- Statistical summary of small RNA (sRNA) sequences from non-infected and citrus dwarfing viroid (CDVd)-infected libraries from stem (Citrus sinensis) and root (C. trifoliata) tissues.

Family	miRNA name	Sequence (5'-3')	Length (nt)	Tissue Type	Normalized value		Log 2 Fold Change	P-value	Adjusted P-value	Significance label
					Non-infected	CDVd-infected				
MIR156	csi-miR156	UGACAGAAGAGAGUGAGCAC	20	Stem	944.28	532.04	-0.828	0.001084	0.0412	**
MIR171	csi-miR171b	CGAGCCGAAUCAAUAUCACUC	21	Stem	433.35	264.95	-0.711	0.000740	0.0338	**
MIR171	csi-miR479	UGUGAUAUUGGUUCGGCUCAUC	22	Stem	433.35	264.95	-0.711	0.000740	0.0338	**
MIR166	csi-miR166a	UCGGACCAGGCUUCAUUCCCCC	22	Stem	225444.12	190251.69	-0.24	0.29	0.614	
MIR166	csi-miR166b	UCGGACCAGGCUUCAUUCCCGU	22	Stem	190840.39	211388.61	0.15	0.25	0.610	
MIR166	csi-miR166c	UCGGACCAGGCUUCAUUCCC	20	Stem	248503.49	210279.64	-0.24	0.27	0.613	
MIR166	csi-miR166d	UCGGACCAGGCUUCAUUCCCU	21	Stem	10291.47	9164.90	-0.17	0.35	0.645	
MIR166	csi-miR166e	UCGGACCAGGCUUCAUUCCCC	21	Stem	225437.68	190245.62	-0.24	0.29	0.614	
MIR396	csi-miR396a	UUCCACAGCUUUCUUGAACUG	21	Stem	4439.016609	6389.073731	0.53	0.01	0.10	
MIR396	csi-miR396b	UUCCACAGCUUUCUUGAACUG	21	Stem	4625.81381	6577.736377	0.51	0.01	0.10	
MIR396	csi-miR396c	UUCAAGAAAUCUGUGGGAAG	20	Stem	3340.320865	2152.155423	-0.63	0.02	0.16	
MIR399	csi-miR399a	UGCCAAAGGAGAUUUGCCCGG	21	Stem	0.82	2.04	1.47	0.22	NA	
MIR399	csi-miR399b	UGCCAAAGGAGAGUUGCCCUA	21	Stem	24.93	41.24	0.74	0.08	0.379	
MIR399	csi-miR399c	UGCCAAAGGAGAAUUGCCCUG	21	Stem	2.28	4.29	0.99	0.25	NA	
MIR399	csi-miR399d	UGCCAAAGGAGAGUUGCCCUG	21	Stem	90.63	113.30	0.33	0.32	0.644	
MIR399	csi-miR399e	UGCCAAAGGAGAAUUGCCCUG	21	Stem	2.28	3.93	0.87	0.32	NA	
MIR477	csi-miR477a	ACCUCCCUCGAAGGCUUCCAA	21	Stem	63.15	53.52	-0.23	0.57	0.750	
MIR477	csi-miR477b	CUCUCCCUCAAGGGCUUCUCU	21	Stem	1367.46	1020.24	-0.42	0.05	0.289	
MIR477	csi-miR477c	UCCCUCGAAGGCUUCCAAUAUA	22	Stem	63.15	53.52	-0.23	0.57	0.750	
MIR482	csi-miR482a	UCUUCCCUAUGCCUCCCAUUCC	22	Stem	1029.05	915.31	-0.17	0.35	0.645	
MIR482	csi-miR482b	UCUUGCCCACCCCUCCCAUUCC	22	Stem	632.93	519.99	-0.28	0.06	0.316	
MIR482	csi-miR482c	UUCCCUAGUCCCCCUAUUCCUA	22	Stem	207.25	288.14	0.48	0.06	0.316	

Table 4.4- Subsets of the conserved microRNAs (miRNAs) and their recovery profile in response to citrus dwarfing viroid (CDVd)-infection in stem (*Citrus sinensis*) and root (*C. trifoliata*) tissues. miRNAs with statistically significant values are noted with **.

miRNA name	Sequence (5'-3')	Length (nt)	Tissue Type	Normalized value		Log 2 Fold Change	P-value	Adjusted P-value	Significance label
				Non-infected	CDVd-infected				
csi-miRNA-75	GUGACAGAAGAGAGUGAGCAC	21	Stem	82.35	35.66	-1.219	0.000074	0.0084	**
csi-miRNA-114	UUGGGCUCUCUUCCUCUCAUG	21	Stem	30.71	6.73	-2.247	0.000023	0.0052	**
csi-miRNA-435	GUCCCUCUCACAGCUACAGUACCC	24	Stem	45.62	23.46	-0.984	0.000380	0.0289	**
csi-miRNA-02	AAAAGGAGGACUAAGUUAAAAGCA	24	Stem	77.68	59.82	-0.39	0.08	0.38	
csi-miRNA-23	AUAUUGGAGUGUUUGACCAGU	21	Stem	60.26	46.28	-0.38	0.14	0.53	
csi-miRNA-87	ACAAGAGUUUGUGACUGUAUCAUU	24	Stem	8.55	10.60	0.20	0.67	1.00	
csi-miRNA-20	GUGACAGAAGAGAGUGAGCAC	21	Root	48.73	39.25	-0.29	0.44	1.00	
csi-miRNA-57	AUUCCUCAUUGUUUGGUCAACAGC	24	Root	13.49	9.75	-0.42	0.41	1.00	
csi-miRNA-63	UUCCAAAGGGAUCGCAUUGAUC	22	Root	59.08	53.41	-0.17	0.59	1.00	
csi-miRNA-77	AGGCAGUCUCCUUGGCUAAG	20	Root	9.54	5.30	-0.90	0.08	1.00	
csi-miRNA-91	AAGCACGAGAGAAAGACGAGAGAA	24	Root	5.21	5.17	-0.05	0.94	1.00	
csi-miRNA-100	AUUUCGGUAACUAAUAGGAUAUAC	24	Root	3.48	3.24	-0.07	0.93	1.00	

Table 4.5- Subset of the conserved and novel microRNAs (miRNAs) and their recovery profile in response to citrus dwarfing viroid (CDVd)-infection in stem (Citrus sinensis) and root (C. trifoliata) tissues. miRNAs with statistically significant values are noted with **.

Table 4.6

miRNA name	Sequence (5'-3')	Length (nt)	Normalized value		Log 2 Fold Change	P-value	Adjusted P-value	Significance label
			Non-infected	CDVd-infected				
csi-miR156	UGACAGAAGAGAGUGAGCAC	20	944.3	532.0	-0.83	0.00	0.04	**
csi-miR159	UUUGGAUUGAAGGGAGCUCUA	21	9271.0	10765.1	0.22	0.23	0.60	
csi-miR160	GCCUGGCUCCCUGUAUGCCAU	21	16.0	28.0	0.81	0.06	0.33	
csi-miR162	UGGAGGCAGCGGUUCAUCGAUC	22	231.8	153.6	-0.60	0.00	0.09	
csi-miR164	UGGAGAAGCAGGGCACGUGCA	21	172.2	124.9	-0.45	0.09	0.40	
csi-miR166a	UCGGACCAGGCUUCAUUCCCCC	22	225444.1	190251.7	-0.24	0.29	0.61	
csi-miR166b	UCGGACCAGGCUUCAUUCCCGU	22	190840.4	211388.6	0.15	0.25	0.61	
csi-miR166c	UCGGACCAGGCUUCAUUCCC	20	248503.5	210279.6	-0.24	0.27	0.61	
csi-miR166d	UCGGACCAGGCUUCAUUCCCU	21	10291.5	9164.9	-0.17	0.35	0.65	
csi-miR166e	UCGGACCAGGCUUCAUUCCCC	21	225437.7	190245.6	-0.24	0.29	0.61	
csi-miR167a	UGAAGCUGCCAGCAUGAUCUG	21	269.9	258.4	-0.06	0.77	0.85	
csi-miR167b	UGAAGCUGCCAGCAUGAUCUU	21	158.6	158.5	0.01	0.98	0.99	
csi-miR167c	UGAAGCUGCCAGCAUGAUCUG	21	163.7	166.0	0.03	0.89	0.95	

csi-miR169	GAGCCAAGAAUGACUUGCCGA	21	0.0	0.0	NA	NA	NA	
csi-miR171a	UUGAGCCGCGCCAAUAUCAC	20	55.1	58.2	0.07	0.76	0.84	
csi-miR171b	CGAGCCGAAUCAAUAUCACUC	21	433.3	265.0	-0.71	0.00	0.03	**
csi-miR172a	AGAAUCUUGAUGAUGCUGCA	20	225.9	228.7	0.01	0.94	0.98	
csi-miR172b	AGAAUCUUGAUGAUGCGGCAA	21	0.8	0.0	-1.92	0.27	NA	
csi-miR172c	UGGAAUCUUGAUGAUGCUGCAG	22	135.6	120.0	-0.18	0.33	0.65	
csi-miR319	UUUGGACUGAAGGGAGCUCCU	21	1239.4	1401.5	0.18	0.39	0.65	
csi-miR390	AAGCUCAGGAGGGAUAGCGCC	21	234.9	221.2	-0.09	0.58	0.75	
csi-miR393	AUCCAAAGGGAUCGCAUUGAUC	22	18.3	14.5	-0.32	0.37	0.65	
csi-miR394	UUGGCAUUCUGUCCACCUCC	20	103.8	130.5	0.34	0.26	0.61	
csi-miR395	CUGAAGUGUUUGGGGGAACUC	21	0.3	0.0	-0.64	0.79	NA	
csi-miR396a	UUCCACAGCUUUCUUGAACUG	21	4439.0	6389.1	0.53	0.01	0.10	
csi-miR396b	UUCCACAGCUUUCUUGAACUG	21	4625.8	6577.7	0.51	0.01	0.10	
csi-miR396c	UUCAAGAAAUCUGUGGGAAG	20	3340.3	2152.2	-0.63	0.02	0.16	
csi-miR397	UCAUUGAGUGCAGCGUUGAUG	21	0.4	0.8	0.79	0.64	NA	
csi-miR398	UGUGUUCUCAGGUCACCCCUU	21	72.1	96.0	0.40	0.17	0.55	
csi-miR399a	UGCCAAAGGAGAUUUGCCCGG	21	0.8	2.0	1.47	0.22	NA	

csi-miR399b	UGCCAAAGGAGAGUUGCCCUA	21	24.9	41.2	0.74	0.08	0.38	
csi-miR399c	UGCCAAAGGAGAAUUGCCCUG	21	2.3	4.3	0.99	0.25	NA	
csi-miR399d	UGCCAAAGGAGAGUUGCCCUG	21	90.6	113.3	0.33	0.32	0.64	
csi-miR399e	UGCCAAAGGAGAAUUGCCCUG	21	2.3	3.9	0.87	0.32	NA	
csi-miR403	UUAGAUUCACGCACAAACUCG	21	3964.4	4058.5	0.03	0.85	0.93	
csi-miR408	AUGCACUGCCUCUUCCCUGGC	21	2.7	4.6	0.75	0.29	NA	
csi-miR472	UUUUCCCACACCUCCCAUCCC	21	982.2	927.8	-0.08	0.66	0.78	
csi-miR473	ACUCUCCCUCAAGGGCUUCGC	21	594.3	539.2	-0.14	0.60	0.76	
csi-miR477a	ACCUCCCUCGAAGGCUUCCAA	21	63.1	53.5	-0.23	0.57	0.75	
csi-miR477b	CUCUCCCUCAAGGGCUUCUCU	21	1367.5	1020.2	-0.42	0.05	0.29	
csi-miR477c	UCCCUCGAAGGCUUCCAAUAUA	22	63.1	53.5	-0.23	0.57	0.75	
csi-miR479	UGUGAUAUUGGUUCGGCUCAUC	22	433.3	265.0	-0.71	0.00	0.03	**
csi-miR482a	UCUUCCCUAUGCCUCCCAUUCC	22	1029.0	915.3	-0.17	0.35	0.65	
csi-miR482b	UCUUGCCCACCCCUCCCAUUCC	22	632.9	520.0	-0.28	0.06	0.32	
csi-miR482c	UUCCCUAGUCCCCCUAUUCCUA	22	207.3	288.1	0.48	0.06	0.32	
csi-miR530a	UGCAUUUGCACCUGCACCUUG	21	11.6	12.8	0.16	0.73	NA	
csi-miR530b	UGCAUUUGCACCUGCAUCUUG	21	123.3	212.9	0.79	0.02	0.18	

csi-miR535	UGACAAUGAGAGAGAGCACAC	21	165.9	101.6	-0.72	0.01	0.13
csi-miR827	UUAGAUGACCAUCAACAAACA	21	123.6	212.2	0.78	0.02	0.14
csi-miR857	UUUUGAAUGUUGAAUGGUGGCUAU	24	0.2	0.7	1.61	0.41	NA
csi-miR1515	UCAUUUUUGCGUGCAAUGAUCC	22	4.8	4.6	-0.14	0.83	NA
csi-miR3946	UUGUAGAGAAAGAGAAGAGAGCAC	24	1.3	2.1	0.55	0.58	NA
csi-miR3947	UUAUUUCAGUAGACGACGUCACA	23	9.4	12.6	0.40	0.35	NA
csi-miR3948	UGGAGUGGGAGUGGGAGUAGGGUG	24	156.5	139.8	-0.16	0.36	0.65
csi-miR3949	UGAUGUUGAGGCAAAAAUGUAG	22	0.0	0.0	NA	NA	NA
csi-miR3950	UUUUUCGGCAACAUGAUUUCU	21	3.4	7.3	1.23	0.05	NA
csi-miR3951	UAGAUAAAGAUGAGAGAAAAA	21	1264.5	1455.1	0.20	0.26	0.61
csi-miR3952	UGAAGGGCCUUUCUAGAGCAC	21	3387.4	3078.5	-0.14	0.34	0.65
csi-miR3953	UUGAGUUCUGCAAGCCGUCGA	21	24.9	28.2	0.16	0.56	0.75
csi-miR3954	UGGACAGAGAAAUCACGGUCA	21	136.7	127.1	-0.10	0.60	0.76

Table 4.6 List of all conserved miRNA found in *Citrus sinensis* stems.

Table 4.7

miRNA name	Sequence (5'-3')	Length (nt)	Normalized value		Log 2 Fold Change	P-value	Adjusted P-value	Significance label
			Non-infected	CDVd-infected				
csi-miR156	UGACAGAAGAGAGUGAGCAC	20	331.2	291.3	-0.18	0.62	0.997	
csi-miR159	UUUGGAUUGAAGGGAGCUCUA	21	1334.7	1369.8	0.04	0.88	0.997	
csi-miR160	GCCUGGCUCCCUGUAUGCCAU	21	2.9	1.9	-0.84	0.31	0.997	
csi-miR162	UGGAGGCAGCGGUUCAUCGAUC	22	45.2	35.7	-0.3	0.4	0.997	
csi-miR164	UGGAGAAGCAGGGCACGUGCA	21	16.2	14.7	-0.2	0.59	0.997	
csi-miR166a	UCGGACCAGGCUUCAUUCCCCC	22	40255.2	37986.8	-0.08	0.76	0.997	
csi-miR166b	UCGGACCAGGCUUCAUUCCCGU	22	56293	48592.7	-0.21	0.37	0.997	
csi-miR166c	UCGGACCAGGCUUCAUUCCC	20	41752	39585.5	-0.08	0.78	0.997	
csi-miR166d	UCGGACCAGGCUUCAUUCCCU	21	1451	1455	0.01	0.98	0.997	
csi-miR166e	UCGGACCAGGCUUCAUUCCCC	21	40249.8	37980.1	-0.08	0.76	0.997	
csi-miR167a	UGAAGCUGCCAGCAUGAUCUG	21	196.3	146.2	-0.41	0.19	0.997	
csi-miR167b	UGAAGCUGCCAGCAUGAUCUU	21	247.1	243.5	-0.02	0.96	0.997	
csi-miR167c	UGAAGCUGCCAGCAUGAUCUG	21	35.6	32.6	-0.07	0.82	0.997	
csi-miR169	GAGCCAAGAAUGACUUGCCGA	21	0	0.3	0.84	0.81	0.997	

csi-miR171a	UUGAGCCGCGCCAAUAUCAC	20	0.3	0.3	0.29	0.9	0.997
csi-miR171b	CGAGCCGAAUCAAUAUCACUC	21	57.6	30.3	-0.96	0.01	0.479
csi-miR172a	AGAAUCUUGAUGAUGCUGCA	20	72.9	57.8	-0.32	0.4	0.997
csi-miR172b	AGAAUCUUGAUGAUGCGGCAA	21	0.3	0.4	0.3	0.89	0.997
csi-miR172c	UGGAAUCUUGAUGAUGCUGCAG	22	50.8	45.4	-0.15	0.73	0.997
csi-miR319	UUUGGACUGAAGGGAGCUCCU	21	59.4	74.6	0.3	0.4	0.997
csi-miR390	AAGCUCAGGAGGGAUAGCGCC	21	121.3	124.9	0.05	0.9	0.997
csi-miR393	AUCCAAAGGGAUCGCAUUGAUC	22	4.5	3.5	-0.37	0.59	0.997
csi-miR394	UUGGCAUUCUGUCCACCUCC	20	21.1	19.7	-0.09	0.81	0.997
csi-miR395	CUGAAGUGUUUGGGGGAACUC	21	1.5	2.4	0.98	0.34	0.997
csi-miR396a	UUCCACAGCUUUCUUGAACUG	21	2594.9	2916	0.17	0.54	0.997
csi-miR396b	UUCCACAGCUUUCUUGAACUG	21	2621.4	2935.8	0.16	0.55	0.997
csi-miR396c	UUCAAGAAAUCUGUGGGAAG	20	315	333.1	0.08	0.72	0.997
csi-miR397	UCAUUGAGUGCAGCGUUGAUG	21	2.4	3	0.62	0.46	0.997
csi-miR398	UGUGUUCUCAGGUCACCCCUU	21	6.1	5.6	0.06	0.92	0.997
csi-miR399a	UGCCAAAGGAGAUUUGCCCGG	21	0.1	0.4	-0.01	1	0.997
csi-miR399b	UGCCAAAGGAGAGUUGCCCUA	21	21	28.2	0.37	0.46	0.997

csi-miR399c	UGCCAAAGGAGAAUUGCCCUG	21	0.2	1.6	1.93	0.17	0.997	
csi-miR399d	UGCCAAAGGAGAGUUGCCCUG	21	37.8	42.1	0.14	0.87	0.997	
csi-miR399e	UGCCAAAGGAGAAUUGCCCUG	21	0.2	1.6	1.93	0.17	0.997	
csi-miR403	UUAGAUUCACGCACAAACUCG	21	250.6	263.8	0.08	0.74	0.997	
csi-miR408	AUGCACUGCCUCUUCCCUGGC	21	0.6	0.9	0.02	0.99	0.997	
csi-miR472	UUUUCCCACACCUCCCAUCCC	21	427	387.8	-0.14	0.5	0.997	
csi-miR473	ACUCUCCCUCAAGGGCUUCGC	21	92.1	61.2	-0.6	0.08	0.997	
csi-miR477a	ACCUCCCUCGAAGGCUUCCAA	21	42.5	43.3	0.01	0.99	0.997	
csi-miR477b	CUCUCCCUCAAGGGCUUCUCU	21	38.4	27.6	-0.52	0.14	0.997	
csi-miR477c	UCCCUCGAAGGCUUCCAAUAUA	22	42.5	43.3	0.01	0.99	0.997	
csi-miR479	UGUGAUAUUGGUUCGGCUCAUC	22	57.6	30.3	-0.96	0.01	0.479	
csi-miR482a	UCUUCCCUAUGCCUCCCAUUCC	22	71.8	65.9	-0.1	0.74	0.997	
csi-miR482b	UCUUGCCCACCCCUCCCAUUCC	22	89.3	89.2	-0.03	0.92	0.997	
csi-miR482c	UUCCCUAGUCCCCCUAUUCCUA	22	27.6	29.6	0.14	0.7	0.997	
csi-miR530a	UGCAUUUGCACCUGCACCUUG	21	0.8	0.6	-0.89	0.57	0.997	
csi-miR530b	UGCAUUUGCACCUGCAUCUUG	21	0.7	1	0.51	0.7	0.997	
csi-miR535	UGACAAUGAGAGAGAGCACAC	21	64	24.4	-1.42	0.00004	0.007	**

csi-miR827	UUAGAUGACCAUCAACAAACA	21	28.4	34.4	0.29	0.55	0.997
csi-miR857	UUUUGAAUGUUGAAUGGUGGCUAU	24	0.3	0	-0.69	0.8	0.997
csi-miR1515	UCAUUUUUGCGUGCAAUGAUCC	22	3.7	1.9	-0.96	0.24	0.997
csi-miR3946	UUGUAGAGAAAGAGAAGAGAGCAC	24	0.4	0	-1.08	0.63	0.997
csi-miR3947	UUAUUUCAGUAGACGACGUCACA	23	0	0	NA	NA	NA
csi-miR3948	UGGAGUGGGAGUGGGAGUAGGGUG	24	12	13	0.18	0.66	0.997
csi-miR3949	UGAUGUUGAGGCAAAAAUGUAG	22	0	0	NA	NA	NA
csi-miR3950	UUUUUCGGCAACAUGAUUUCU	21	0.3	0.3	0.3	0.89	0.997
csi-miR3951	UAGAUAAAGAUGAGAGAAAAA	21	464.4	359.6	-0.37	0.2	0.997
csi-miR3952	UGAAGGGCCUUUCUAGAGCAC	21	279.8	252	-0.16	0.46	0.997
csi-miR3953	UUGAGUUCUGCAAGCCGUCGA	21	0.6	0.8	0.8	0.6	0.997
csi-miR3954	UGGACAGAGAAAUCACGGUCA	21	14.6	17.7	0.18	0.64	0.997

Table 4.7 List of all conserved miRNAs found in *Citrus trifoliata* roots.

REFERENCES

1. Adkar-Purushothama, C. R., Brosseau, C., Giguère, T., Sano, T., Moffett, P., and Perreault, J.-P. (2015). Small RNA Derived from the Virulence Modulating Region of the Potato spindle tuber viroid Silences callose synthase Genes of Tomato Plants. *Plant Cell* 27, 2178–2194.

2. Adkar-Purushothama, C. R., Iyer, P. S., and Perreault, J.-P. (2017). Potato spindle tuber viroid infection triggers degradation of chloride channel protein CLC-b-like and Ribosomal protein S3a-like mRNAs in tomato plants. *Sci. Rep.* 7, 8341.

3. Altenburg, E. (1946). The “viroid” theory in relation to plasmagenes, viruses, cancer and plastids. *Am. Nat.* 80, 559–567.

4. Axtell, M. J., and Bartel, D. P. (2005). Antiquity of microRNAs and their targets in land plants. *Plant Cell* 17, 1658–1673.

5. Axtell, M. J., Snyder, J. A., and Bartel, D. P. (2007). Common functions for diverse small RNAs of land plants. *Plant Cell* 19, 1750–1769.

6. Babcock, B. (2018). Economic impact of California’s citrus industry. *Citrograph* 9, 36–39.

7. Bartling, D., Radzio, R., Steiner, U., and Weiler, E. W. (1993). A glutathione S-transferase with glutathione-peroxidase activity from Arabidopsis thaliana. Molecular cloning and functional characterization. *Eur. J. Biochem.* 216, 579–586.

8. Bolduc, F., Hoareau, C., St-Pierre, P., and Perreault, J.-P. (2010). In-depth sequencing of the siRNAs associated with peach latent mosaic viroid infection. *BMC Mol. Biol.* 11, 16.

9. Borges, F., and Martienssen, R. A. (2015). The expanding world of small RNAs in plants. *Nat. Rev. Mol. Cell Biol.* 16, 727–741.

10. Boswell, S. B., and Others (1970). Tree spacing of ’Washington' navel orange. *J. Am. Soc. Hortic. Sci.* 95, 523–528.

11. Bustin, S. A., Benes, V., Garson, J. A., Hellemans, J., Huggett, J., Kubista, M., et al. (2009). The MIQE guidelines: minimum information for publication of quantitative real-time PCR experiments. *Clin. Chem.* 55, 611–622.

12. Cai, Y., Zhuang, X., Gao, C., Wang, X., and Jiang, L. (2014). The Arabidopsis Endosomal Sorting Complex Required for Transport III Regulates Internal Vesicle Formation of the Prevacuolar Compartment and Is Required for Plant Development. *Plant Physiol.* 165, 1328–1343.

13. Cardon, G., Höhmann, S., Klein, J., Nettesheim, K., Saedler, H., and Huijser, P. (1999). Molecular characterisation of the Arabidopsis SBP-box genes. *Gene* 237, 91–104.

14. Cheng, X., Peng, J., Ma, J., Tang, Y., Chen, R., Mysore, K. S., et al. (2012). NO APICAL MERISTEM (MtNAM) regulates floral organ identity and lateral organ separation in Medicago truncatula. *New Phytol.* 195, 71–84.

15. Chen, H.-M., Chen, L.-T., Patel, K., Li, Y.-H., Baulcombe, D. C., and Wu, S.-H. (2010a). 22-Nucleotide RNAs trigger secondary siRNA biogenesis in plants. *Proc. Natl. Acad. Sci. U. S. A.* 107, 15269–15274.

16. Chen, X., Zhang, Z., Liu, D., Zhang, K., Li, A., and Mao, L. (2010b). SQUAMOSA promoter-binding protein-like transcription factors: star players for plant growth and development. *J. Integr. Plant Biol.* 52, 946–951.

17. Czech, B., Munafò, M., Ciabrelli, F., Eastwood, E. L., Fabry, M. H., Kneuss, E., et al. (2018). piRNA-Guided Genome Defense: From Biogenesis to Silencing. *Annu. Rev. Genet.* 52, 131–157.

18. Dadami, E., Boutla, A., Vrettos, N., Tzortzakaki, S., Karakasilioti, I., and Kalantidis, K. (2013). DICER-LIKE 4 but not DICER-LIKE 2 may have a positive effect on potato spindle tuber viroid accumulation in Nicotiana benthamiana. *Mol. Plant* 6, 232–234.

19. Dadami, E., Dalakouras, A., and Wassenegger, M. (2017). “Chapter 11 - Viroids and RNA Silencing,” in *Viroids and Satellites*, eds. A. Hadidi, R. Flores, J. W. Randles, and P. Palukaitis (Boston: Academic Press), 115–124.

20. da Graça, J. V., Douhan, G. W., Halbert, S. E., Keremane, M. L., Lee, R. F., Vidalakis, G., et al. (2016). Huanglongbing: An overview of a complex pathosystem ravaging the world’s citrus. *J. Integr. Plant Biol.* 58, 373–387.

21. Dai, X., Zhuang, Z., and Zhao, P. X. (2018). psRNATarget: a plant small RNA target analysis server (2017 release). *Nucleic Acids Res.* 46, W49–W54.

22. Diermann, N., Matoušek, J., Junge, M., Riesner, D., and Steger, G. (2010). Characterization of plant miRNAs and small RNAs derived from potato spindle tuber viroid (PSTVd) in infected tomato. *Biol. Chem.* 391, 1379–1390.

23. Ding, B. (2009). The biology of viroid-host interactions. *Annu. Rev. Phytopathol.* 47, 105–131.

24. Eamens, A. L., Smith, N. A., Dennis, E. S., Wassenegger, M., and Wang, M.-B. (2014). In Nicotiana species, an artificial microRNA corresponding to the virulence modulating region of Potato spindle tuber viroid directs RNA silencing of a soluble inorganic pyrophosphatase gene and the development of abnormal phenotypes. *Virology* 450-451, 266–277.

25. Farooq, M., Mansoor, S., Guo, H., Amin, I., Chee, P. W., Azim, M. K., et al. (2017). Identification and Characterization of miRNA Transcriptome in Asiatic Cotton (Gossypium arboreum) Using High Throughput Sequencing. *Front. Plant Sci.* 8, 969.

26. Ferdous, J., Sanchez-Ferrero, J. C., Langridge, P., Milne, L., Chowdhury, J., Brien, C., et al. (2017). Differential expression of microRNAs and potential targets under drought stress in barley. *Plant Cell Environ.* 40, 11–24.

27. Flores, R., Di Serio, F., Navarro, B., and Owens, R. A. (2017). "Chapter 9 - Viroid Pathogenesis," in *Viroids and Satellites*, eds. A. Hadidi, R. Flores, J. W. Randles, and P. Palukaitis (Boston: Academic Press), 93–103.

28. Flores, R., Gas, M.-E., Molina-Serrano, D., Nohales, M.-Á., Carbonell, A., Gago, S., et al. (2009). Viroid replication: rolling-circles, enzymes and ribozymes. *Viruses* 1, 317–334.

29. Gandikota, M., Birkenbihl, R. P., Höhmann, S., Cardon, G. H., Saedler, H., and Huijser, P. (2007). The miRNA156/157 recognition element in the 3' UTR of the Arabidopsis SBP box gene SPL3 prevents early flowering by translational inhibition in seedlings. *Plant J.* 49, 683–693.

30. Gao, J., Yin, F., Liu, M., Luo, M., Qin, C., Yang, A., et al. (2015). Identification and characterisation of tobacco microRNA transcriptome using high-throughput sequencing. *Plant Biol.* 17, 591–598.

31. Gómez, G., Martínez, G., and Pallás, V. (2009). Interplay between viroid-induced pathogenesis and RNA silencing pathways. *Trends Plant Sci.* 14, 264–269.

32. Gottwald (2010). Current Epidemiological Understanding of Citrus Huanglongbing. *Annu. Rev. Phytopathol.* 48, 119–139.

33. Götz, S., García-Gómez, J. M., Terol, J., Williams, T. D., Nagaraj, S. H., Nueda, M. J., et al. (2008). High-throughput functional annotation and data mining with the Blast2GO suite. *Nucleic Acids Res.* 36, 3420–3435.

34. Gullner, G., Komives, T., Király, L., and Schröder, P. (2018). Glutathione S-Transferase Enzymes in Plant-Pathogen Interactions. *Front. Plant Sci.* 9, 1836.

35. Huang, J.-H., Lin, X.-J., Zhang, L.-Y., Wang, X.-D., Fan, G.-C., and Chen, L.-S. (2019). MicroRNA Sequencing Revealed Citrus Adaptation to Long-Term Boron Toxicity through Modulation of Root Development by miR319 and miR171. *Int. J. Mol. Sci.* 20. doi:10.3390/ijms20061422.

36. Itaya, A., Zhong, X., Bundschuh, R., Qi, Y., Wang, Y., Takeda, R., et al. (2007). A structured viroid RNA serves as a substrate for dicer-like cleavage to produce biologically active small RNAs but is resistant to RNA-induced silencing complex-mediated degradation. *J. Virol.* 81, 2980–2994.

37. Jagadeeswaran, G., Zheng, Y., Sumathipala, N., Jiang, H., Arrese, E. L., Soulages, J. L., et al. (2010). Deep sequencing of small RNA libraries reveals dynamic regulation of conserved and novel microRNAs and microRNA-stars during silkworm development. *BMC Genomics* 11, 52.

38. Jia, L., Zhang, D., Qi, X., Ma, B., Xiang, Z., and He, N. (2014). Identification of the conserved and novel miRNAs in Mulberry by high-throughput sequencing. *PLoS One* 9, e104409.

39. Kalvari, I., Argasinska, J., Quinones-Olvera, N., Nawrocki, E. P., Rivas, E., Eddy, S. R., et al. (2018). Rfam 13.0: shifting to a genome-centric resource for non-coding RNA families. *Nucleic Acids Res.* 46, D335–D342.

40. Kanaoka, M. M., Urban, S., Freeman, M., and Okada, K. (2005). An Arabidopsis Rhomboid homolog is an intramembrane protease in plants. *FEBS Lett.* 579, 5723–5728.

41. Kawahara, Y., Endo, T., Omura, M., Teramoto, Y., Itoh, T., Fujii, H., et al. (2020). Mikan Genome Database (MiGD): integrated database of genome annotation, genomic diversity, and CAPS marker information for mandarin molecular breeding. *Breed. Sci.* 70, 200–211.

42. Kou, S.-J., Wu, X.-M., Liu, Z., Liu, Y.-L., Xu, Q., and Guo, W.-W. (2012). Selection and validation of suitable reference genes for miRNA expression normalization by quantitative RT-PCR in citrus somatic embryogenic and adult tissues. *Plant Cell Rep.* 31, 2151–2163.

43. Kozomara, A., Birgaoanu, M., and Griffiths-Jones, S. (2019). miRBase: from microRNA sequences to function. *Nucleic Acids Res.* 47, D155–D162.

44. Kozomara, A., and Griffiths-Jones, S. (2011). miRBase: integrating microRNA annotation and deep-sequencing data. *Nucleic Acids Res.* 39, D152–7.

45. Kozomara, A., and Griffiths-Jones, S. (2014). miRBase: annotating high confidence microRNAs using deep sequencing data. *Nucleic Acids Res.* 42, D68–73.

46. Lambin, E. F. (2012). Global land availability: Malthus versus Ricardo. *Global Food Security* 1, 83–87.

47. Lavagi-Craddock, I., Campos, R., Pagliaccia, D., Kapaun, T., Lovatt, C., and Vidalakis, G. (2020). Citrus dwarfing viroid reduces canopy volume by affecting shoot apical growth of navel orange trees grown on trifoliate orange rootstock. *Journal of Citrus Pathology* 7. Available at: https://escholarship.org/uc/item/2497h2fp.

48. Lee, M.-H., Kim, B., Song, S.-K., Heo, J.-O., Yu, N.-I., Lee, S. A., et al. (2008). Large-scale analysis of the GRAS gene family in Arabidopsis thaliana. *Plant Mol. Biol.* 67, 659–670.

49. Lei, J., and Sun, Y. (2014). miR-PREFeR: an accurate, fast and easy-to-use plant miRNA prediction tool using small RNA-Seq data. *Bioinformatics* 30, 2837–2839.

50. Leitner-Dagan, Y., Ovadis, M., Shklarman, E., Elad, Y., Rav David, D., and Vainstein, A. (2006). Expression and functional analyses of the plastid lipid-associated protein CHRC suggest its role in chromoplastogenesis and stress. *Plant Physiol.* 142, 233–244.

51. Liang, W.-W., Huang, J.-H., Li, C.-P., Yang, L.-T., Ye, X., Lin, D., et al. (2017). MicroRNA-mediated responses to long-term magnesium-deficiency in Citrus sinensis roots revealed by Illumina sequencing. *BMC Genomics* 18, 657.

52. Liu, X., Lin, C., Ma, X., Tan, Y., Wang, J., and Zeng, M. (2018). Functional Characterization of a Flavonoid Glycosyltransferase in Sweet Orange (Citrus sinensis). *Front. Plant Sci.* 9, 166.

53. Love, M. I., Huber, W., and Anders, S. (2014). Moderated estimation of fold change and dispersion for RNA-seq data with DESeq2. *Genome Biol.* 15, 550.

54. Lu, Y.-B., Qi, Y.-P., Yang, L.-T., Guo, P., Li, Y., and Chen, L.-S. (2015). Boron-deficiency-responsive microRNAs and their targets in Citrus sinensis leaves. *BMC Plant Biol.* 15, 271.

55. Ma, C.-L., Qi, Y.-P., Liang, W.-W., Yang, L.-T., Lu, Y.-B., Guo, P., et al. (2016). MicroRNA Regulatory Mechanisms on Citrus sinensis leaves to Magnesium-Deficiency. *Front. Plant Sci.* 7, 201.

56. Macovei, A., Vaid, N., Tula, S., and Tuteja, N. (2012). A new DEAD-box helicase ATP-binding protein (OsABP) from rice is responsive to abiotic stress. *Plant Signal. Behav.* 7, 1138–1143.

57. Mafra, V., Kubo, K. S., Alves-Ferreira, M., Ribeiro-Alves, M., Stuart, R. M., Boava, L. P., et al. (2012). Reference genes for accurate transcript normalization in citrus genotypes under different experimental conditions. *PLoS One* 7, e31263.

58. Martin, M. (2011). Cutadapt removes adapter sequences from high-throughput sequencing reads. *EMBnet.journal* 17, 10–12.

59. Ma, Z., Hu, X., Cai, W., Huang, W., Zhou, X., Luo, Q., et al. (2014). Arabidopsis miR171-targeted scarecrow-like proteins bind to GT cis-elements and mediate gibberellin-regulated chlorophyll biosynthesis under light conditions. *PLoS Genet.* 10, e1004519.

60. Minoia, S., Carbonell, A., Di Serio, F., Gisel, A., Carrington, J. C., Navarro, B., et al. (2014). Specific argonautes selectively bind small RNAs derived from potato spindle tuber viroid and attenuate viroid accumulation in vivo. *J. Virol.* 88, 11933–11945.

61. Mishra, A. K., Duraisamy, G. S., Matoušek, J., Radisek, S., Javornik, B., and Jakse, J. (2016). Identification and characterization of microRNAs in Humulus lupulus using high-throughput sequencing and their response to Citrus bark cracking viroid (CBCVd) infection. *BMC Genomics* 17, 919.

62. Moriguchi, T., Kita, M., Endo-Inagaki, T., Ikoma, Y., and Omura, M. (1998). Characterization of a cDNA homologous to carotenoid-associated protein in citrus fruits1The nucleotide sequence reported in this paper has been submitted to DDBJ under accession No. AB011797 (CitPAP). Contribution No. 1112 of the NIFTS.1. *Biochimica et Biophysica Acta (BBA) - Gene Structure and Expression* 1442, 334–338.

63. Motameny, S., Wolters, S., Nürnberg, P., and Schumacher, B. (2010). Next generation sequencing of miRNAs - strategies, resources and methods. *Genes* 1, 70–84.

64. Moxon, S., Jing, R., Szittya, G., Schwach, F., Rusholme Pilcher, R. L., Moulton, V., et al. (2008). Deep sequencing of tomato short RNAs identifies microRNAs targeting genes involved in fruit ripening. *Genome Res.* 18, 1602–1609.

65. Murcia, N., Bernad, L., Serra, P., Hashemian, S. M. B., and Duran-Vila, N. (2009). Molecular and biological characterization of natural variants of Citrus dwarfing viroid. *Arch. Virol.* 154, 1329–1334.

66. Navarro, B., Gisel, A., Rodio, M. E., Delgado, S., Flores, R., and Di Serio, F. (2012). Small RNAs containing the pathogenic determinant of a chloroplast-replicating viroid guide the degradation of a host mRNA as predicted by RNA silencing. *Plant J.* 70, 991–1003.

67. Navarro, B., Pantaleo, V., Gisel, A., Moxon, S., Dalmay, T., Bisztray, G., et al. (2009). Deep sequencing of viroid-derived small RNAs from grapevine provides new insights on the role of RNA silencing in plant-viroid interaction. *PLoS One* 4, e7686.

68. Offen, W., Martinez-Fleites, C., Yang, M., Kiat-Lim, E., Davis, B. G., Tarling, C. A., et al. (2006). Structure of a flavonoid glucosyltransferase reveals the basis for plant natural product modification. *EMBO J.* 25, 1396–1405.

69. Owens, D. K., and McIntosh, C. A. (2009). Identification, recombinant expression, and biochemical characterization of a flavonol 3-O-glucosyltransferase clone from Citrus paradisi. *Phytochemistry* 70, 1382–1391.

70. Owens, R. A., and Hammond, R. W. (2009). Viroid pathogenicity: one process, many faces. *Viruses* 1, 298–316.

71. Owens, R. A., Tech, K. B., Shao, J. Y., Sano, T., and Baker, C. J. (2012). Global analysis of tomato gene expression during Potato spindle tuber viroid infection reveals a complex array of changes affecting hormone signaling. *Mol. Plant. Microbe. Interact.* 25, 582–598.

72. Platt, R. G. (1973). Treatment of frost-inured citrus, avocados. *California citrograph*. Available at: http://agris.fao.org/agris-search/search.do?recordID=US201303229376.

73. Reis, R. S., Eamens, A. L., Roberts, T. H., and Waterhouse, P. M. (2015). Chimeric DCL1-Partnering Proteins Provide Insights into the MicroRNA Pathway. *Front. Plant Sci.* 6, 1201.

74. Rhoades, M. W., Reinhart, B. J., Lim, L. P., Burge, C. B., Bartel, B., and Bartel, D. P. (2002). Prediction of plant microRNA targets. *Cell* 110, 513–520.

75. Riese, M., Höhmann, S., Saedler, H., Münster, T., and Huijser, P. (2007). Comparative analysis of the SBP-box gene families in P. patens and seed plants. *Gene* 401, 28–37.

76. Schmittgen, T. D., and Livak, K. J. (2008). Analyzing real-time PCR data by the comparative C(T) method. *Nat. Protoc.* 3, 1101–1108.

77. Semancik, J.S., (2003). Considerations for the introduction of viroids for economic advantage. In: Hadidi, A., Flores, R., Randles, J.W., Semancik, J.S. (Eds.), *Viroids*. CSIROPublishing, Collingwood, VIC, pp. 357-362.

78. Semancik, J. S., Rakowski, A. G., Bash, J. A., and Gumpf, D. J. (1997). Application of selected viroids for dwarfing and enhancement of production of "Valencia" orange. *J. Hortic. Sci.* 72, 563–570.

79. Treiber, T., Treiber, N., and Meister, G. (2019). Regulation of microRNA biogenesis and its crosstalk with other cellular pathways. *Nat. Rev. Mol. Cell Biol.* 20, 5–20.

80. Tsushima, T., Murakami, S., Ito, H., He, Y.-H., Charith Raj, A. P., and Sano, T. (2011). Molecular characterization of Potato spindle tuber viroid in dahlia. *J. Gen. Plant Pathol.* 77, 253–256.

81. Tucker, D. P. H., and Wheaton, T. A. (1978). Trends in higher citrus planting densities. in *Proc. Fla. State Hort. Soc*, 36–40.

82. USDA-NASS (8/2019). Citrus Fruits 2019 Summary. Available at: https://www.nass.usda.gov/Publications/Todays_Reports/reports/cfrt0819.pdf.

83. Van Duyn, M. A., and Pivonka, E. (2000). Overview of the health benefits of fruit and vegetable consumption for the dietetics professional: selected literature. *J. Am. Diet. Assoc.* 100, 1511–1521.

84. Van Sandt, V. S. T., Suslov, D., Verbelen, J.-P., and Vissenberg, K. (2007). Xyloglucan endotransglucosylase activity loosens a plant cell wall. *Ann. Bot.* 100, 1467–1473.

85. Verburg, P. H., Mertz, O., Erb, K.-H., Haberl, H., and Wu, W. (2013). Land system change and food security: towards multi-scale land system solutions. *Curr Opin Environ Sustain* 5, 494–502.

86. Vernière, C., Perrier, X., Dubois, C., Dubois, A., Botella, L., Chabrier, C., et al. (2006). Interactions between citrus viroids affect symptom expression and field performance of clementine trees grafted on trifoliate orange. *Phytopathology* 96, 356–368.

87. Vidalakis, G., Gumpf, D. J., Bash, J. A., and Semancik, J. S. (2004). Finger Imprint of Poncirus trifoliata: A Specific Interaction of a Viroid, a Host, and Irrigation. *Plant Dis.* 88, 709–713.

88. Vidalakis, G., Pagliaccia, D., Bash, J. A., Afunian, M., and Semancik, J. S. (2011). Citrus dwarfing viroid: effects on tree size and scion performance specific to Poncirus trifoliata rootstock for high-density planting. *Ann. Appl. Biol.* 158, 204–217.

89. Vogt, T., and Jones, P. (2000). Glycosyltransferases in plant natural product synthesis: characterization of a supergene family. *Trends Plant Sci.* 5, 380–386.

90. Wang, J., Mei, J., and Ren, G. (2019). Plant microRNAs: Biogenesis, Homeostasis, and Degradation. *Front. Plant Sci.* 10, 360.

91. Wang, M.-B., Bian, X.-Y., Wu, L.-M., Liu, L.-X., Smith, N. A., Isenegger, D., et al. (2004). On the role of RNA silencing in the pathogenicity and evolution of viroids and viral satellites. *Proc. Natl. Acad. Sci. U. S. A.* 101, 3275–3280.

92. Wang, Y., Shibuya, M., Taneda, A., Kurauchi, T., Senda, M., Owens, R. A., et al. (2011). Accumulation of Potato spindle tuber viroid-specific small RNAs is accompanied by specific changes in gene expression in two tomato cultivars. *Virology* 413, 72–83.

93. Wassenegger, M., Heimes, S., and Sänger, H. L. (1994). An infectious viroid RNA replicon evolved from an in vitro-generated non-infectious viroid deletion mutant via a complementary deletion in vivo. *EMBO J.* 13, 6172–6177.

94. Wu, G., and Poethig, R. S. (2006). Temporal regulation of shoot development in Arabidopsis thaliana by miR156 and its target SPL3. *Development* 133, 3539–3547.

95. Xiang, L., Etxeberria, E., and Van den Ende, W. (2013). Vacuolar protein sorting mechanisms in plants. *FEBS J.* 280, 979–993.

96. Xie, K., Wu, C., and Xiong, L. (2006). Genomic organization, differential expression, and interaction of SQUAMOSA promoter-binding-like transcription factors and microRNA156 in rice. *Plant Physiol.* 142, 280–293.

97. Xie, R., Zhang, J., Ma, Y., Pan, X., Dong, C., Pang, S., et al. (2017). Combined analysis of mRNA and miRNA identifies dehydration and salinity responsive key molecular players in citrus roots. *Sci. Rep.* 7, 42094.

98. Yao, L. H., Jiang, Y. M., Shi, J., Tomás-Barberán, F. A., Datta, N., Singanusong, R., et al. (2004). Flavonoids in food and their health benefits. *Plant Foods Hum. Nutr.* 59, 113–122.

99. Yu, S., Galvão, V. C., Zhang, Y.-C., Horrer, D., Zhang, T.-Q., Hao, Y.-H., et al. (2012). Gibberellin Regulates the Arabidopsis Floral Transition through miR156-Targeted SQUAMOSA PROMOTER BINDING–LIKE Transcription Factors. *Plant Cell* 24, 3320–3332.

100. Zavallo, D., Debat, H. J., Conti, G., Manacorda, C. A., Rodriguez, M. C., and Asurmendi, S. (2015). Differential mRNA Accumulation upon Early Arabidopsis thaliana Infection with ORMV and TMV-Cg Is Associated with Distinct Endogenous Small RNAs Level. *PLoS One* 10, e0134719.

101. Zhang, B., Pan, X., and Stellwag, E. J. (2008). Identification of soybean microRNAs and their targets. *Planta* 229, 161–182.

102. Zhang, L., Chia, J.-M., Kumari, S., Stein, J. C., Liu, Z., Narechania, A., et al. (2009). A genome-wide characterization of microRNA genes in maize. *PLoS Genet.* 5, e1000716.

103. Zhang, R., Marshall, D., Bryan, G. J., and Hornyik, C. (2013). Identification and characterization of miRNA transcriptome in potato by high-throughput sequencing. *PLoS One* 8, e57233.

104. Zhang, T., Hu, S., Yan, C., Li, C., Zhao, X., Wan, S., et al. (2017). Mining, identification and function analysis of microRNAs and target genes in peanut (Arachis hypogaea L.). *Plant Physiol. Biochem.* 111, 85–96.

105. Zhang, Y., Wang, Y., Gao, X., Liu, C., and Gai, S. (2018). Identification and characterization of microRNAs in tree peony during chilling induced dormancy release by high-throughput sequencing. *Sci. Rep.* 8, 4537.

106. Zhu, L., Ow, D. W., and Dong, Z. (2018). Transfer RNA-derived small RNAs in plants. *Sci. China Life Sci.* 61, 155–161.

GENERAL CONCLUSIONS

A comprehensive study of the application of high-throughput technologies for citrus pathogen detection and the characterization of citrus host response in response to pathogen infections was presented in this dissertation. High-throughput extraction adoption was integral for nursery stock testing and field surveys, which resulted in significantly lowering the virus and viroid infections in the CA nursery and the led to the discovery of the first cases citrus viroid V (CVd V) and citrus leaf blotch virus (CLBV).

The high-throughput technology was then expanded to high-throughput sequencing (HTS) for the detection of citrus pathogens, and which utilized the e-probe diagnostic nucleic acid analysis (EDNA) online platform to simplify the data analysis. As proof-of-concept e-probes were developed for citrus tristeza virus (CTV), citrus exocortis viroid (CEVd), and *Candidatus* Liberibacter asiaticus (CLas). HTS was also applied for elucidation of viroid-host interactions by characterizing the miRNA citrus response in response to citrus dwarfing viroid (CDVd) infection.

Some of the research presented in these studies have had real world impact and are actively being used at the Citrus Clonal Protection Program (CCPP) for pathogen detection and exlusion. The viroid-host interaction in response to CDVd infection may not have immediate impact but understanding some of the underlying mechanisms for the dwarfing phenotype is important for future research.

Overall, this research will provide a lasting impact for the CCPP as the program continues the natural progression towards implementing and improving diagnostics for pathogen detection in citrus. This is especially important because citrus is a multi-billion-

dollar industry in the state of California that needs to be preserved through continuous disease management strategies and maintaining and distributing clean plant materials.